LB-877

DEFLECTION SYSTEMS WITH REGULATED KICKBACK HIGH-VOLTAGE SUPPLIES FOR TRI-COLOR KINESCOPES

Property of
Albert E. Linden

RADIO CORPORATION OF AMERICA
RCA LABORATORIES DIVISION
INDUSTRY SERVICE LABORATORY

RADIO CORPORATION OF AMERICA
RCA LABORATORIES DIVISION
INDUSTRY SERVICE LABORATORY

LB-877

Deflection Systems with Regulated Kickback

High-Voltage Supplies for Tri-Color Kinescopes

This report is the property of the Radio Corporation of America and is loaned for confidential use with the understanding that it will not be published in any manner, in whole or in part. The statements and data included herein are based upon information and measurements which we believe accurate and reliable. No responsibility is assumed for the application or interpretation of such statements or data or for any infringement of patent or other rights of third parties which may result from the use of circuits, systems and processes described or referred to herein or in any previous reports or bulletins or in any written or oral discussions supplementary thereto.

Approved

Stuart W. Seeley

Deflection Systems with Regulated Kickback High-Voltage Supplies for Tri-Color Kinescopes

Introduction

This bulletin describes a system that provides both horizontal deflection and regulated high voltage for tri-color kinescopes. It employs a horizontal-deflection circuit with a kick-back rectifier, similar to that normally employed in black-and-white receivers, to which means for regulating the high voltage has been added. The circuit is capable of supplying a relatively large amount of regulated high-voltage power, providing a maximum output of 700 μa at 20 kv to the final anode and convergence circuits and 600 μa at 3.6 kv to the focus circuit. Regulation for load changes is better than 2 per cent. The regulation level can be fixed during line-voltage changes, or automatically referenced to the line voltage. In one version a power pentode and a triode are added to the normal tube complement of a black-and-white receiver with electrostatic focus. Another version requires only the addition of a dual triode but is capable of delivering less peak high-voltage power.

Principles of Operation

In an unregulated horizontal-deflection and high-voltage supply system, a substantial increase in beam current causes the rectified high voltage to drop. It also reduces the peak pulse amplitude in the deflection transformer and therefore the energy returned to the output circuit after flyback. This in turn results in reduced boosted voltage, in changes in linearity and size, and in variation of the output-tube plate current. Attempts to regulate the high voltage by systems that automatically alter the screen voltage, plate voltage, or the amplitude of the drive of the horizontal output tube usually result in picture foldover in the center of the raster, changes in size and linearity, and in greatly increased plate dissipation. It was therefore considered advantageous to regulate the high voltage by maintaining a constant load on the horizontal output circuit. One method of doing this is by adding a "dummy" load tube in shunt with the kinescope. The dummy tube's beam current is made to vary in a manner complementary to that of the kinescope. The total current supplied by the rectifier to the dummy tube and kinescope is thus kept constant, and the high-voltage rectifier reflects a fixed load to the deflection circuit.

The basic principle is illustrated in Fig. 1. The dummy load may be a second kinescope, or an RCA type 5890 "Remote Cutoff Beam Pentode Tube", which consists of a kinescope gun and final anode enclosed in a smaller envelope. The dummy tube must be capable of dissipating, during such times as the picture tube is dark, all the energy the kinescope may utilize at full brightness. Fig. 1 shows, for illustrative purposes, a phase splitter that supplies a video signal to the dummy tube opposite in polarity to that supplied to the active kinescope. Thus when the current decreases in the kinescope, it increases in the

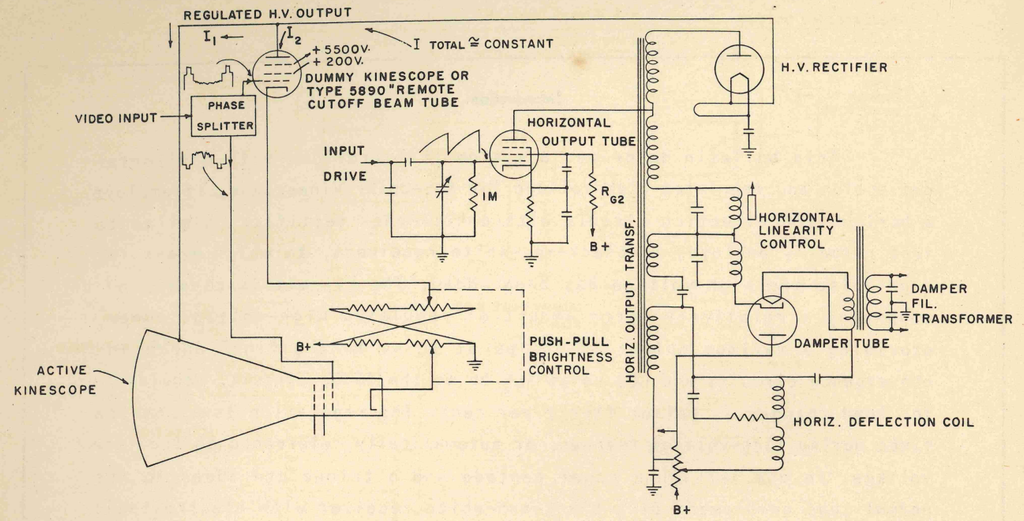

Fig. 1 – D–C type of dummy load tube controlled by inverted video and push-pull brightness potentiometer.

dummy tube so that the total remains unchanged. A push-pull brightness control is similarly employed.

Since the grid voltage-beam current characteristics of the kinescope and the 5890 pentode are not linear, the increase in current in the dummy tube may not fully match the current decrease in the kinescope unless the voltage applied to the grid of the dummy load tube is modified in accordance with these characteristics. Because of the additional circuitry required, this method of regulation was not further pursued.

The high-voltage rise occurring when the picture tube brightness is reduced may be used in another method of control. In this arrangement the rise which is within the regulation limits causes the beam current in the dummy load tube to increase and thus to keep the total drain constant. The resulting percentage regulation can be quite small since the change in output voltage can be kept to the minimum needed to control the dummy tube. This is a very small fraction of the final anode voltage and is usually less than 1 per cent.

Fig. 2 shows how a high-voltage corona regulator may be used to sense the rise in the high-voltage output and apply it to the dummy load tube. The characteristic of the corona regulator is similar to that of low-voltage regulators in that conduction rises sharply when the applied voltage increases above the designed starting voltage. Corona regulators are presently manufactured mainly for experimental applications and consequently are expensive. They are usually designed for low maximum current (less than 100 μa) and low power dissipation. Further information regarding corona regulators may be found in Naval Research Laboratory Bulletins 3140[1] and 3635[2].

If the picture tube brightness is reduced, the rise in high voltage above the starting level of the corona regulator in Fig. 2 appears mainly across the series resistor R_g, which is connected to the grid of the dummy load tube. This causes the dummy tube to conduct, thus effecting the regulation of the high voltage. This method of regulation tends to drain a constant total current from the high-voltage rectifier which reflects a constant load on the deflection circuit. Corona tubes having a

[1] NRL Report N-3140, "Voltage Stabilization by Means of The Corona Discharge Between Coaxial Cylinders" by H. B. Blifford, R. G. Arnold and H. Friedman, June, 1947.

[2] NRL Report 3635, "High Voltage Stabilization by Means Of The Corona Discharge Between Coaxial Cylinders" by S. W. Lichtman, March 13, 1950.

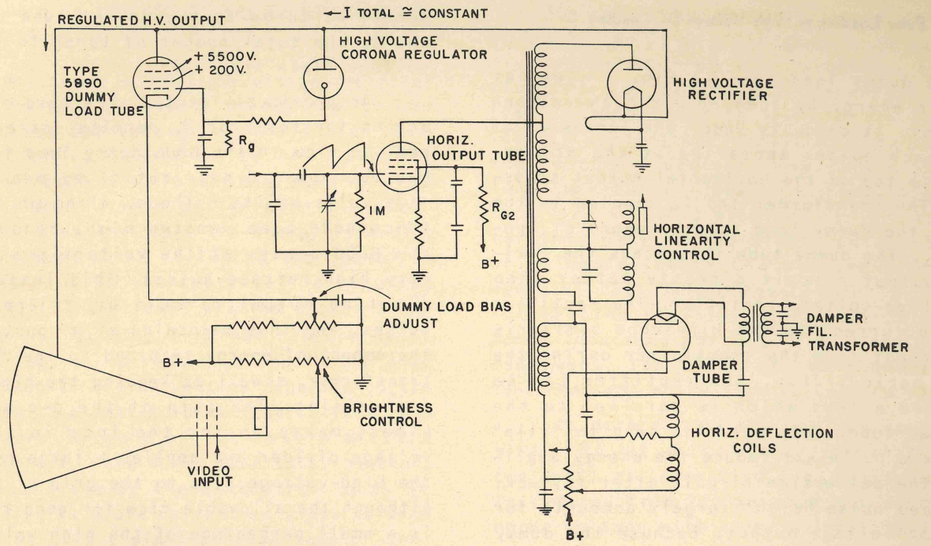

Fig. 2 – D–C type of dummy load tube controlled by high-voltage corona regulator.

good regulation characteristic and capable of larger dissipation have been built for experimental purposes and have served without the addition of dummy load tubes as high-voltage regulators with the characteristic of reflecting a constant total load to the deflection circuit. However, some difficulty was encountered with erratic behavior at high currents.

DC Amplifier Control of the Dummy Load

Fig. 3 shows an arrangement utilizing a commercially available triode in place of the corona regulator shown in Fig. 2 for control of the dummy load tube. A low-voltage d-c amplifier which senses the voltage rise appearing at a tap on a voltage divider connected to the high-voltage output is used for this purpose. The dummy load may be of the "beam current" variety such as the RCA 5890 pentode shown in Fig. 2 or of the pulse type shown in Fig. 4 and described below. When the kinescope beam current is reduced from its maximum value, the high voltage tends to rise. The rise is sensed at the grid of the d-c amplifier (12AX7) by means of the voltage divider. The cathode of the amplifier is biased positively with a fixed reference voltage which is the operating voltage of the neon tube. This initially keeps the amplifier near cutoff. With reduced beam current, the increased output voltage raises the grid of the d-c amplifier so that its plate current increases and causes the voltage across the resistor R_2 to rise. This increases current flow in the dummy load tube which also is initially biased near cutoff by means of the positive voltage applied to its cathode.

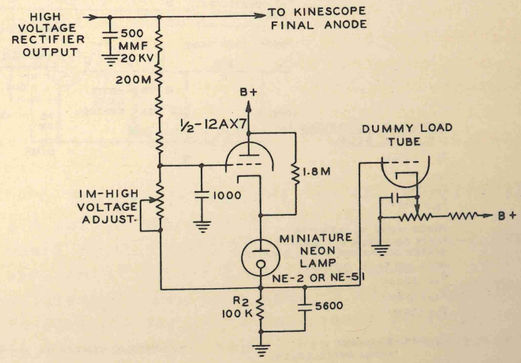

Fig. 3 – A d-c amplifier for control of the dummy load tube.

Pulse Loading vs High-Voltage DC Loading

The dummy load tube in Fig. 4 does not dissipate energy by loading the high-voltage d-c output. It conducts under the influence of the flyback pulses appearing at the driver-tube plate tap of the horizontal output transformer. The transformer tap is coupled to the plate of the dummy load tube by means of condenser C_1. The dummy tube thus loads the horizontal output circuit directly rather than via the high-voltage rectifier. The rectifier supplying current to the kinescope similarly draws current from the transformer during the flyback period. Thus, the rectifier can be considered a load which is parallel to the dummy load tube. Both circuits tend to "clip" the retrace pulse and reduce the energy available to the deflection circuit after flyback. The reduced pulse height largely accounts for lower high-voltage output. Because the dummy load tube is connected to a lower tap on the transformer, it must draw a larger current than the high-voltage rectifier to produce the same loading effect on the output circuit. This larger current should equal N_2/N_1 times the change in rectifier current. N_1 is the total number of turns to the driver-tube plate tap and N_2 the total number of turns to the high-voltage plate terminal.

As previously stated, the rise of voltage across the resistor R_2 permits increased current to flow in the 6BQ6 dummy load tube which has been biased near cutoff by means of the +105 volts on its cathode. Although the grid-to-cathode bias remains high, conduction in the 6BQ6 occurs at the voltage peaks of the very high retrace pulses. This loads the deflection output circuit by "clipping" the pulses, and thus maintains at a constant level the amount of energy returned to the deflection transformer, aswell as keeping the high voltage from rising. The gain of the d-c amplifier almost makes up for the loss in the high-voltage divider and applies a large portion of the high-voltage rise to the grid of the 6BQ6. Although the allowable rise for good regulation is a small percentage of the high voltage, the absolute amount is quite adequate for the 6BQ6 to produce enough loading to prevent the much greater voltage rise that would otherwise occur. In circuits where the peak voltage applied to the plate exceeds 5 kv or where the dissipation requirement is over 10 watts, a tube of higher

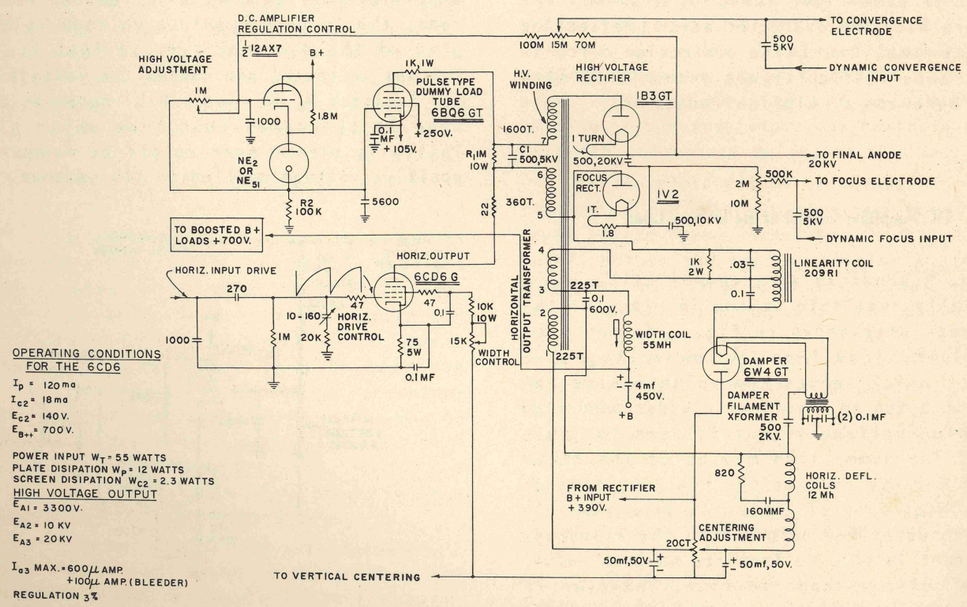

Fig. 4 – D. C. amplifier and pulse type dummy load tube regulator.

ratings, such as the 6BG6G, may be used as the dummy load tube.

Current flows in the high-voltage rectifier when the voltage of the pulse applied to the plate exceeds the voltage of the filter condenser which is connected to the cathode. Therefore, current flows only during that portion of the retrace period when the kickback pulse is at its peak. The energy remaining in the kickback pulse following the cessation of current flow in the rectifier is returned to the deflection circuit via the damper tube. The energy returned in this way produces part of the deflection current supplied to the yoke coils and boosts the B+ voltage supplied to the output tube. The peak-to-peak yoke current thus depends very largely on the return of this energy. Current in the dummy load tube, however, is not restricted by the d-ccontrol bias in this manner. Its plate current vs plate voltage characteristic is typical of a pentode in that the decrease in plate current is relatively gradual with the decrease in plate voltage. Thus when the control bias of the dummy load tube is reduced to effect regulation, the current flow in the first half of the retrace period loads the deflection circuit, reduces the peak voltage generated in the flyback pulse and prevents the rise in high voltage above the regulation level. Continued conduction after the voltage peak, however, tends further to reduce the energy returned to the deflection circuit and causes the picture width to decrease, even though the high voltage is regulated, and even though the output tube plate current tends to increase because of increased power losses.

To remedy this condition resistor R_1 and capacitor C_1 are added in series with the high-voltage winding. The dummy tube current develops a bias across the resistor and capacitor and restricts current flow more nearly to the period of the voltage peak. The bias developed also produces some regulating effect since it is applied to the high-voltage rectifier. The dummy load tube thus regulates by means of pulse loading, which is of primary importance in effecting regulation, and also by means of the bias applied to the rectifier. The bias developed in this manner should not exceed the maximum negative voltage rating of the dummy load tube.

The regulating action produced by the bias across R_1 and C_1 on the high-voltage output, as distinguished from that produced by pulse clipping, can be used to compensate for the loss in output due to the drop in the high-voltage winding and rectifier tube caused by the rectifier current flow. Since the dummy load tube current does not flow through the rectifier and this winding, it may compensate for this drop by additional pulse clipping, which would reduce the picture width, or by means of this supplementary bias produced by introducing resistor R_1 in the path of the dummy load tube current. With the latter arrangement, the width of the picture may be kept constant while high voltage is regulated.

In determining the optimum value of resistor R_1, it will be observed that if R_1 is too small or is omitted, and the beam current is reduced from its maximum value, the final anode voltage will nevertheless remain fairly constant because of the action of the d-c amplifier. However, the width of the picture would decrease, largely because of the reduced peak-to-peak deflection current. The dummy load tube, in its attempt to keep the high voltage constant, "clips" the retrace pulses by the amount required to regulate the high voltage but by continued conduction reduces energy available to the deflection circuit after flyback more than does the high-voltage rectifier when it is supplying full beam current. On the other hand, if R_1 is made too large the width of the picture increases with reduced brightness because the rectifier regulating bias is obtained with reduced pulse clipping, allowing more energy to be returned to the deflection circuit.

The Design of the Deflection Transformer

The remaining parts of the circuit are similar to those in deflection circuits commonly found in black-and-white receivers. The horizontal output transformer used is of the autotransformer type because closer coupling is possible for given inductance windings than in an isolation type. The transformer was designed to give greater second anode power and better regulation than normally produced

in such circuits. Since the initial regulation improves when the ratio of stored energy to dissipated energy is increased, the use of higher circulating power seemed desirable. The stored energy at the end of each sweep is given by $W_o = \frac{1}{2}L\hat{i}^2$ where L is the inductance reflected back to the yoke. This inductance includes the secondary inductance of the transformer which is in parallel with the yoke and which must be energized to the same peak-to-peak voltage. The peak current supplied to the parallel inductances is represented by $\hat{i}$. Thus, if a low-inductance transformer is used, and a substantial amount of power is circulated in it as well as in the yoke, an advantage is secured in regulation. Another alternative is to employ a yoke of relatively low deflection sensitivity (wide-angle yoke) so that a large peak deflection current and therefore large stored energy is utilized.

The deflection transformer shown in Fig. 5 was designed for use with the 45-degree (XT6875) tri-color tube deflection yoke having horizontal coil inductance of 15 mh. The transformer inductance was made low relative to the yoke--6.0 mh at the yoke tap. The leakage reactance is proportionately low in such an autotransformer. In contrast, the transformer inductance at the yoke tap in conventional circuits is considerably larger than the yoke inductance.

The low reflected inductance also permits the use of a high-voltage step-up winding to the rectifier which reflects a relatively large capacitance back to the yoke without resulting in an excessive retrace time. Thus with this arrangement the use of a single rectifier to produce the high-voltage output is possible. Before adding the regulator the high voltage at zero load is 27 kv. With a 700-μampere load it drops to 20 kv. The regulator is set at the lower level and prevents any voltage rise above this value when the beam current is reduced.

The design of the deflection transformer requires consideration of size, core losses, copper losses, and adequate insulation of the high-voltage coil. Fig. 5 shows a transformer design that was employed with the circuits shown in this bulletin. To obtain the required low value of inductance for a given size, a single U-shaped core was used instead of a

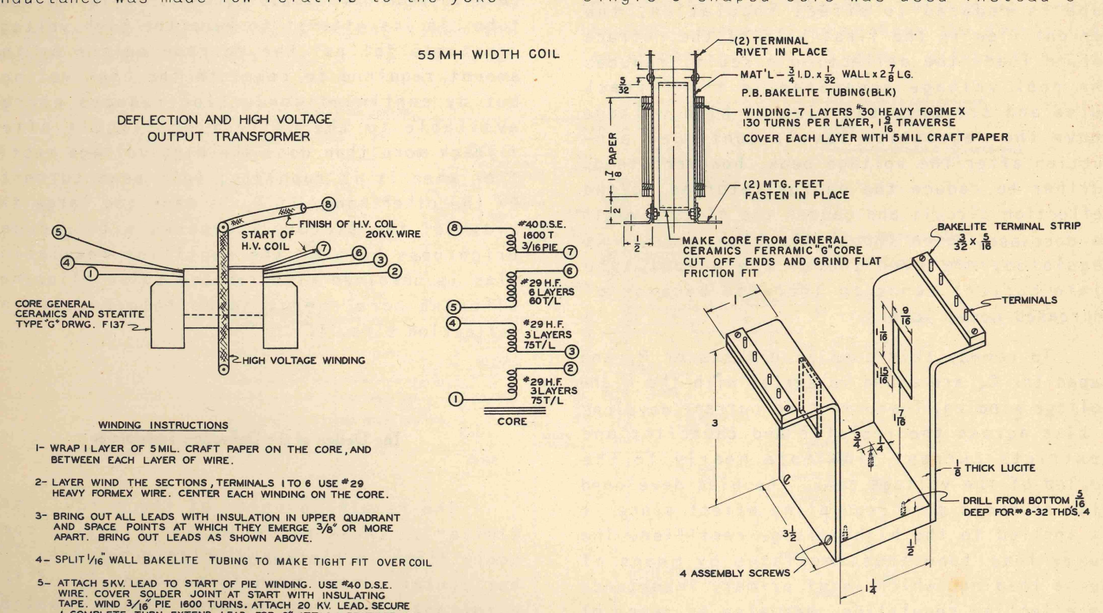
55 MH WIDTH COIL
DEFLECTION AND HIGH VOLTAGE OUTPUT TRANSFORMER
FINISH OF H.V. COIL
20KV. WIRE
START OF H.V. COIL
CORE GENERAL CERAMICS AND STEATITE TYPE "G" DRWG. F137-2
HIGH VOLTAGE WINDING
#40 D.S.E. 1600 T 3/16 PIE
#29 H.F. 6 LAYERS 60 T/L
#29 H.F. 3 LAYERS 75 T/L
#29 H.F. 3 LAYERS 75 T/L
CORE
(2) TERMINAL RIVET IN PLACE
MAT'L - 3/4 I.D. x 1/32 WALL x 2 7/8 LG.
P.B. BAKELITE TUBING (BLK)
WINDING - 7 LAYERS #30 HEAVY FORMEX 130 TURNS PER LAYER, 1 5/16 TRAVERSE
COVER EACH LAYER WITH 5 MIL CRAFT PAPER
7/8 PAPER
(2) MTG. FEET FASTEN IN PLACE
MAKE CORE FROM GENERAL CERAMICS FERRAMIC "G" CORE
CUT OFF ENDS AND GRIND FLAT
FRICTION FIT
BAKELITE TERMINAL STRIP 3/32 x 5/18
TERMINALS
1/8 THICK LUCITE
DRILL FROM BOTTOM 5/16 DEEP FOR #8-32 THDS. 4
4 ASSEMBLY SCREWS
WINDING INSTRUCTIONS
1- WRAP 1 LAYER OF 5 MIL. CRAFT PAPER ON THE CORE, AND BETWEEN EACH LAYER OF WIRE.
2- LAYER WIND THE SECTIONS, TERMINALS 1 TO 6 USE #29 HEAVY FORMEX WIRE. CENTER EACH WINDING ON THE CORE.
3- BRING OUT ALL LEADS WITH INSULATION IN UPPER QUADRANT AND SPACE POINTS AT WHICH THEY EMERGE 3/8" OR MORE APART. BRING OUT LEADS AS SHOWN ABOVE.
4- SPLIT 1/16" WALL BAKELITE TUBING TO MAKE TIGHT FIT OVER COIL
5- ATTACH 5 KV. LEAD TO START OF PIE WINDING. USE #40 D.S.E. WIRE. COVER SOLDER JOINT AT START WITH INSULATING TAPE. WIND 3/16" PIE 1600 TURNS. ATTACH 20 KV. LEAD. SECURE 1 COMPLETE TURN, EXTEND LEAD FOR 8" ATTACH RECTIFIER CAP. FOR UNIVERSAL 84B WINDING MACHINE USE DOUBLE THROW CAM AND 118/40 GEARS
6- COVER H.V. WINDING WITH A SMOOTH COAT HIGH TEMPERATURE MELTING POINT WAX. SUCH AS A.T. COMPOUND.
7- AFTER ASSEMBLY AFFIX THE HIGH VOLTAGE WIRE LOOPS FOR THE FILAMENTS OF THE RECTIFIERS FLUSH WITH LUCITE WALLS.

Fig. 5 - Deflection transformer and width coil construction.

pair as is normally employed to make a closed magnetic circuit. Thus the magnetic circuit is largely through air. The use of the corepermits a reduction of the number of turns and the amount of copper required for the desired inductance and therefore minimizes copper losses. Further reduction in the number of turns and the use of both cores was not feasible because of increased core losses due to saturation. Furthermore, enclosing the high-voltage coil in the relatively small window space of a pair of commercially available cores introduces serious insulation problems. However, cores of greater cross-sectional area and with windows larger than conventional may be used, but result in a larger transformer. The single core with the coil windings on it was mounted in a compact lucite transformer housing. This construction allows for adequate clearance and insulation surrounding the high-voltage coil, which operates with 20-kv pulse voltage, and thereby avoids corona and breakdown which otherwise would be a danger.

While the coils shown in Fig. 4 are wound directly on the core they may be wound on a close-fitting round coil form if the end of the core is first cut off and then cemented in place during assembly. Alternatively, a cylindrical ferrite core of equivalent reluctance may be substituted for the U-shaped core.

The transformer coil information for the circuit shown in Fig. 4 is given in Fig. 5. Similar transformer coils are used in Figs. 7 and 9 except for the number of turns, which is shown on these drawings. These result in more deflection when operating with lower B+ voltage, but supply somewhat reduced high voltage.

The output-tube grid drive should be adjusted almost to the point of picture foldover. The picture width and the high-voltage power output are at a maximum whereas the driver tube and damper tube currents are at a minimum value. To decrease these currents further, the transformer inductance may be increased. This may be done by adding pieces of ferrite about 1 inch long to one or both ends of the core. The reduction of power input in the latter case, however, results in less high-voltage power, but greater picture width. The circuits shown in Figs. 4, 7 and 9 should be adjusted so that the damper tube and driver tube currents are within tube ratings.

In addition, the width coil, shown in Fig. 4 in shunt with the yoke, may be used in conjunction with the output tube screen grid voltage control for adjusting picture width. The construction of the width coil is shown in Fig. 5. It stores a portion of the total circulating energy of the deflection circuit. When the shunt inductance is decreased, by moving the core partially out of the coil, the picture width is reduced, but the output-tube plate current and the available high-voltage power are increased. On the other hand, when the screen-grid voltage is decreased, the picture width as well as the output tube plate current and the available high-voltage power are reduced. By adjusting both the inductance and the screen-grid voltage, the picture width can be set as desired while maintaining the high-voltage power output, and keeping the driver tube and damper tube currents within ratings.

The lower section of the output transformer is used for centering, and both this section and the yoke operate at B+ potential. The width coil however, operates at the boosted B+ voltage. This voltage, which is available from the lower end of the width coil, is used as the plate supply for the horizontal and vertical blocking oscillators and is also supplied to the kinescope screen grids. The width coil may be replaced by a 100 K (5 watt) resistor with some sacrifice in boosted B+ voltage, and high-voltage power output.

This method of adjusting the circuit may be used to determine experimentally the design values of the components to be employed in a horizontal deflection and regulated kick-back high-voltage supply circuit of this type. A trial transformer, whose inductance can be varied by adding core sections is used. The output tube, the damper tube and B+ supply for this test, should be more than adequate to deliver the desired peak-to-peak current to the yoke coils, as well as the additional current to be circulated in the low-inductance transformer and width coil. The circuit is adjusted so that the yoke current is suitable for full width at the design value of the final anode voltage, and the deflection transformer and width coil are circulating enough additional power to yield the desired high voltage when second anode current is increased to the desired maximum value. The circulating current can now

be measured and then the required transformer inductance and the inductance of the width coil, if one is to be used, can be determined. Similarly the output tube, the damper tube, and the B+ supply necessary to circulate this current can be selected. The means for regulating the high voltage are then added to the circuit.

The power circulated is greater in the circuits illustrated than in conventional circuits in order to increase the high-voltage power output. Nevertheless, it is supplied by means of a tube complement no greater than the minimum commonly used for black-and-white receiver deflection circuits, except for those added for regulation. The total power input required for deflection and high voltage is substantially less than if an r-f supply is employed for the high voltage. The total plate and screen current is 140 ma when the B+ supply is 390 volts. Note that the 6BQ6 is used in this circuit, and in the circuit shown in Fig. 7, in a manner for which tube ratings are not available. Further experience is needed at this time to determine whether the tube is suitable for this purpose. It may be replaced by a 6BG6G for more conservative design.

Gating Amplifier Control of the Dummy Load

A gating pulse amplifier is shown in Fig. 6 that may be used in place of the d-c amplifier shown in Figs. 3 and 5. The gain of the 12AT7 gating amplifier is varied by the d-c voltage applied to its grid. The grid voltage in turn depends upon the high-voltage output and also upon the 135-volt negative supply because of the voltage divider connecting these points in the circuit. Thus the negative supply serves the same purpose as the fixed bias voltage supplied by the neon tube connected to the cathode of the 12AX7 in Fig. 3. The divided high voltage must exceed the bias of the negative supply, to put the gating amplifier in operation. It will be noted, however, that now the bias is not fixed, but varies with line voltage since it is supplied from a nonregulated source. Thus the high voltage is regulated at a level that depends upon line voltage rather than being independent of it. This feature is desirable in receivers using unregulated B supplies. When the line voltage drops, the B+ voltage delivered to the deflection circuit in such receivers drops accordingly. This would normally result in a decrease in both vertical and horizontal deflection. Also under these conditions the high-voltage supply would not be capable of delivering the normal peak current at the nominal final anode voltage and loss of regulation, change of picture size and some defocusing would result at peak picture brightness. In addition, in some tri-color tube receivers the lower B+ may reduce the output of the dynamic convergence circuits with possible color separation. When the regulation level follows line voltage, the changes in picture size and the possibility of deconvergence of the three beams in the tri-color tube can be minimized. Similarly, with reduced line voltage if the high-voltage regulating level is adequately reduced, a higher peak beam current can be supplied with good regulation when brightness is varied.

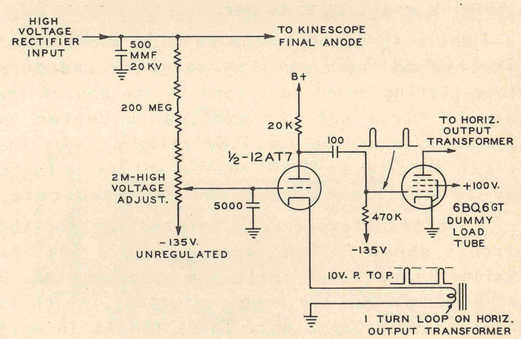

Fig. 6 – A gating pulse amplifier for control of the dummy load tube.

In the arrangement shown in Fig. 9 the bias voltage for the gating pulse amplifier is obtained from the grid of the blocking oscillator. This method may be applied to the circuit in Figs. 6 and 7. The grid self bias of the blocking oscillator was found to vary with line voltage and was used in place of a negative supply which was not available in this receiver. The high-voltage divider connected to the grid of the blocking oscillator should be sufficiently high in resistance not to upset the normal operation of the oscillator. If, in an alternative arrangement, the cathode of the gating pulse amplifier returns through the winding that pulses it to B+, and the low end

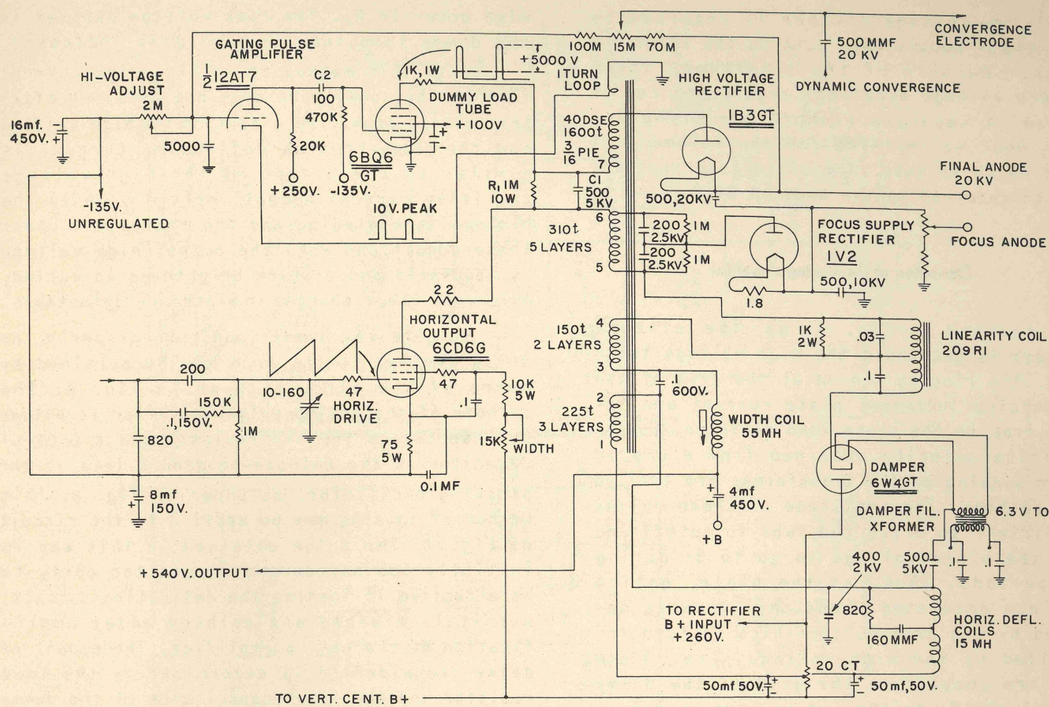

Fig. 7 – The gating pulse amplifier and pulse type dummy load tube regulator.

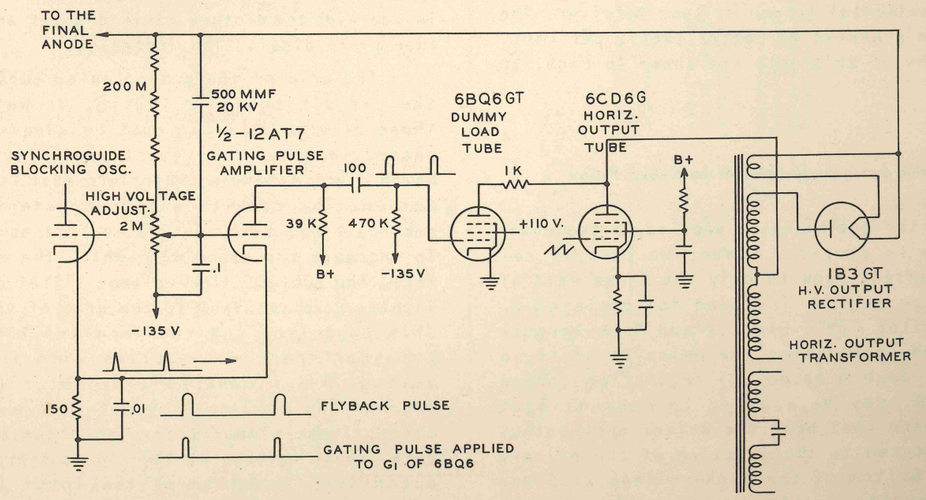

Fig. 8 – A method for gating the pulse amplifier during the first half of the flyback period.

of the high-voltage divider is returned to ground, the B+ supply then acts as the reference voltage. Because of the relatively large reference voltage excellent regulation can be achieved. A separate transformer or heater winding must be employed for the filament of the gating pulse tube. The plate load resistor should be returned to the boosted B+.

Operation of the Gating Amplifier

Referring to Fig. 7, as the picture brightness is decreased the high voltage tends to rise. The rise is sensed at the grid of the 12AT7 causing increased plate current and increased drop in the plate load resistor. Pulses of positive polarity obtained from a one or two turn winding on the transformer are applied to the cathode. The amplitude of these pulses is sufficient to drive the tube to cutoff and causes the plate voltage to go to B+ during these periods. Thus, at the plate, gating pulses are generated whose amplitude is determined by the grid voltage which in turn is controlled by the high-voltage rise. These pulses are coupled to the grid of the dummy load tube via C_2 causing it to conduct during this period and thereby to effect the regulation desired.

The circuit shown in Fig. 7 is being used in an experimental tri-color tube receiver. The regulation achieved is better than 2 per cent. Photographs of this unit are shown in Figs. 10 and 11.

Gating during the First Half of the Flyback Period

When the gating pulse applied to the dummy load tube is properly timed, so that it restricts current flow to only the first half of the retrace period. The need for resistor R_1 and capacitor C_1 in Figs. 4 and 7 is largely eliminated, permitting the omission of these elements. Such a method of regulation, shown in Fig. 8, may be applied to conventional transformers that have the driver tube output lead connected to the junction of the primary with the bottom of the high-voltage winding. The high-voltage output obtainable at full load is increased by the drop that would otherwise occur in R_1. The peak voltage applied to the dummy load tube is similarly increased.

With this method of pulsing, the current flow in the dummy tube does not continue after the voltage peak. Its effect on the high voltage and the peak-to-peak deflection current is similar to the effect of the high-voltage rectifier current except for the drop in the high-voltage winding and the rectifier. Under these conditions when the output high voltage is regulated and picture brightness is varied, only very minor changes in width are detectable.

To gate the dummy load tube properly the pulse applied to its grid may be obtained by means of the circuit shown in Fig. 8. The cathode of the gating-pulse amplifier is pulsed by inserting a 150-ohm resistor and a 0.01-µf capacitor in the cathode-to-ground lead of the blocking oscillator, as shown in Fig. 8. This method of pulsing may be applied to the circuit of Fig. 7. The pulse obtained in this way is initially too narrow and occurs too early to be effective in loading the deflection circuit, but it is widened and delayed after amplification by the gating amplifier. The amount of delay and widening is determined by the load resistor and the input capacitance of the dummy load tube. A plate load resistor of 39 K was found optimum in one circuit. Should the pulse be inadequately widened it is ineffective in producing regulation. On the other hand, if it is too wide the picture width changes and driver tube plate dissipation increases.

The grid of the gating pulse amplifier in the circuit shown in Fig. 8, as well as in those previously shown must be adequately bypassed in order to prevent capacitive pickup which might otherwise interfere with its control action. The resulting time constant of the control circuit may not be as fast as desired. To increase the speed with which the regulator acts, the 500-µµf high-voltage filter capacitor in Fig. 8 is returned to the grid of the 12AT7. This capacitor and the parallel 200-megohm resistor are now in series with the high-voltage adjustment potentiometer (about 1 megohm) and the parallel 0.1-µf bypass capacitor. These elements form an attenuator network, whose voltage at the tap is approximately a constant fraction of the input from the high-voltage rectifier, for both d-c and low- and high-frequency voltage changes.

Deflection Systems with Regulated Kickback High-Voltage Supplies for Tri-Color Kinescopes

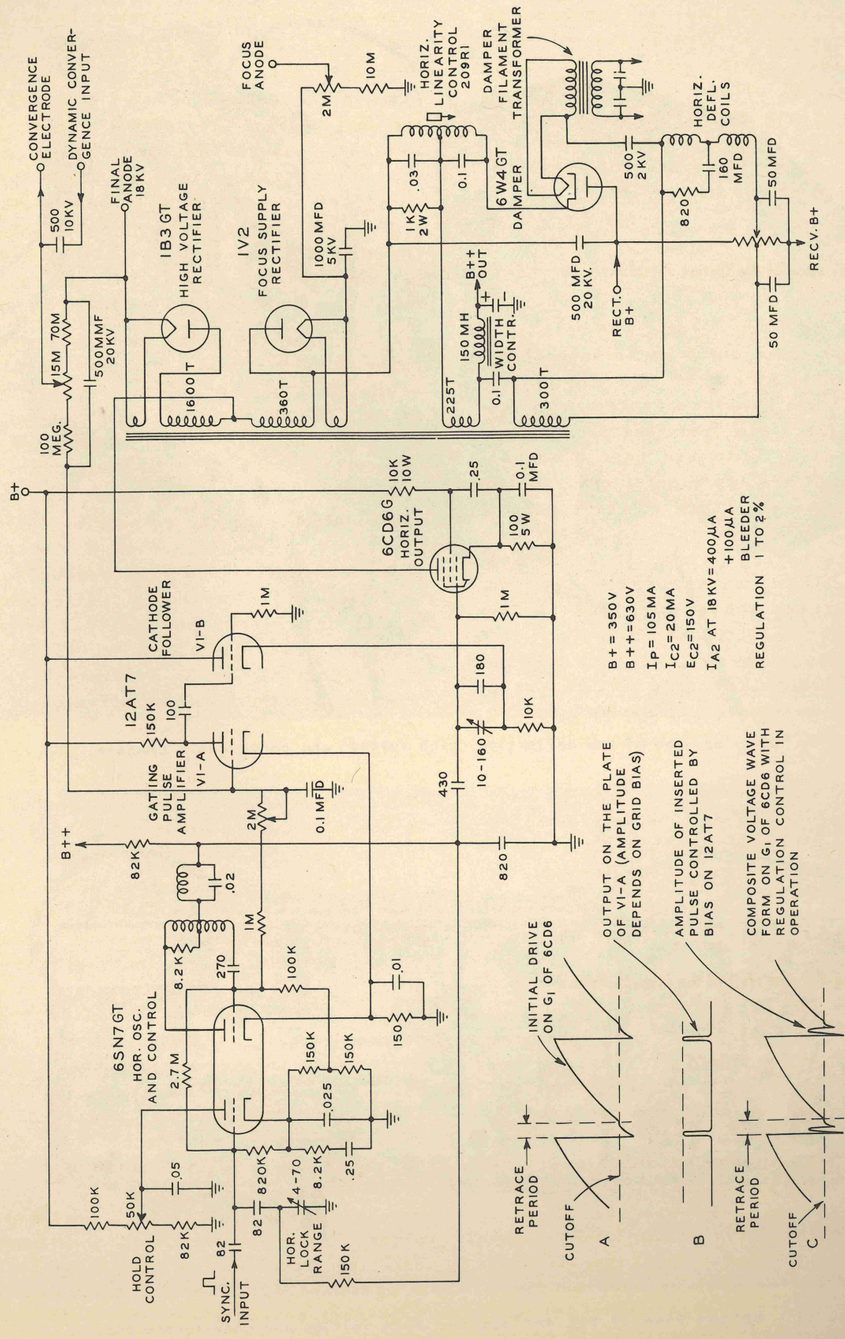

Fig. 9 – Regulated high voltage pulse supply with the dummy load tube eliminated.

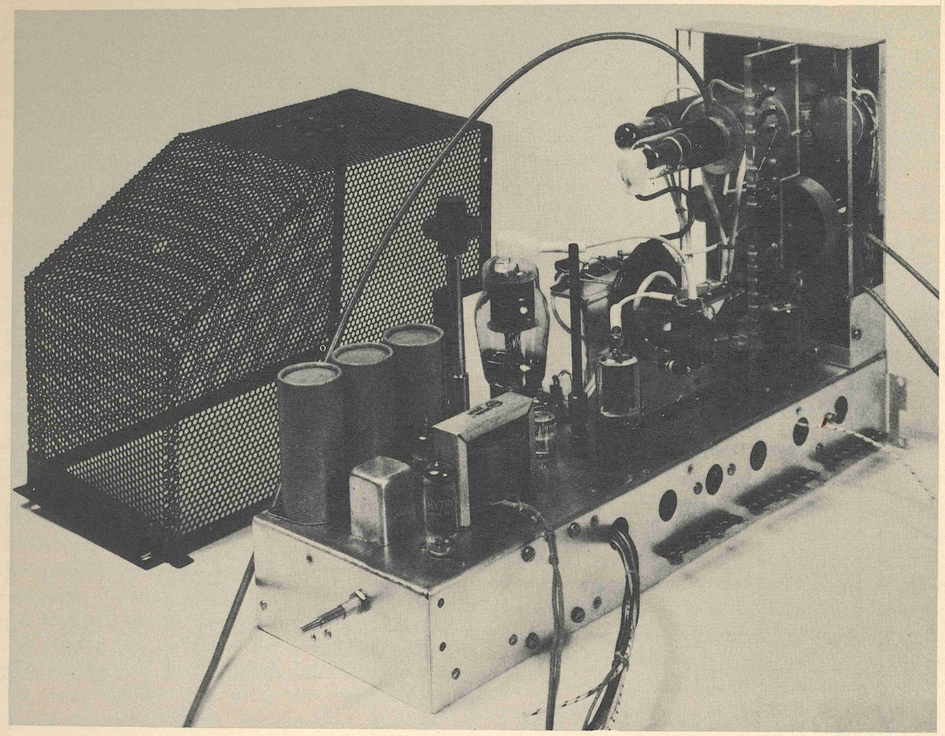

Fig. 10 – Top view of the deflection, high voltage and convergence chassis.

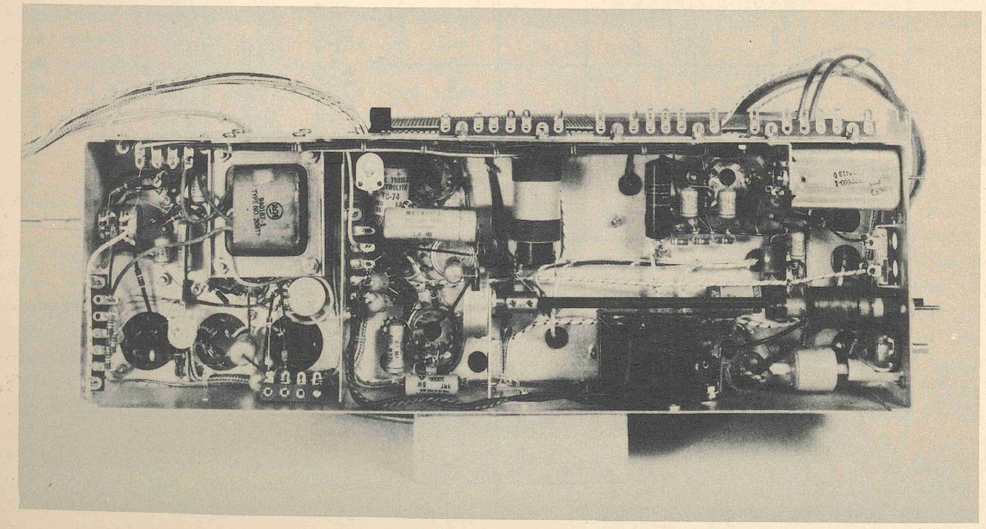

Fig. 11 – Bottom view of the deflection, high voltage and convergence chassis.

Elimination of the Dummy Load Tube

In the circuit shown in Fig. 9 the dummy load tube has been eliminated. The horizontal output tube now serves as the driver for the deflection circuit during the go sweep and as a dummy load tube during retrace. A gating pulse of appropriate width, timing, and amplitude is super-imposed upon the sawtooth input signal at the grid of the driver tube by means of a gating pulse amplifier and a cathode follower. One dual triode is employed for this purpose. In conventional circuits the horizontal output tube is normally cut off during the flyback period. In this circuit it is made to conduct by a pulse added to the input signal shortly after it is initially cut off by the sawtooth drive. This causes it to clip the retrace pulses and to prevent high-voltage rise in the manner of the separate dummy load tube.

Since the dummy load current can no longer be made to flow in a separate path from that of the driver-tube plate current, the resistor R_1 and capacitor C_1 cannot be used. A small change in width, with full change in brightness, may be detected even though the high voltage is regulated. The change in width, however, is substantially less than with non-regulated supplies.

Note that the plate dissipation of the horizontal output tube is now increased by the amount of power formerly absorbed by the separate dummy load tube. When a dark picture is presented, the additional plate dissipation equals the power supplied to the high-voltage rectifier at peak picture brightness. Satisfactory life of the output tube may be impaired if the total dissipation is allowed to be excessive. The 6CD6 plate dissipation, in the circuit shown in Fig. 9, may be somewhat excessive for the condition of picture-tube cutoff, but this circuit is nevertheless presented for purposes of illustration. This arrangement may be used in circuits in which the plate dissipation of the output tube is originally sufficiently below the maximum allowable dissipation to permit it safely to absorb the additional high-voltage power. If the 6CD6 in Fig. 9 is replaced by two 6BG6's, the total maximum allowable plate dissipation is increased from 15 to 40 watts. The peak high-voltage power output and the yoke deflection available in the circuit of Fig. 4 can be obtained with substantially lower B+ voltage (300 volts). In circuits where the damper tube current is increased above the allowable maximum for the 6W4, it must be replaced by two damper tubes.

Morris D. Nelson

Morris D. Nelson

LB-907

A STUDY OF TRANSISTOR CIRCUITS FOR TELEVISION RECEIVERS

Property of
Albert E. Linden

RADIO CORPORATION OF AMERICA
RCA LABORATORIES DIVISION
INDUSTRY SERVICE LABORATORY

RADIO CORPORATION OF AMERICA
RCA LABORATORIES DIVISION
INDUSTRY SERVICE LABORATORY

LB-907

A Study of Transistor Circuits for Television Receivers

This report is the property of the Radio Corporation of America and is loaned for confidential use with the understanding that it will not be published in any manner, in whole or in part. The statements and data included herein are based upon information and measurements which we believe accurate and reliable. No responsibility is assumed for the application or interpretation of such statements or data or for any infringement of patent or other rights of third parties which may result from the use of circuits, systems and processes described or referred to herein or in any previous reports or bulletins or in any written or oral discussions supplementary thereto.

Approved

Stuart W. Seeley

A Study of Transistor Circuits for Television Receivers

Introduction

This bulletin describes a general study of transistors in television receivers. For this purpose, the development of a completely transistorized television receiver was undertaken. An experimental model using 37 transistors and a 5-inch kinescope, housed in a plastic cabinet 13 x 12 x 7 inches, was constructed. This portable receiver operates on a single channel using a self-contained loop, and has a total battery-power consumption of 13 watts, more than 25 per cent of which is consumed by the kinescope heater.

The development of a complete experimental receiver, even with a number of compromises, provided an opportunity to deal with the problems found in every stage and circuit of the receiver. Although experimental point-contact transistors have recently been developed which will provide oscillations for the entire v-h-f television band, considerable difficulty was found in providing wide-band r-f gain using transistors at these frequencies. This problem was much less difficult at intermediate frequencies and at the intercarrier-sound frequency. The second-detector problem of obtaining high rectification efficiency with low load impedances was solved by using a transistor detector. The video amplifier problem was complicated by the requirement for a high input impedance; however, with a combination of junction and contact transistors a stable, high gain video amplifier with a relatively high input impedance was built. An audio system using complementary symmetrical junction transistors was designed to produce high output with good efficiency.

In the synchronization and deflection portion of the receiver circuits were devised for using transistors in ways which differ from the analogues of amplifier tubes. A single transistor was used as a d-c setter, sync separator and sync amplifier. A simple and reliable horizontal a-f-c system was developed by utilizing the symmetrical properties of transistors. Point-contact transistors were found to be particularly economical pulse and sawtooth oscillators. The complementary symmetry principle was used to provide vertical deflection with high linearity and efficiency. In the horizontal deflection circuits, the fast high-current switching ability of transistors was used advantageously. An efficient circuit using the symmetrical property of the transistor, which has no analogue in electron tubes, was devised for horizontal deflection.

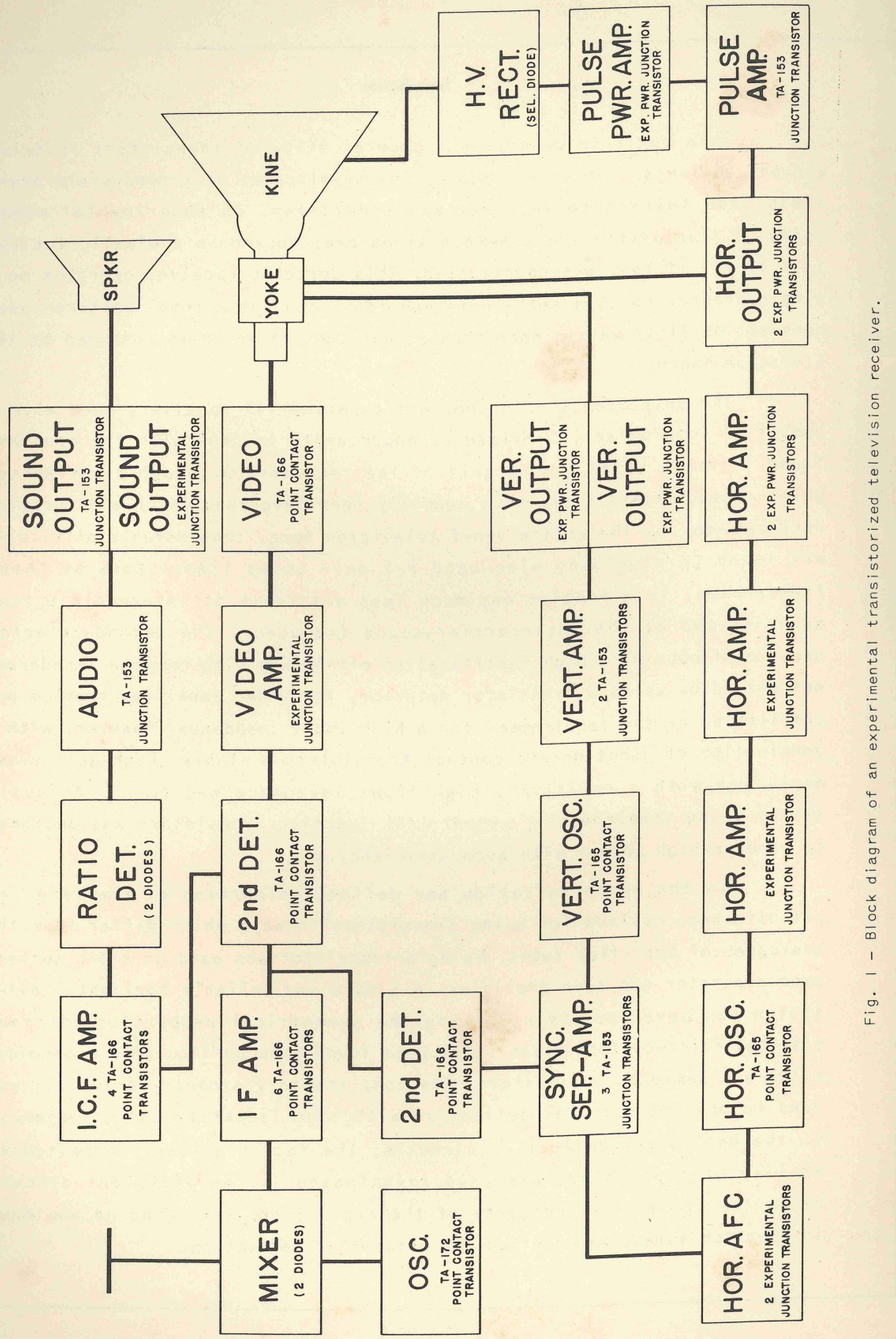
H.V. RECT. (SEL. DIODE)
PULSE PWR. AMP. EXP. PWR. JUNCTION TRANSISTOR
PULSE AMP. TA-153 JUNCTION TRANSISTOR
KINE
SPKR
YOKE
HOR. OUTPUT 2 EXP. PWR. JUNCTION TRANSISTORS
SOUND OUTPUT TA-153 JUNCTION TRANSISTOR
SOUND OUTPUT EXPERIMENTAL JUNCTION TRANSISTOR
VIDEO TA-166 POINT CONTACT TRANSISTOR
VER. OUTPUT EXP. PWR. JUNCTION TRANSISTOR
VER. OUTPUT EXP. PWR. JUNCTION TRANSISTOR
HOR. AMP. 2 EXP. PWR. JUNCTION TRANSISTORS
AUDIO TA-153 JUNCTION TRANSISTOR
VIDEO AMP. EXPERIMENTAL JUNCTION TRANSISTOR
VERT. AMP. 2 TA-153 JUNCTION TRANSISTORS
HOR. AMP. EXPERIMENTAL JUNCTION TRANSISTOR
RATIO DET. (2 DIODES)
2nd DET. TA-166 POINT CONTACT TRANSISTOR
VERT. OSC. TA-165 POINT CONTACT TRANSISTOR
HOR. AMP. EXPERIMENTAL JUNCTION TRANSISTOR
I.C.F. AMP. 4 TA-166 POINT CONTACT TRANSISTORS
IF AMP. 6 TA-166 POINT CONTACT TRANSISTORS
2nd DET. TA-166 POINT CONTACT TRANSISTOR
SYNC. SEP-AMP. 3 TA-153 JUNCTION TRANSISTORS
HOR. OSC. TA-165 POINT CONTACT TRANSISTOR
MIXER (2 DIODES)
OSC. TA-172 POINT CONTACT TRANSISTOR
HOR. AFC 2 EXPERIMENTAL JUNCTION TRANSISTORS

Fig. 1 - Block diagram of an experimental transistorized television receiver.

Signal Channel

The first part of this bulletin treats the signal channel consisting of the mixer, the intermediate-frequency amplifiers, the second detector, the sound channel and the video amplifier. The second part treats the deflection channel including the synchronizing and deflection circuits and the high voltage generator. A block diagram of the receiver is shown in Fig. 1.

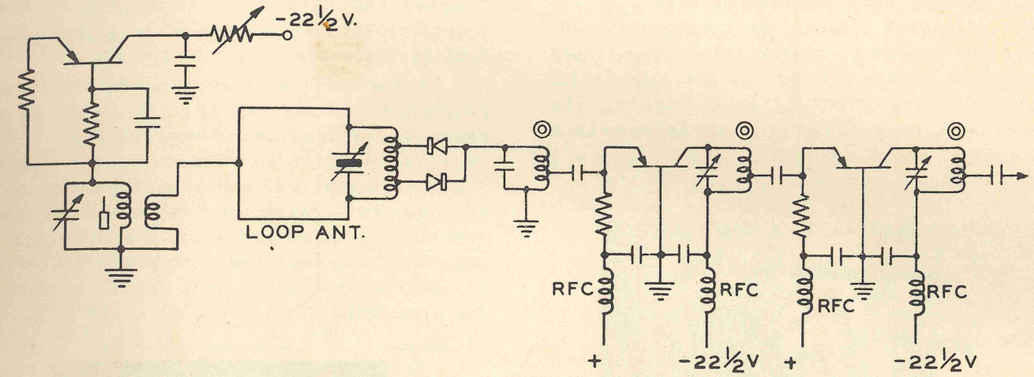

Fig. 2 - Schematic of local oscillator, mixer, and first IF amplifier.

The signal is picked up by a loop antenna, mixed with the local oscillator in a pair of crystal diodes, and the resulting difference signal amplified by six stages of grounded-base point-contact transistors. Two second detectors provide independent signals for the sync and video amplifiers. Intercarrier sound from the video second detector is amplified by four intercarrier frequency stages and demodulated by a ratio detector. The resulting audio signal is applied to an emitter follower stage driving a complementary type push-pull output stage.[1]

The video signal is amplified by a system combining the higher input impedance of a grounded emitter junction transistor with the high-frequency response of a point-contact type.

The tuned loop antenna was decided upon after a comparison of various antenna types which could be included in a case only 12 x 13 x 7 inches. The tuning capacitor is located at a break in the loop at the middle of the front side. To provide a means of impedance matching to the mixer diodes, a coil is used in shunt with the loop and tuning capacity. The combination of the loop and coil have an inductance of approximately one-half microhenry allowing a larger minimum tuning capacity. Optimum power transfer to the mixer diodes is achieved by connecting the diodes to balanced taps at an intermediate impedance point on the coil.

The local oscillator employs a type TA-172 point-contact transistor designed for high-frequency oscillator use.[2] The oscillator circuit provides a signal at 60 Mc for mixing with the Channel 4 carrier of 67.25 Mc. The local oscillator signal is coupled to the midpoint of the loop by a two-turn pickup coil wound over the oscillator tank.

The mixer circuit consists of two 1N54A crystal diodes in a balanced arrangement as shown in Fig. 2. The difference frequency is impedance matched to the first i-f amplifier by a tuned circuit which has a tapped coil. This 50-microhenry coil is wound on a ferrite toroid. By the use of the ferrite toroids for all coils in the tuned i-f stages, the effect of stray magnetic fields is reduced and shielding problems minimized. Large impedance transformation ratios are easily obtained because of

[1] LB-906, *Symmetrical Properties of Transistors and Their Application.*

[2] LB-867, *The Control of Frequency Response and Stability of Point-Contact Transistors.*

the high coupling coefficient obtainable. With a total diode mixer current of 1 milliampere the mixer circuit gain is -6 db or a 2 to 1 loss of signal voltage.

For simplicity the i-f amplifiers are stagger tuned. Each of the i-f amplifier stages consists of a point-contact transistor, type TA-166, operated in a grounded-base circuit. The collector of one stage is matched to the succeeding stage by a tapped coil similar to that previously mentioned. Collector voltage is supplied by a 22½-volt battery common to the entire receiver but decoupled by an L-C filter in each collector circuit. No attempt was made to keep the impedance of the collector circuit high outside of the bandpass as the type TA-166 transistors are short-circuit stable. The emitter bias was fixed at approximately 1 milliampere and supplied by a penlite cell battery. The photograph of one of the i-f stages in Fig. 3 shows the ferrite toroid used in the interstage tuned circuits.

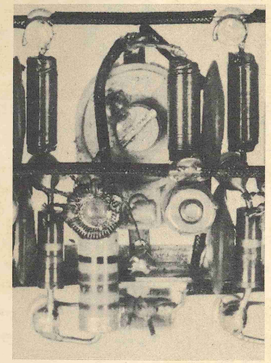

Fig. 3 - Close-up of ferrite toroid coil in i-f stage.

Overall power gain of the six stages and the second detector in the band pass shown in Fig. 4 is 47 db. The markers shown are at 5 Mc and 10 Mc showing the rising characteristic between 6.5 and 7.5 Mc and the flat top between 7.5 and 9.5 Mc.

The second detector presented a problem because of the relatively low input impedance of the video amplifier. The first proposal was a crystal detector, but because of the low impedances involved, the rectification efficiency was extremely low. Severe negative peak clipping occurred since the a-c load resistance was comparable or even less than the d-c load of the crystal rectifier. The logical step was to use a transistor as the detector.

The last i-f transformer is different from the preceding ones in that it has two windings and is double tuned. The second winding is tapped and feeds the emitter of the detector transistor, a point-contact type TA-166. This transistor does not have any bias applied to its emitter, the low side of the secondary winding being connected to ground. The emitter-base electrodes in the transistor act as a crystal rectifier, the resulting rectified signal appears in the collector circuit amplified by the current gain of the transistor.

Since the rectified signal is internally coupled to an amplifying part of the circuit there is no problem of keeping the d-c load resistance small in respect to the a-c load and hence negative peak clipping problems are avoided and a resulting improvement in rectifier efficiency is obtained. The collector load impedance was kept small to avoid the effects of the frequency-dependent input impedance of the video amplifier.

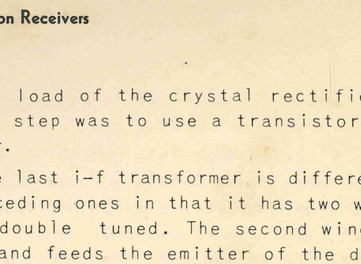

Fig. 4 - Frequency response of video amplifier.

The video amplifier was one of the first units of the receiver built and consequently was completed before other parts of the receiver were started. This presented the problem of building an amplifier to work from an unknown source impedance. Since junction transistors which could serve as video amplifiers were not then available, it was necessary to use a point-contact type of transistor in the amplifier to get sufficient high-frequency response. Unfortunately, point-contact transistors are most successfully used in a grounded-base circuit in which they have very low input impedance. To overcome this problem of low

input impedance, a selected junction transistor was used in a base input circuit to drive the emitter of a point-contact unit as shown in Fig. 5.

The low-frequency voltage gain of the amplifier is 20 and the video response is shown in Fig. 6. The response of the basic amplifier with no equalization is shown in (a). The addition of a conventional video peaking coil (L_3) in the collector circuit of the contact unit alters the response as shown in (b). Further equalization is accomplished by the degenerative feedback provided by the resistance (R_1) in the emitter of the junction unit (c). The high output impedance of the junction unit permits the use of positive feedback in the base of the point-contact unit and the effect of this feedback provided by R_2 and L_2 is shown in (d). The result of bypassing R_1 at 1 Mc with a low-Q series resonant circuit is illustrated in (e). In all photographs the marker is at 2 Mc and the source impedance of the input signal generator is 1000 ohms.

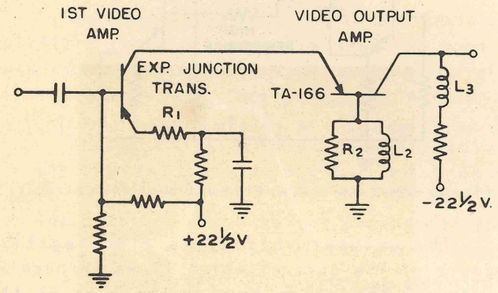

Fig. 5 - Video amplifier.

The use of a point-contact transistor in the output stage limited the voltage swing obtainable consistent with good frequency response and limited power dissipation. With the 2700-ohm load resistance used, the bias was adjusted to allow an 8-volt peak-to-peak swing in the output, since previous measurements had shown that this value was adequate to provide good picture contrast. However, in later operation of the amplifier it was found desirable to utilize all of this allowable swing for actual picture signal and consequently the sync pulses were permitted to drive the amplifier into the saturation region.

Because of this sync crushing it was necessary to provide a separate sync amplifier. To prevent this amplifier from loading the second detector excessively, a separate second detector was provided. This detector, which is similar to the video detector, is fed from a lower impedance tap on the driving transformer, thereby taking less of the available signal power. The sync amplifier is described later in connection with the deflection circuits.

A sound take-off trap is located in the video-detector circuit and provides the intercarrier-sound signal which is amplified by four stages tuned to the intercarrier frequency, 4.5 Mc. The first three of these stages are similar to the picture amplifier stage except that they are not stagger tuned, but peaked to 4.5 Mc. The fourth stage drives a standard ratio-detector transformer modified to operate from a lower source impedance. The demodulator has a peak separation of 120 kc and gives an audio output signal on the order of a volt.

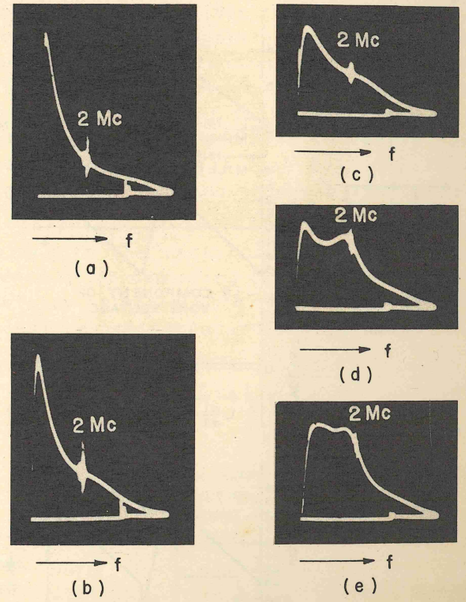

Fig. 6 - Frequency response of video amplifier.

This signal is amplified by a system of unusual design. An emitter follower circuit is used to drive a combination of a p-n-p and n-p-n transistor in the output circuit. This combination utilizes the complementary symmetry properties described in LB-906[1].

Deflection and Synchronization

The deflection and synchronization circuits are described in the following sections in the order in which they were developed, rather than in the order shown on the block diagram. This procedure is followed to indicate the manner in which the several circuits were evolved.

Vertical Deflection

The equivalent circuit of the vertical yoke consists of a resistance of 65 ohms in series with an inductance of 45 mh. A peak-to-peak current of 100 ma is required to deflect the beam three inches--the proposed picture height. Fig. 7 shows the ideal waveforms necessary to obtain linear deflection.

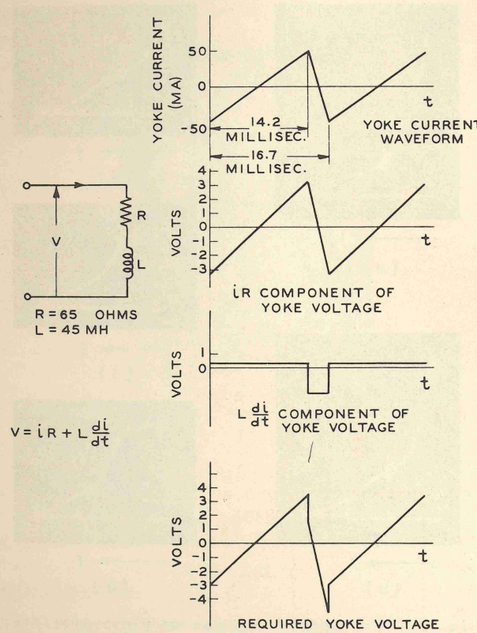

Fig. 7 - Theoretical vertical yoke waveforms

The waveform to energize the yoke is obtained from a synchronized relaxation oscillator using one TA-165 point-contact transistor. The operation of this circuit may be briefly described with reference to the simplified schematic shown in Fig. 8. The application of voltage causes the base of the transistor to assume a negative potential equal to the product of the base resistor, R_3, and the leakage current across the collector rectifying contact. (Appendix A)

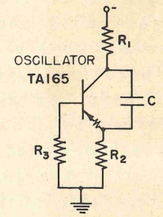

Fig. 8 - Vertical oscillator.

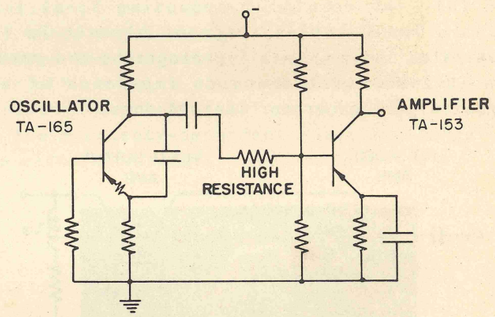

Fig. 9 - Vertical oscillator and amplifier circuit.

The emitter voltage is also negative because of the current which flows through R_2 to charge the capacitor, C. As long as the emitter is more negative than the base, the conduction through the emitter-collector path of the transistor is negligible. As the capacitor becomes charged, however, the leakage current increases while the charging current through R_2 falls off exponentially. Eventually a point is reached when the emitter is positive with respect to the base. The capacitor then begins to discharge through the emitter-collector path. Since the current gain of the transistor is greater than unity, the base current increases faster than the emitter current and the action becomes self-sustaining and continues until the capacitor is discharged. The cycle is then repeated. Synchronization is accomplished by applying positive pulses to the emitter at a rate somewhat faster than the free-running rate. The voltage waveform across R_1 is shown in Fig. 10a. The ratio of sawtooth to pulse may be altered by changing the ratio of the collector resistance to the emitter resistance.

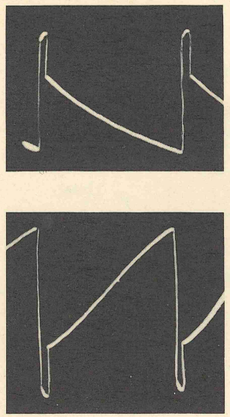

(a) Vertical oscillator output

(b) Vertical yoke voltage

Fig. 10 - Waveforms.

In coupling the oscillator to a transistor amplifier, it is necessary to meet two conditions if the amplifier output is to be an undistorted replica of the generated waveform:

(1) The loading effect of the amplifier on the oscillator must be negligible.

(2) The amplifier must be fed from a current rather than a voltage source.

The first of these arises because of the reactive output impedance of the oscillator. Any loading of the oscillator therefore not only attenuates the output but also alters the shape of the waveform. The second condition is imposed because of the non-linear input impedance of the transistor amplifier. Equal increments of collector current are generated by equal increments of base current, which, because of the non-linear input impedance of the transistor, do not correspond to equal increments in base voltage.

The two conditions are met by using high-resistance coupling as shown in Fig. 9. This resistance prevents loading of the oscillator and at the same time approximates a constant current source for the amplifier.

Fig. 11 shows the three-stage vertical amplifier. The first stage consists of a grounded-emitter stabilized class A amplifier using a TA-153 junction transistor. The second stage is a grounded collector power junction transistor which provides the necessary drive at low impedance to operate the output stage. Frequency selective feedback, provided by R_1 and C_1 serves to compensate for distortion introduced by the first two stages. The output stage consists of a grounded-collector complementary-symmetrical push-pull amplifier using both a p-n-p and an n-p-n transistor.

This type of amplifier permits direct coupling to the vertical yoke without the presence of de-centering current. The Class-A efficiency obtained with this circuit was 24 per cent, which compares favorably with the

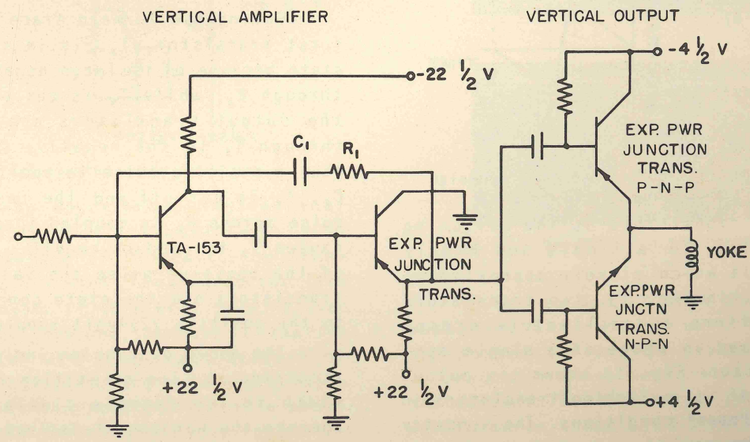

Fig. 11 - Vertical amplifier

maximum theoretically possible value of 33 per cent (for a sawtooth wave). The voltage waveform across the yoke is shown in Fig. 10b.

Horizontal Deflection

The operation of the horizontal-deflection system is based on the fact that linear bi-directional currents may be made to flow in an inductive yoke if a source of energy is periodically connected and disconnected with a fast switch.[1] An investigation of such a system is included in Appendix B and the results of this investigation are tabulated in Fig. 12.

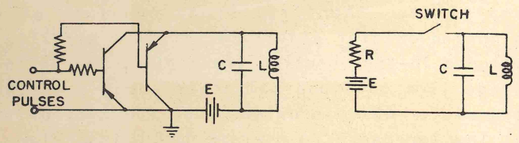

Actual circuit Equivalent circuit

$$E = \frac{E_{T\,MAX}}{1 + \frac{\pi(1-\delta)}{2\delta}}$$

$$L = \left(\frac{K(1-\delta)E}{Df_h}\right)^2$$

$$I_{PP} = \frac{f_h D^2}{k^2 E(1-\delta)}$$

$$\sqrt{LC} = \frac{\delta}{\pi f_h}$$

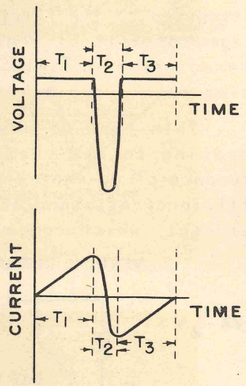

Design equations Yoke waveforms

Fig. 12 – Horizontal deflection circuit and design equations.

The use of transistors as the switching mechanism results in a simple and highly efficient circuit which closely approximates an ideal switch. In Fig. 13, two transistors with their emitters and collectors cross-connected are used in place of a single symmetrical transistor. Fig. 13 shows the output characteristics of the switching transistors in the "closed" and "open" conditions. The symmetry and low effective resistance of the "closed" condition (a) and the high effective resistance of the "open" condition (b) are apparent.

In order to control the output transistors, it is necessary that their bases be returned to a source of negative potential while they are conducting, and to a source of positive potential while they are cut off. This is accomplished with another form of switching circuit employing two transistors as shown in Fig. 14. The arrangement, which is essentially a single-pole double-throw switch, has been referred to as the "totem pole" circuit.

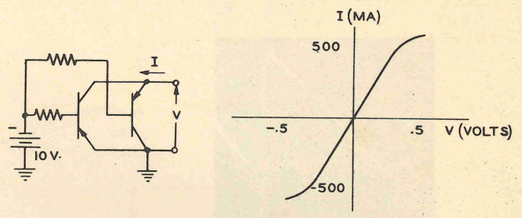

Circuit VI characteristic

(a) "Closed" connection

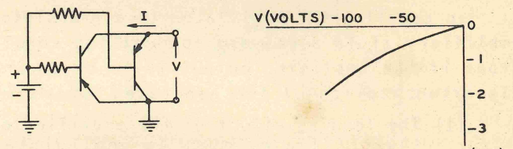

Circuit VI characteristic

(b) "Open" connection

Fig. 13 – Output characteristics of switching transistors.

During the forward trace of the beam, the first transistor, T_1, is in a high-conduction state because of the large negative bias applied through R_1, while T_2 is cut off. The bases of the output transistors are thus connected through T_1 to the negative $22\frac{1}{2}$-volt supply. When a positive pulse is applied to T_1 through C_1, T_1 is cut off and the resulting negative pulse across R_2 is coupled through C_2 to T_2 and causes T_2 to conduct heavily. For the duration of the positive pulse the bases of the output transistors are therefore connected through T_2 to the positive $22\frac{1}{2}$-volt supply.

The above discussion indicates that pulses occurring at line repetition rate and equal in width to the retrace time are necessary to operate the horizontal-deflection system. These pulses are obtained from an oscillator essentially the same as is used for the vertical deflection except for the frequency determining components. Amplification of the pulses is provided by the direct-coupled complementary-symmetrical Class-B pulse amplifier shown in Fig. 15.

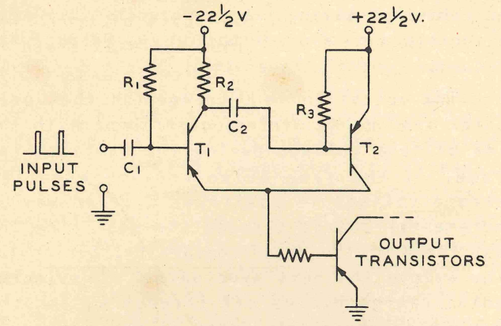

Fig. 14 – Totem pole circuit.

With no input signal, both transistors are nearly cut off, and the output terminal is connected through R_2 to the negative $22\frac{1}{2}$-volt supply. A positive pulse at the input causes both transistors to conduct heavily and connects the output terminal to the positive $22\frac{1}{2}$-volt supply through the p-n-p unit. With this circuit it is possible to obtain approximately 40-volt peak-to-peak output pulses from a peak-to-peak input of 0.5 volt.

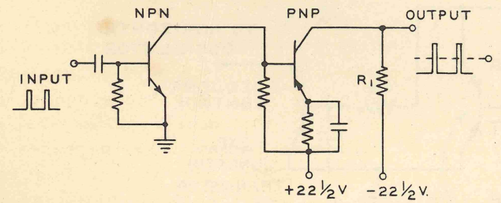

Fig. 15 – Direct-coupled pulse amplifier.

The preceding description implies that the elapsed time between the oscillator discharge and the opening of the switching transistors is negligible when compared to the time for one line retrace. If this were true, driven sync could be used. However, because of reactive effects associated with the input circuit of the switching transistors, there is appreciable time delay between the application of a positive pulse and the "opening" of the yoke circuit. Experimentally it was found that this delay is approximately 15 μsec which is about 5 μsec longer than the time allotted for horizontal retrace.

One effect of such a delay on the television picture is to place a black vertical bar at the right of the screen which corresponds to the horizontal blanking in the video signal. In addition, a portion of the picture appears immediately to the right of the black bar. It is apparent that an a-f-c system can compensate for the delay described above by re-phasing the horizontal oscillator. A simple and reliable transistor a-f-c system will be described in a later section.

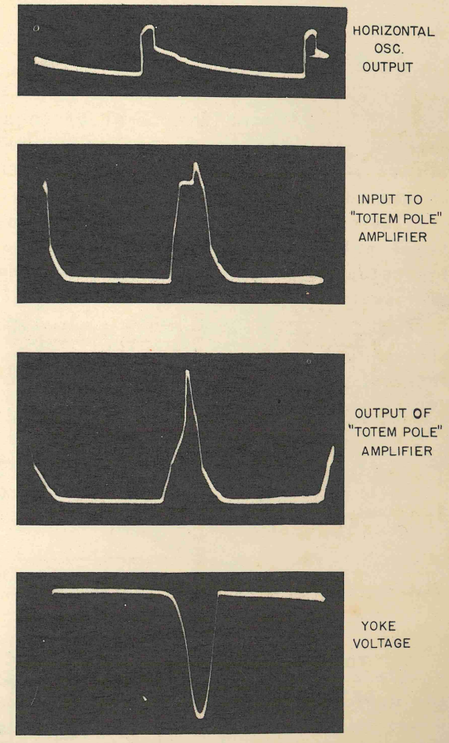

Fig. 16 – Waveforms in the horizontal deflection circuit.

Figs. 16 and 17 show photographs of the waveforms observed at several points in the horizontal deflection system. Of particular interest are those concerning the yoke voltage and current. The similarity of the photographed waveforms to those predicted by the elementary theory in Appendix B is evident.

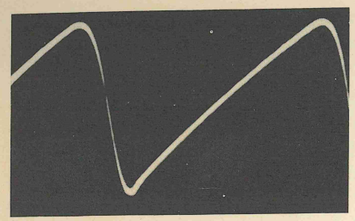

Fig. 17 – Horizontal yoke current waveform.

Sync Channel

A schematic of the synchronizing circuits of the receiver is shown in Fig. 18. The sync separator and amplifier consist of two TA-153 junction transistors. The first of these is connected grounded base. The emitter-base rectifier serves to separate the sync pulses which are coupled by the collector circuit to the following amplifier. After integration, the vertical pulses are amplified by a grounded emitter stage and are then used to synchronize the vertical oscillator.

The horizontal a-f-c system mentioned previously depends for its operation on the symmetrical properties of the phase comparator transistor. The retrace voltage pulse from the deflection yoke is integrated by a network consisting of R_1 and C_1. In the absence of a negative sync pulse on its base, the phase comparator functions simply as a high resistance and the integrated retrace pulse appears as a symmetrical sawtooth wave, its d-c component having been removed by C_2. There is therefore no d-c voltage on the base of the frequency control transistor.

The operation is unchanged if the horizontal sync pulse arrives coincident with the time of zero voltage during the sawtooth retrace. If the sync pulse arrives when the retrace voltage is positive, C_2 receives an incremental charge through the resulting low resistance of the phase comparator. During the time before the next sync pulse, this incremental charge drains off through R_4 and the frequency control transistor. A small negative bias is thus generated on the base of the frequency control transistor which lowers its effective resistance and causes the horizontal oscillator to fire sooner than on the previous cycle. The action continues until the sync pulse occurs simultaneously with the zero voltage point of the sawtooth retrace. The sequence of operation is reversed in the event the sync pulse originally arrives while the sawtooth retrace is negative.

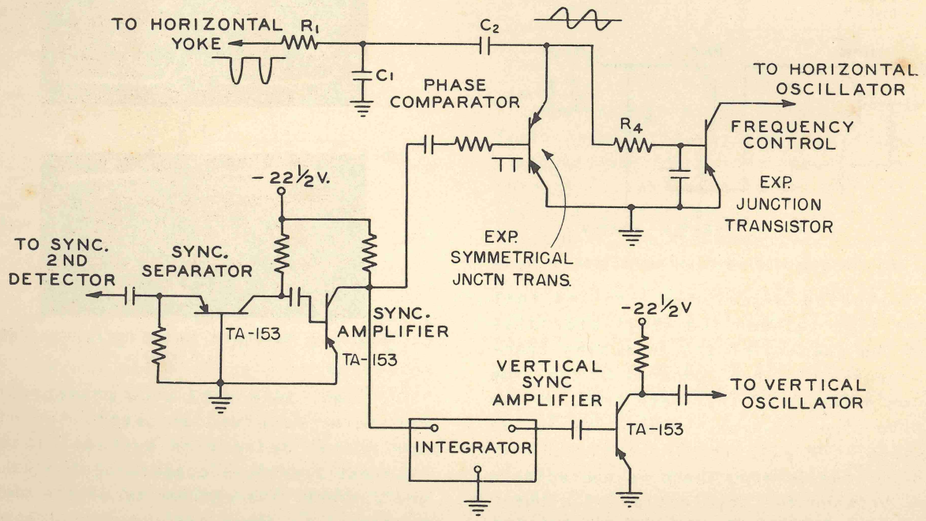

Fig. 18 – Sync channel and AFC circuits.

High-Voltage Supply

Because the flyback voltage of the horizontal deflection system is limited by transistor characteristics and since no transformer is used, it is not convenient to get the 2000-volt d.c. for the kinescope directly from the deflection system. For this reason a separate system shown in Fig. 19 was used. This is essentially a two-stage class-B amplifier driving a tuned transformer in the output. The negative flyback pulse is lightly coupled to the amplifier and causes the first transistor to conduct, thereby applying a conduction bias to the output stage. The output transistor, a power type, conducts heavily and supplies power to the tuned transformer at a horizontal frequency. The choke in the base circuit of the output transistor provides a low-impedance d-c path and insures that any leakage current in either transistor does not bias the output to conduction except when the system is pulsed. A half-wave selenium rectifier and filter provides the 2000-volt d.c. from the secondary of the tuned transformer.

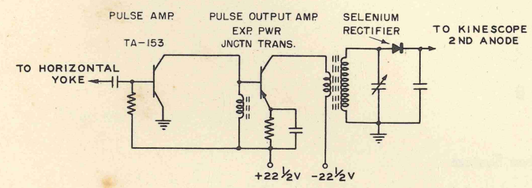

Fig. 19 – High voltage system.

Receiver Description

The receiver was built in a portable form with self-contained batteries in a clear plastic case. The total power consumption of the receiver is 13 watts. Of these 13 watts, 3.6 watts or more than 25 per cent, goes into the filament of the kinescope. The kinescope is the 5FP4 type and provides a 3 x 4-inch picture with a highlight brightness of approximately 10 foot-lamberts. The general layout of the receiver is shown in Fig. 20. The signal channel is built on the vertical plastic shelf in the center of the receiver. The deflection chassis is under the neck and the socket of the kinescope. The high-voltage supply is placed beyond the batteries to provide the least disturbance to the rest of the receiver. Fig. 21 shows the receiver in its normal viewing position. The total weight of the receiver with the batteries is 27 pounds.

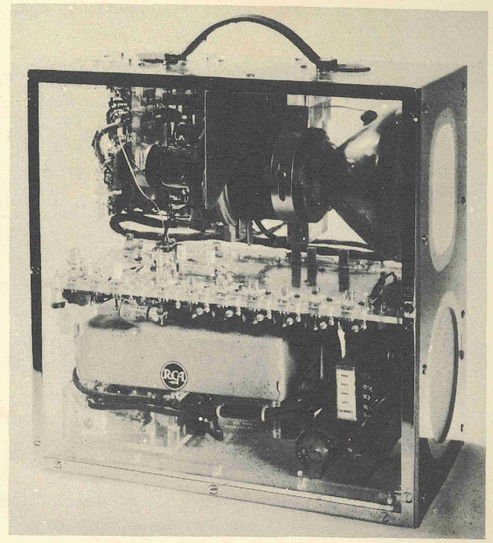

Fig. 20 – General layout of receiver.

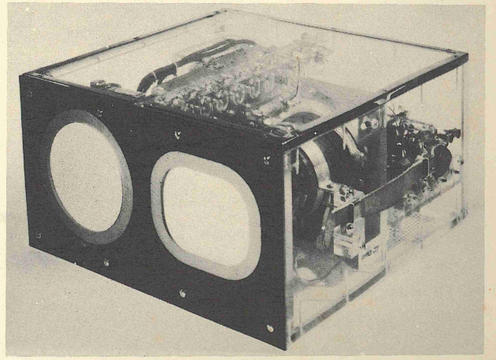

Fig. 21 – Front view of receiver.

Gerald B. Herzog
Robert D. Lohman
George C. Sziklai

Appendix A

With reference to Fig. 8:

$$V_b = - I_{co} R_3,$$

$$V_e = - \frac{V R_2}{R_1 + R_2} e^{\frac{-t}{(R_1 + R_2)}}$$

The condition for negligible emitter-collector conduction is:

$$|V_b| < |V_e|.$$

When this condition is no longer met, the discharge begins and is cumulative since:

$$I_b = I_{co} + I_E (\alpha - 1).$$

$$\alpha > 1.$$

Appendix B

Horizontal Deflection System

The operation of the horizontal deflection will be described by assuming:

(1) that the yoke is a perfect inductance,
(2) that the transistor is a bi-directional switch with a constant resistance when closed and infinite resistance when open.

The circuit operation will be considered during three durations of time:

(1) T_1, during which the switch is closed
(2) T_2, during which the switch is open
(3) T_3, during which the switch is closed

The relationships between these time durations are:

$$T_1 = T_3, \tag{1}$$

$$\frac{T_2}{T_1 + T_2 + T_3} = \delta, \tag{2}$$

$$T_1 + T_2 + T_3 = 1/f_h \tag{3}$$

where δ is the ratio of the retrace time to the time for one complete cycle and f_h is the line repetition rate. The simplified circuit is shown in Fig. 22a.

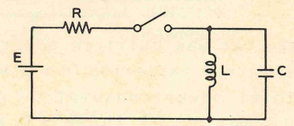

(a) Simplified equivalent circuit.

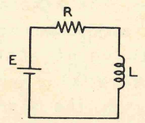

(b) Circuit during T_1 and T_3

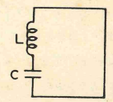

(c) Circuit during T_2

Fig. 22 - Circuits of Appendix B analysis.

The circuit may be further simplified as shown in Fig. 22b and c for each of the three time intervals if the following additional assumptions are made:

$$RC \ll T_1; \qquad \frac{R}{L} T_1 \ll 1 \tag{4}$$

The operation during the interval T_1 is as follows:

$$I(t)R + L \frac{dI(t)}{dt} = E, \tag{5}$$

$$I(0) = 0 \tag{6}$$

The solution is:

$$I(t) = \frac{E}{R} (1 - e^{\frac{-tR}{L}}), \tag{7}$$

$$I(t) \approx \frac{E}{L} t, \text{ since } \frac{R}{L} T_1 \ll 1 \tag{8}$$

The operation during T_2 while the switch is open is as follows:

$$L \frac{dI(t)}{dt} + \frac{1}{C} \int I(t)dt = 0, \tag{9}$$

$$I(0) = \frac{E}{L} T_1. \tag{10}$$

The solution is:

$$I(t) = \frac{E}{L} T_1 \cos t/\sqrt{LC}. \tag{11}$$

where time is measured from the instant of opening the switch. If the switch remains open for a time such that:

$$\frac{t}{\sqrt{LC}} = \pi = \frac{T_2}{\sqrt{LC}}, \tag{12}$$

then,

$$T_2 = \pi\sqrt{LC}. \tag{13}$$

Thus, at the end of T_2 the current in the yoke has reversed and the resonant circuit has gone through one-half cycle of oscillation.

The operation during T_3 is as follows:

$$RI(t) + L \frac{dI(t)}{dt} = E, \tag{14}$$

$$I(0) = - \frac{E}{L} T_1. \tag{15}$$

The solution in this case is:

$$I(t) \approx \frac{E}{L} t - \frac{E}{L} T_1 + \frac{RE}{L^2} T_1 t, \tag{16}$$

$$I(t) = \frac{E}{L} t \left(1 + \frac{T_1}{L/R}\right) - \frac{E}{L} T_1,$$

$$I(t) \approx \frac{E}{L} t - \frac{E}{L} T_1. \tag{17}$$

since the assumption that $RT_1/L \ll 1$ has already been made. The current during T_3 is therefore a linear time function minus a constant current. At the end of T_3 the linear term equals the constant term and the current is zero. The cycle then repeats.

It is desirable to eliminate the three intervals of time T_1, T_2 and T_3 from the equations since they can be expressed in terms of L, C, δ, and f_h. This may be done as follows: From Eqs. (13), (2), and (3):

$$T_2 = \pi\sqrt{LC}, \tag{18}$$

$$T_1 = \frac{T_2(1-\delta)}{2\delta} = \frac{\pi\sqrt{LC}(1-\delta)}{2\delta} = T_3, \tag{19}$$

$$\sqrt{LC} = \frac{\delta}{\pi f_h} \tag{20}$$

The idealized waveforms for the complete cycle are shown in Fig. 12.

In designing the horizontal deflection system it is necessary to derive several relationships which connect the magnitude of the deflection to the equations determined in the previous discussion. The design is limited by the voltage rating of the switching transistors, the particular yoke and kinescope construction used, and the anode voltage chosen for the kinescope.

Let:

K = a measurable constant depending on yoke construction and anode voltage,
D = deflection width in inches,
δ = ratio of retrace time to the time for one complete cycle,
L = inductance of yoke in henries,
f_h = line repetition rate in cycles/sec.,
E = battery voltage in volts.

If I_{pp} = peak-to-peak deflection current in amperes, it can be shown that:

$$I_{pp} = \frac{D}{K\sqrt{L}} = \frac{E}{L}(T_1+T_3). \qquad (21)$$

From Eqs. (1) and (19):

$$T_1+T_3 = 2T_1 = \frac{\pi\sqrt{LC}(1-\delta)}{\delta}. \qquad (22)$$

From Eq. (20):

$$\sqrt{LC} = \frac{\delta}{\pi f_h}. \qquad (20)$$

Therefore:

$$L = \left[\frac{K(1-\delta)E}{Df_h}\right]^2, \qquad (23)$$

$$I_{pp} = \frac{f_h D^2}{K^2 E(1-\delta)}. \qquad (24)$$

For a given deflection width, repetition rate, yoke construction, kinescope construction, and anode voltage, it is seen that both L and I_{pp} are dependent only on E and δ. With the transistors used, E is uniquely determined by δ and the maximum allowable voltage across the transistors.

The maximum voltage across the yoke inductance may be found from Eq. (11).

$$I_L = \frac{E}{L}T_1 \cos t/\sqrt{LC}, \qquad (11)$$

$$E_L = L\frac{dI_L}{dt} = -\frac{E\pi(1-\delta)}{2\delta} \sin T/\sqrt{LC} \qquad (25)$$

This expression is a maximum when:

$$\sin t/LC = 1 .$$

Therefore,

$$\hat{E}_L = \frac{-\pi(1-\delta)E}{2\delta}. \qquad (26)$$

The maximum voltage across the transistors, E_T, is:

$$\hat{E}_T = \hat{E}_L + E. \qquad (27)$$

where the signs must be chosen so the voltages add:

$$\hat{E}_T = -E\ 1 + \frac{\pi(1-\delta)}{2\delta} \qquad (28)$$

LB-863

A CRYSTAL RINGING CIRCUIT FOR COLOR SYNCHRONIZATION

Property of
Albert E. Linder

RADIO CORPORATION OF AMERICA
RCA LABORATORIES DIVISION
INDUSTRY SERVICE LABORATORY

RADIO CORPORATION OF AMERICA

RCA LABORATORIES DIVISION

INDUSTRY SERVICE LABORATORY

LB-863

A Crystal Ringing Circuit for Color Synchronization

This report is the property of the Radio Corporation of America and is loaned for confidential use with the understanding that it will not be published in any manner, in whole or in part. The statements and data included herein are based upon information and measurements which we believe accurate and reliable. No responsibility is assumed for the application or interpretation of such statements or data or for any infringement of patent or other rights of third parties which may result from the use of circuits, systems and processes described or referred to herein or in any previous reports or bulletins or in any written or oral discussions supplementary thereto.

Approved

Stuart W. Seeley

A Crystal Ringing Circuit for Color Synchronization

Introduction

This bulletin describes a receiver color synchronization circuit which uses the ringing of a quartz crystal to produce the required color reference frequency from the separated color synchronization burst. This circuit has both advantages and disadvantages as compared with other circuitry and complete evaluation must depend on field experience. Alternative methods of providing color synchronization have been described in earlier bulletins including LB-843, *AFC Color Synchronization Circuits*.

The circuit described in this bulletin is similar in principle to that in LB-838, with a quartz crystal rather than a coil-condenser combination being used as the ringing circuit. The crystal provides improved long-term stability and less susceptibility to noise because of its higher Q.

Circuit

The basic circuit is shown in Fig. 1 which gives the electrical equivalent circuit for the crystal and shows the crystal being driven by a generator of impedance Z_G into a load of impedance Z_L. It is assumed that the burst has been separated from the composite video signal so that the driving voltage is zero except for the 10 cycles of burst (2.5 μseconds) during each line interval.

It was observed early in this investigation that under certain conditions the output voltage across Z_L contained oscillations at two frequencies, corresponding to the two circuit meshes. These frequencies are separated by a few kilocycles and correspond to the so-called series and parallel resonant frequencies of the crystal. The presence of the two frequencies was readily observed by the resulting beat envelope of the output voltage. Under conditions of high values of terminal resistance, the parallel resonant mode predominated; with low terminal resistances the shunt capacitance of the crystal was effectively shorted and only the series oscillatory mode was effective.

The parallel mode was investigated initially. As might be expected from the relatively high terminal resistances (10K ohms or higher), this mode of operation resulted in an output frequency and phase which were affected by the terminal reactances as well as by the crystal shunt capacitance. There was also a tendency toward ringing of the input coil (the effect of which could be neutralized). Because of these undesirable characteristics, the series mode of operation was investigated and found to offer substantial improvement in circuit stability and ease of alignment.

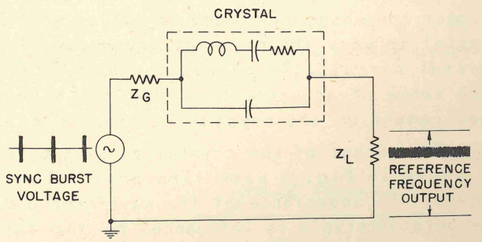

Fig. 1 – Electrical equivalent of crystal ringing circuit.

Series Operation

In order to achieve series operation, it is necessary to work the crystal out of, and into, relatively low resistances in the order of 100 to 2000 ohms. In the circuits shown in Fig. 2, a crossover in the mode of operation appears when the source and load impedances are in the region of 4000 ohms.

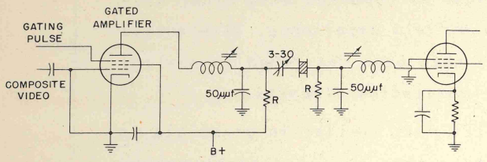

(a)

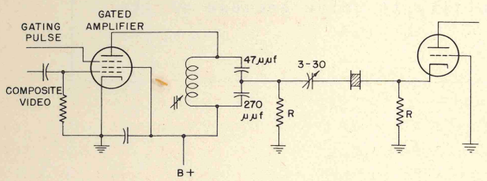

(b)

Fig. 2 – Two forms of the crystal ringing circuit. The effect of varying R is shown in Fig. 4. The series trimmer enables tuning the crystal frequency over a range of a few kilocycles.

A series arrangement used is shown in Fig. 2a. The crystal is driven from the 6AS6 gated burst amplifier through an impedance transforming π network. An alternate method of driving the crystal is shown in Fig. 2b. This lends itself for use with a grounded-grid triode amplifier. The Q of the impedance matching networks in these circuits is relatively low and their effect on the phase of the output is negligible.

In both these circuits, an adjustable trimmer condenser is placed in series with the crystal to vary the resonant frequency of the crystal circuit. This provides a relatively wide range of adjustment so that the accuracy requirement on the crystal is greatly eased.

The output of the crystal ringing circuit is shown in Fig. 3 with line and field rate sweeps. The appearance of the waveforms during the burst intervals is influenced by the tuning of the crystal circuit and in general proper tuning is accompanied by maximum output and minimum discontinuity. The decay of the output voltage during the vertical interval is of course the result of absence of burst during this interval, in accordance with the present NTSC standards. The amount of decay as well as the discontinuity during the line interval are related to the circuit Q. Generally, higher circuit Q's, i.e., lower values of R, will result in more uniform output.

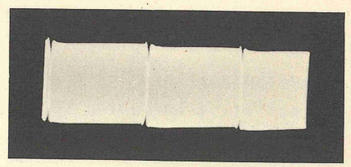

(a) – Output of crystal ringing circuit – horizontal sweep.

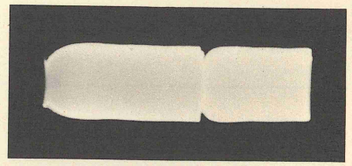

(b) – Output of crystal ringing circuit – vertical sweep.

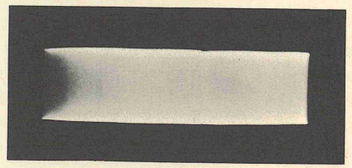

(c) – Output of limiter – vertical sweep.

Fig. 3 – Output of crystal ringing circuit.

Phase Stability and Noise Immunity

The operating characteristics of this circuit are shown in Fig. 4 which displays the phase variation of the output as a function of the frequency separation between the transmitted color sync burst and the receiver crystal circuit resonance. Curves are given for several values of load resistance R. These curves show that, for a given frequency separation, the phase shift decreases for increasing values of series resistance, i.e., for lower values of circuit Q.

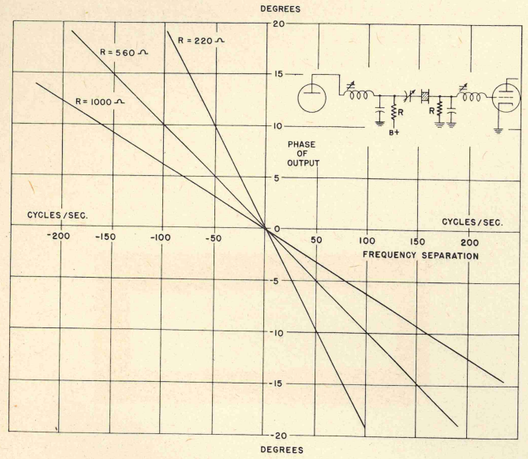

Fig. 4 – Variation in phase of output with frequency separation between burst and crystal circuit. The higher the load resistance, the lower the phase shift for a given frequency separation.

Pictures were observed under weak signal conditions using the circuits of Fig. 2 incorporated in a complete television receiver operating on NTSC standards. It was found that random noise enabled a more critical evaluation of color sync performance and was preferable to impulse noise in this respect. In general, the noise immunity was found to improve with increasing circuit Q, as is to be expected. The phase stability, with 1000-ohm terminating resistors, was such that a frequency change of ±80 cycles in the color subcarrier frequency produced a phase shift of ±5 degrees in the receiver sampling frequency. In addition to producing phase shift, detuning of the receiver crystal circuits also resulted in degradation of the picture in the form of streaking when the separation exceeded approximately ±100 cycles. With 220-ohm terminating resistors, this streaking became noticeable for a detuning of approximately ±60 cycles. Because of the greater phase stability and reduction in streaking under weak signal conditions with the crystal circuit detuned from the color sync burst, operation with 1000-ohm load resistors appeared preferable.

The crystal ringing circuit differs from AFC or locked-in oscillators in that the latter exhibit only phase variations under noise conditions. In order to eliminate amplitude variations resulting from noise and changes in signal level, it has been found essential to provide limiting so that a color sync signal of substantially constant amplitude is fed to the color demodulators. The degree of limiting required will depend on the sensitivity of the color demodulators to amplitude changes in the sampling (color reference) frequency.

Crystal Frequency

In general, it has been possible to use crystals interchangeably in the transmitter and receiver color reference frequency circuits. This comes about since in both circuits frequency is determined by the crystal in series with an adjustable capacitance of the same order of magnitude.

The color sync circuit is aligned by peaking all tuned circuits (including the crystal) for maximum output. When the series crystal trimmer is properly adjusted, minimum discontinuity will result during the sync interval. Optimum adjustment of the crystal tuning is most readily made with a weak signal input to the antenna terminals, by adjusting for minimum noise streaking.

The requirement on the accuracy of the crystal frequency is considerably less stringent than Fig. 4 would indicate. Although the crystal circuit must be tuned accurately by the associated series trimmer, the crystal itself may be ground to limits of the order of ±1000 cycles of the design center.

Jack Avins

LB-883

A SWEEP METHOD FOR MEASURING ENVELOPE DELAY

Property of
Albert E. Linden

RADIO CORPORATION OF AMERICA
RCA LABORATORIES DIVISION
INDUSTRY SERVICE LABORATORY

RADIO CORPORATION OF AMERICA
RCA LABORATORIES DIVISION
INDUSTRY SERVICE LABORATORY

LB-883

A Sweep Method for Measuring Envelope Delay

This report is the property of the Radio Corporation of America and is loaned for confidential use with the understanding that it will not be published in any manner, in whole or in part. The statements and data included herein are based upon information and measurements which we believe accurate and reliable. No responsibility is assumed for the application or interpretation of such statements or data or for any infringement of patent or other rights of third parties which may result from the use of circuits, systems and processes described or referred to herein or in any previous reports or bulletins or in any written or oral discussions supplementary thereto.

Approved

Stuart W. Seeley

A Sweep Method for Measuring Envelope Delay

Introduction

Equipment has been developed which in conjunction with generally available sweep generators and oscilloscopes, makes it possible to determine rapidly the envelope delay characteristic as well as the amplitude characteristic of any amplifier or system. Measurement made with it when compared with other methods of determining envelope delay agreed within 0.01 microsecond in absolute value and even better in relative values.

Theory of Operation

If a signal consisting of two frequencies is fed into an amplifier, the signal at the output will consist of these same two frequencies but each will have had its phase shifted by an amount determined by the phase shift of the amplifier at each of the two frequencies.

That is, if the input signal is

$$S_i = \cos(2\pi f_1 t+\varphi_1)+\cos(2\pi f_2 t+\varphi_2)$$

the output will be

$$S_o = A\cos(2\pi f_1 t+\varphi_1+\theta_1)+B\cos(2\pi f_2 t+\varphi_2+\theta_2)$$

If the two frequencies are close enough together so that the envelope delay is constant in the interval between f_1 and f_2 the envelope delay will be

$$T_E = \frac{d\theta}{d\omega} = \frac{\Delta\theta}{2\pi\Delta f} = \frac{\theta_2-\theta_1}{2\pi(f_2-f_1)}$$

Since f_1 and f_2 are known the measurement of T_E resolves itself into measuring $\theta_2-\theta_1$.

If the output signal is detected in a square law detector,

$$S_o^2 = A^2\cos^2(2\pi f_1 t+\varphi_1+\theta_1)+B^2\cos^2(2\pi f_2 t+\varphi_2+\theta_2)$$

$$+2AB\cos(2\pi f_1 t+\varphi_1+\theta_1)\times\cos(2\pi f_2 t+\varphi_2+\theta_2)$$

$$= \frac{A^2+B^2}{2} + \frac{A}{2}\cos(4\pi f_1 t+2\varphi_1+2\theta_1)+\frac{B}{2}\cos(4\pi f_2 t+2\varphi_2+2\theta_2)$$

$$+AB\cos[2\pi(f_1+f_2)t+\varphi_1+\varphi_2+\theta_1+\theta_2]$$

$$+AB\cos[2\pi(f_2-f_1)t+\varphi_2-\varphi_1+\theta_2-\theta_1]$$

This shows that there is a d-c term, three high-frequency terms (roughly 2f) and a term, the last term above, at a frequency of the difference of the two frequencies and shifted in phase by the difference in phase shift of the two frequencies.

It should be noted that $\Delta\theta = \theta_2-\theta_1$ is not dependent on A or B.

By selecting just the $\Delta f = f_2-f_1$ term by circuits tuned to it, a sine wave is obtained;

$$AB\cos(2\pi\Delta f t+\varphi+\Delta\theta)$$

By measuring this phase of this detected output signal relative to the same signal at the input to the amplifier where $\Delta\theta = 0$,

$$\varphi+\Delta\theta-\varphi = \Delta\theta.$$

This shows that the phase of this Δf signal is $\Delta\theta$ and since Δf is known,

$$T_E = \frac{\Delta\theta}{2\pi\Delta f}.$$

To get the delay at any other frequency, f_1 and f_2 are changed, keeping Δf constant. Then, the envelope delay will always be proportional to the $\Delta\theta$, since Δf is constant. This may be written

$$T_E = \frac{1}{2\pi f\Delta} \times \Delta\theta$$

An easy way to measure $\Delta\theta$ is to feed the sine wave at Δf of unknown phase into a modulator with a sine wave of the same frequency but constant phase. The output is then proportional to

$$K \sin \Delta\theta$$

This can be seen by considering what a modulator does. It multiplies the two waves. Therefore the output

$$S_T = \cos(2\pi\Delta ft+\varphi)\times\cos(2\pi\Delta ft+\varphi+\Delta\theta)$$

$$= \tfrac{1}{2}\cos(2\pi 2\Delta ft+2\varphi+\Delta\theta)+\tfrac{1}{2}\cos\Delta\theta$$

By filtering out $2\Delta f$ there is only

$$S_T = \tfrac{1}{2}\cos\Delta\theta.$$

If the phase of the reference signal is shifted by 90 degrees this would be $S_T = \frac{1}{2} \sin \Delta\theta$.

In most simple modulators (not balanced) there is a d-c term which can easily be balanced out.

Instead of using just two frequencies, a group of frequencies can be used. Two practical cases are those obtained by modulating a carrier either in amplitude or frequency. When this is done, the phase of the modulating frequency after detection can be used, provided the amplitude of the two side bands have been made equal before detection by an amplitude limiter before the discriminator in the case of frequency modulation, or by a frequency limiter before the amplitude detector in the case of amplitude modulation. Both these systems have the disadvantage that the probe used for looking at the point in the amplifier under test cannot be a simple detector but must be a wide-band cathode follower to take the signal into the measuring equipment. The beat between the two side bands can be used in either of these cases (twice the modulating frequency) as is done when just two frequencies are used. However, the second harmonic of the modulating frequency generated in the simple type of detector is of the same frequency and gives spurious results.

For these reasons it was decided to use just two frequencies and a simple diode detector. In order to generate two frequencies whose difference is constant while their absolute frequency is varied rapidly as is done in a sweep, it is necessary to modulate the signal from the sweep generator by a constant frequency in a double balanced modulator.

Equipment

A block diagram of the equipment for accomplishing the above is shown in Fig. 1.

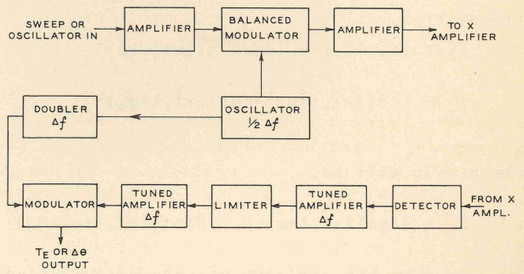

Fig. 1 – Block diagram of the equipment.

A signal at the frequency for which the envelope delay is to be measured is fed through an amplifier into a doubly balanced modulator where it is modulated by the output of an oscillator at $\frac{1}{2}\Delta f$. Neither of the input signals appear at the output of the modulator, but only the products, that is, $f + \frac{1}{2}\Delta f$ and $f - \frac{1}{2}\Delta f$. After further amplification this signal is fed to the amplifier under test. The signal from the output of the amplifier under test is fed to a detector the output of which is tuned to Δf. After amplification and limiting, this signal is fed to a modulator to be modulated by

a signal of fixed phase at Δf derived by doubling the $\frac{1}{2}\Delta f$ signal from the oscillator. The low-frequency side-band output of the modulator is a d-c signal proportional to

$$K + \sin\Delta\theta = K + aT_E$$

The K can be balanced out and the a determined by calibration. T_E can be read on a calibrated d-c meter if a single frequency input is used or on an oscilloscope if a sweep input is used.

For the equipment which was built a Δf of 200 kc was chosen as a compromise between resolution (ability to measure speed of change of T_E with f) and size of d-c variation in the output meter or scope reading. Lower Δf would increase the resolution but the d-c changes due to a change in T_E would be reduced. The d-c changes could be increased at the expense of some additional circuits by multiplying both the reference and varying Δf by the same factor before feeding them into the phase detector modulator.

Circuit Diagram

The circuit diagram follows the block diagram closely. The signal from the sweep generator, after amplification, goes to the balanced modulator. This consists of two modulator tubes V3 and V4 fed in push pull by both the input signal and the 100-kc fixed frequency. The 100 kc is fed by a balanced transformer and the signal by a plate-cathode phase splitter V2. The balance controls on the modulator are (1) the G_1 bias which, in conjunction with the tuning of the two halves of the secondary of the 100-kc transformer, balances out the 100 kc in the output; (2) the G_3 bias which minimizes the second harmonic in the output; (3) the low-frequency signal balance by means of the potentiometer in the cathode of the phase splitter which makes both halves of the modulator modulate equally; (4) the high-frequency signal balance by means of the cathode condenser which does the same as (3) for the high frequencies, and (5) the neutralizing condenser between the grid and plate of one of the modulators to compensate for the capacity feedthrough at high frequencies of the other modulator due to stray capacity of the wiring, etc.

The output of the modulator is amplified in tube V5 and fed to the amplifier to be tested by the cathode follower tube V6.

The oscillator V9 and the buffers V7 and V8 need no explanation.

The output of the amplifier is detected in the probe whose output is tuned to 200 kc. The tuned circuit has a condenser divider so that the proper signal level may be selected for the tuned amplifier and limiter which follows. Tube V14 is a tuned amplifier and V13 drives a double diode limiter which works satisfactorially without phase shift over about a 10 to 1 range. Care must be taken so that none of the stages before the limiter saturate or draw grid current; otherwise there would be phase shift with amplitude. This is the reason for using a 6AG7 with unbypassed cathode resistor to drive the limiter. The output of the limiter goes through another tuned amplifier V12 to the first grid of modulator V11. The potentiometer across the tuned circuit in the plate of tube V12 serves to put the proper amount of sine wave signal on the modulator to give a calibrated output. G_3 of the modulator V11 is fed a fixed-phase 200-kc signal through the tuned amplifier V10 from the doubler circuit in the plate of tube V8. The primary of the double transformer is tunable so that the phase of the 200-kc output may be changed over about 180 degrees. This changes the amplitude of the 200-kc signal some, but the modulator is insensitive to amplitude of this signal if it is large enough. The output current of the modulator is read on a 0–1.0 ma meter or can be observed by an oscilloscope after filtering out the 200 kc. A 0–1.0-ma meter in the limiter circuit serves to indicate when the signal is within the proper range and can be used to check the amplitude characteristic of the amplifier.

Care must be taken that no unmodulated 100 or 200-kc signal gets into the tuned amplifier. Therefore the first stage of the 200-kc amplifier should be shielded. One side of the filament should be grounded at tube V14.

Photographs of the experimental equipment are shown in Fig. 3.

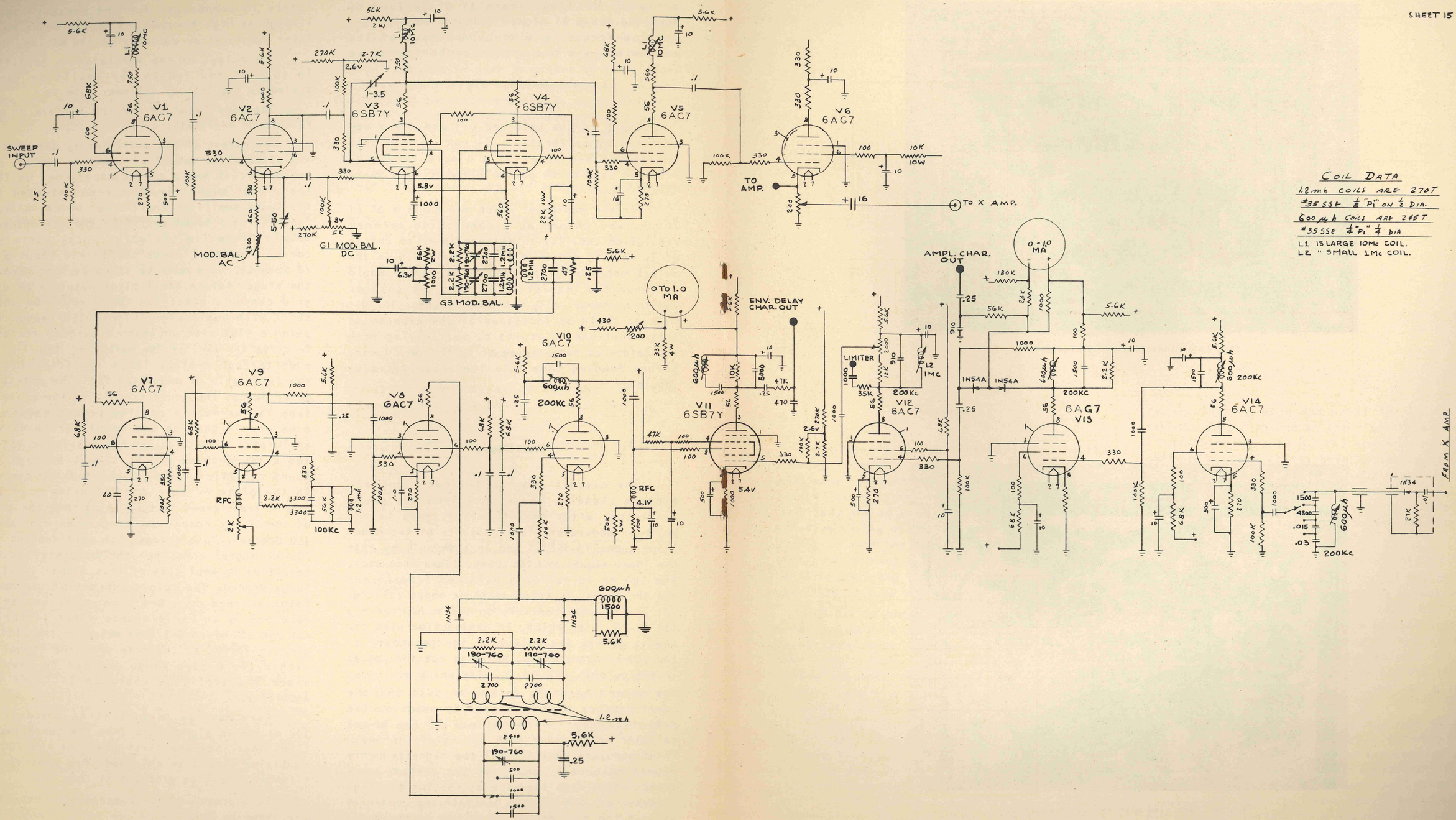

Fig. 2 – Circuit diagram of the equipment.

COIL DATA

1.2 mh COILS ARE 270T #35 SSE ⅛" "Pi" ON ½ DIA.

600 μh COILS ARE 245T #35 SSE ¼" "Pi" ¼ DIA

L1 IS LARGE 10Mc COIL.

L2 " SMALL 1Mc COIL.

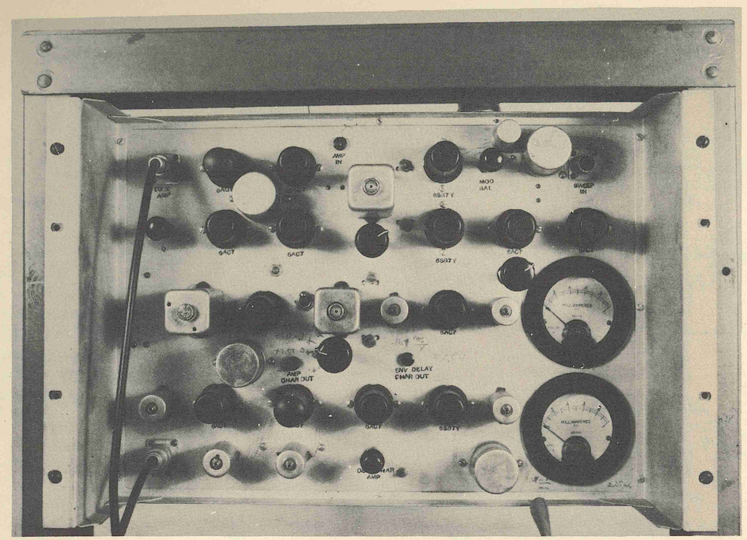

Fig. 3a – Front view of the equipment.

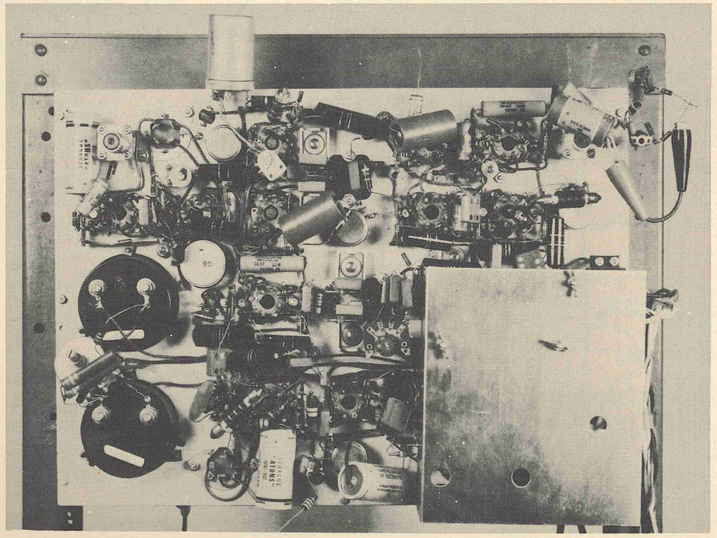

Fig. 3b. Back view with shield in position

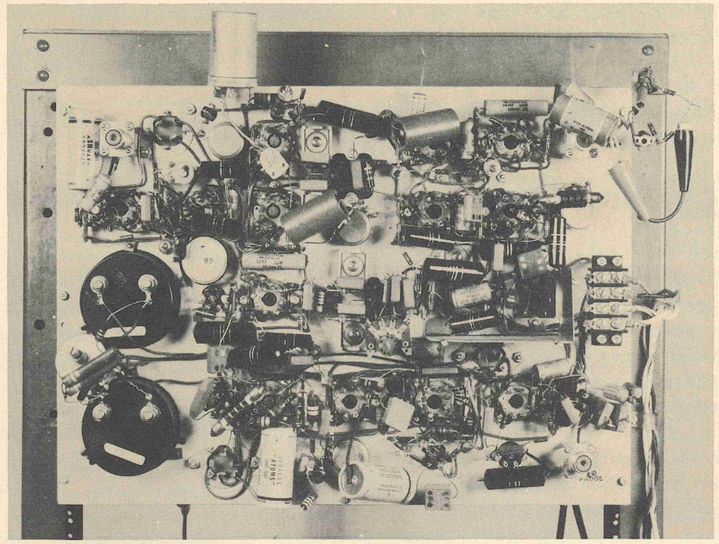

Fig. 3c. Back view with shield removed.

Operation

The oscillator is first adjusted to the desired frequency (100 kc). Then the balanced modulator is balanced. This is done by looking at the output signal. With no input, the G_1 and G_3 biases are adjusted in conjunction with the relative tuning of the two halves of the transformer to make the output 0. This can later be checked more accurately by connecting the probe to the output and looking at the test point on the plate of tube V12.

After the output has been adjusted for 0 with no input, a sweep signal is introduced, being careful not to use more than about 0.3 volt peak to peak. The output should be single valued at both low and high frequencies and should have a single base line. The low-frequency balance potentiometer in the cathode of V2 should be adjusted for a single trace at low frequencies and the condenser in the cathode of tube V2 should be adjusted for the high-frequency end. If the base line spreads out at the high-frequency end it is because there is more capacity between one of the grids and the common plate than the other. A small variable capacitor is added to the low side to make them equal. This is adjusted until the base line becomes single valued at the high frequencies. After this adjustment, the condenser in the cathode of tube V2 may have to be readjusted slightly. The peaking in the plates of tube V1, V3 and V4, and V5 are adjusted to give flat response. These may belater readjusted slightly to give as flat an envelope delay response as possible.

The doubler circuits are tuned in the normal fashion.

The probe is connected to the output with a signal fed to the input, and the circuits in the plates of tubes V13 and V14 and the grid of V14 are tuned for maximum by observing the signal at the amplitude characteristic out or the amplitude meter reading. The circuit in V12 is tuned for maximum by observing the signal at the limiter test point.

With a sweep input and a scope at the envelope delay characteristic output, the tuning of the doubler (the phase control) is adjusted until the sweep is approximately at the same level during sweep as during the blanked off time. The sweep should be adjusted for maximum flatness from about 0.5 Mc and up by slight adjustment of the peaking controls

in the plates of the modulator and tube V5. If this adversely affects the amplitude response it should be corrected by adjustment of the peaking in tube V1. Below 0.5 Mc there will be spurious responses due to harmonics generated in the detector adding to the desired signal.

The delay characteristic meter is calibrated by adjusting the "meter 0" potentiometer until the meter reads center scale for no signal input and then the "delay characteristic calibrate" potentiometer adjusted to give exactly full scale or exactly 0 reading at the maximum or minimum possible excursion with a single-frequency input signal (not sweep) and adjustment of the phase control. The device is now ready to use to check the envelope delay characteristic of an amplifier. If the amplification of the amplifier under test is greater than unity the probe gain should be reduced to keep the amplitude characteristic meter on scale. If it is less than unity, additional gain should be provided but the input to the balanced modulator should not be increased. The sweep input should not be raised higher than 0.5 volt peak-to-peak if accurate results are desired. Point-by-point measurements may be made by reading the meter or sweep measurements may be made by using an oscilloscope.

The probe input condenser size is a compromise. For accurate point-by-point measurements to low frequencies without the need for calibrated correction, it should be as large as possible. For following rapid changes in amplitude such as occur when sweeping a low-pass filter a small condenser is desirable. A 3000-μμf condenser is a fair compromise but should be changed for individual situations. An 0.01-μf condenser is used in the probe which is large enough for low-frequency point-by-point measurements. For sweeping, a small condenser should be used in series with this one.

The envelope delay is:

$$T_E = \frac{\Delta\theta}{2\pi\Delta f}$$

If the 1-ma meter reads 0 degrees to 90 degrees from center scale to full scale it reads 0.5 sin $\Delta\theta$, or if I_m is in ma from center scale

$$2I_m = \sin \Delta\theta; \qquad \Delta\theta = \sin^{-1} 2I_m$$

therefore

$$T_E = \frac{\sin^{-1} 2I_m}{2\pi \times 200 \times 10^3} = 0.798\ (\sin^{-1} 2I_m) \times 10^{-6}$$

Since for small angles $\sin \theta = \theta$ if θ is in radians

$$T_E \cong 0.80 \times 2I_m \times 10^{-6}$$

this is quite accurate in the range between −0.3 to +0.3 microsecond, being in error by less than 0.01 microsecond. Since the scope measures this 0 to ±0.5-ma current as the voltage across a 10K resistor

$$T_E \cong 0.16 V_s \times 10^{-6}$$

in the range ±2 volts.

For larger delays the full formula must be used for accurate results.

$$T_E = 0.798(\sin^{-1} 2I_m) \times 10^{-6} = 0.1596(\sin^{-1} V_s) \times 10^{-6}$$

The meter or scope can of course be calibrated directly in microseconds.

Results

Several devices were measured by other methods and then with this equipment point by point. Some of the results are shown in Figs. 4

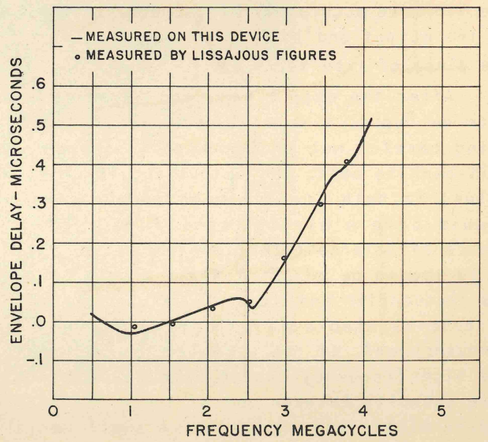

Fig. 4 – Envelope delay of a television receiver.

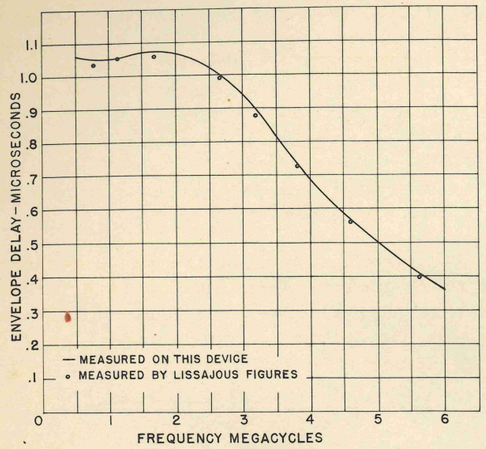

Fig. 5 – Envelope delay of phase correcting circuit.

and 5. It can be seen that they agree within about 0.01 μsec. Most other methods of measuring phase give readings at certain discreet frequencies only, whereas, with this device, any frequency can be used. This makes it possible to find variations between the discreet frequencies which would be missed by the other methods. Fig. 4 shows a variation of this type near 2.5 Mc. Fig. 6 shows two oscillograms of characteristics of circuits taken with a sweep input.

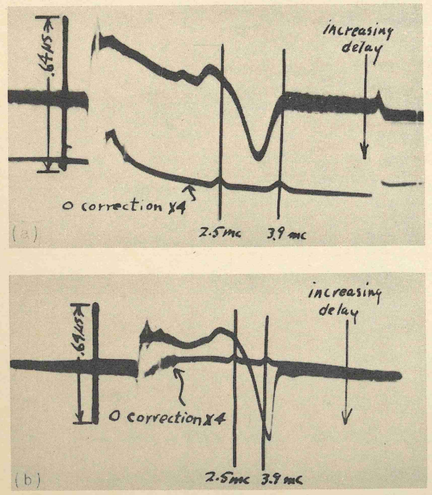

Fig. 6 – Oscillograms of the envelope delay characteristics of two television receivers.

Receivers are measured by modulating a Mega-Pix or other modulator at r.f. with the output of this device, and connecting the probe to some point after the second detector depending on how much of the video is to be measured.

When measuring a receiver, the harmonics of line frequency near 200 kc cause some trouble but usually only outside the band being measured where the limiter is not effective.

Since this experimental equipment is rack mounted, the probe lead was extended with additional coaxial cable to reach the receiver circuits and the input circuit retuned to 200 kc. This caused some small peaks in the characteristic due to the long ground.

Possibilities for Future Development

Since this equipment is experimental there are a number of things which could be done differently if another circuit were built. For instance, there is no need for the extra positive bias on the two modulators over that required for proper biasing. The 100-kc input to the balanced modulator could be reduced in ways other than loading the primary of the transformer with 47 ohms. Other types of oscillators might be used. Other limiters might be used.

In addition to this type of change, there are others which might improve the operation in one respect or another. For instance, the frequency difference might be lowered so that greater resolution would be obtained and also readings at lower frequencies could be used. This would reduce the accuracy unless the reference and unknown frequencies were both multiplied up before application to the detector modulator. These multipliers would also help to limit any amplitude changes.

The oscillator could be locked to horizontal so that the output signal could be blanked and fed through equipment using clamps.

For use of the equipment where the detector must be remote from the input, the reference phase must be reconstructed from the

signal itself. This cannot be done point by point but must be done when using a sweep. One way of doing this is with an a-f-c circuit whose response is so slow that it ignores changes in phase during the sweep. Another way is to feed the signal into a narrow filter which ignores the sweep frequency sidebands.

Instead of using a reference signal one can measure the frequency changes of the 200-kc signal with time as the input is swept through the frequency range by putting this 200-kc signal through a discriminator. By converting this information to phase changes of the 200-kc signal by integration one gets a signal corresponding to envelope delay. A second integration would give phase response. (Integration of the signal out of the phase detector modulator would also give phase response.)

Alfred C. Schroeder

Alfred C. Schroeder

LB-872

BALANCE MEASUREMENTS ON BALUN TRANSFORMERS

Property of
Albert E. Linden

RADIO CORPORATION OF AMERICA
RCA LABORATORIES DIVISION
INDUSTRY SERVICE LABORATORY

RADIO CORPORATION OF AMERICA
RCA LABORATORIES DIVISION
INDUSTRY SERVICE LABORATORY

LB-872

Balance Measurements on Balun Transformers

This report is the property of the Radio Corporation of America and is loaned for confidential use with the understanding that it will not be published in any manner, in whole or in part. The statements and data included herein are based upon information and measurements which we believe accurate and reliable. No responsibility is assumed for the application or interpretation of such statements or data or for any infringement of patent or other rights of third parties which may result from the use of circuits, systems and processes described or referred to herein or in any previous reports or bulletins or in any written or oral discussions supplementary thereto.

Approved

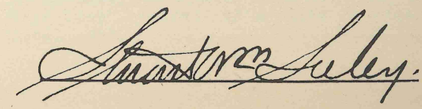

Balance Measurements on Balun Transformers

Introduction

This bulletin discusses means of establishing a figure of merit which expresses the relative quality of balance obtained from balun transformers. This figure of merit, termed the balance efficiency, is defined and expressed in terms of measurable quantities. A balance comparator to measure the balance efficiency of baluns is described, and tests on representative baluns are presented.

General Discussion

Standard antenna systems used in television reception of horizontally-polarized signals are of the balanced, symmetrical type. Modern receivers are almost exclusively designed with unsymmetrical, coaxial inputs because of economic and engineering advantages. Therefore an isolation transformer is required to join the two systems without disturbing their inherent properties.

In past practice, geometrically unsymmetrical systems such as coaxial lines and single-ended loads have been termed as unbalanced systems. Hence the isolation transformer has commonly been called a balun as an abbreviation for balance-to-unbalance transformer.

To avoid confusion and conform with common usage, it is important to note that the terms "balanced" and "unbalanced" are applied in two different manners. Where used in connection with a transmission line or load, reference is made to the physical symmetry of the line construction or the equality of the load terminal impedances to ground. The terms are also used, however, to denote the type of excitation or mode of operation.

A symmetrical system can support simultaneously two transverse electromagnetic (TEM) modes of propagation. The balanced or push-pull mode is obtained where the currents on symmetrically located conductors are equal in magnitude and opposite in phase at all cross sections. This is the normal operating condition of non-radiating open-wire transmission lines and shielded-pair transmission lines with zero net current flow on the inside of the shield. Conversely, equal in-phase currents on the symmetrically located conductors are defined as the unbalanced or push-push mode. Here the potential difference between the conductors is zero at all cross sections. An open-wire transmission line acting as an antenna against ground is an example of unbalanced mode operation. Another example is the shielded-pair line functioning as a coaxial cable with the pair of conductors effectively joined together and return currents flowing on the inside of the shield.

The normal directional and electrical characteristics of the symmetrical receiving antenna system are based on balanced mode design. An unbalanced load termination permits the existence of undesired push-push currents,[1] resulting in extraneous signal pickup by the transmission line and a reduction in gain and signal-to-noise ratio.

The function of the balun is to transfer efficiently the balanced mode energy from the antenna and to prevent unbalanced mode currents

[1] K. Tomiyasu, "Unbalanced Terminations on a Shielded-Pair Line", *Journal of Applied Physics*, p. 552, June, 1950.

from coupling to the receiver input. Frankel[2] has given a general equivalent circuit and necessary requirements for a perfect balun and shows the independence of its operation on source or load impedances.

Some baluns, however, have balance characteristics which are a function of frequency as well as the driving conditions. Since practical installations vary widely in the type of receiving antennas used and the layout of the transmission line in relation to the field configuration in the vicinity, it is obviously impossible to measure the balance quality of a balun for all operating conditions. Therefore, an arbitrary standard setup is presented in this bulletin for comparing the relative balance merits of different baluns. A simple device called the balance comparator is described for obtaining the balance efficiency of baluns.

Theory

Fig. 1a shows the block diagram of a balun joining a balanced mode generator, having an internal impedance of $2Z_o$, to an unbalanced load, Z_L, represented by the television receiver

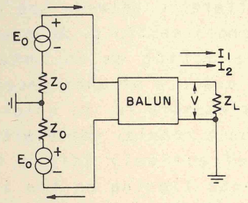

(a) – With a balanced mode generator

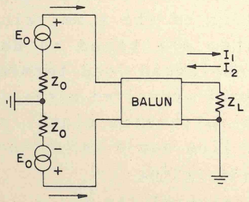

(b) – With an unbalanced mode generator.

Fig. 1 – Block diagram of balun feeding an unbalanced load.

[2] S. Frankel, "Reactance Networks for Coupling Between Unbalanced and Balanced Circuits", *Proc. I.R.E.*, p. 486, Sept. 1941.

input. The balun is assumed to be made of linear, passive, reactive elements. All expressions are complex quantities.

The load current components, I_1 and I_2, result from applying each of the voltages, E_o, separately. Hence, with both voltages applied, the total load current is (I_1+I_2) by the principle of superposition.

Now if one of the input voltages is reversed in phase as in Fig. 1b, an unbalanced mode generator is obtained, and the load current becomes (I_1-I_2). If the balun input is balanced, this unbalanced mode is suppressed and I_1 equals I_2.

If the balun input is unbalanced, the ratio R of the receiver input currents (or voltages) for the two types of balun input feed is a measure of the balance quality.

$$\text{Or} \qquad R = \left| \frac{I_1 - I_2}{I_1 + I_2} \right| = \left| \frac{1-(I_2/I_1)}{1+(I_2/I_1)} \right| \tag{1}$$

It is logical and desirable, however, that the quality of balance be stated as a percentage with perfect balance expressed as 100 per cent and complete unbalance as 0 per cent. Therefore, let the balance efficiency be defined as:

$$\text{balance efficiency} = \frac{100}{1+R} \tag{2}$$

The relation between the balance efficiency and the impedances of the load and generator is considered next.

Applying Thevenin's theorem to the output circuit,

$$I_1 = \frac{V_1}{Z_L + Z_1} \tag{3}$$

and

$$I_2 = \frac{V_2}{Z_L + Z_1} \tag{4}$$

where Z_1 is the impedance measured looking back into the balun output terminals with the input voltages, E_o, turned off, and V_1 and V_2 are the open-circuit output voltages obtained by turning on the input voltages separately.

It is seen that the ratio of I_1 to I_2 is unaffected by the value of the load impedance, Z_L. Therefore, from Eq. (1), the balance efficiency is also independent of the load impedance.

The load current components are proportional, respectively, to the balun input terminal voltages produced by applying the two generators separately. However, since these terminal voltages are dependent upon the generator internal impedance as well as the balun input impedances to ground, then the ratio of I_1 to I_2, and hence the balance efficiency, is a function of the generator internal impedance.

Therefore, for consistent comparison purposes, the balun should be tested with a generator having an internal impedance equal to the nominal value for which the balun was designed to obtain the required impedance transformation. In the usual television practice this value is nominally 300 ohms.

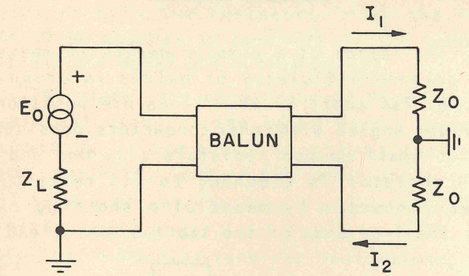

Fig. 2(a) – Block diagram of balun joining an unbalanced mode generator to a balanced load.

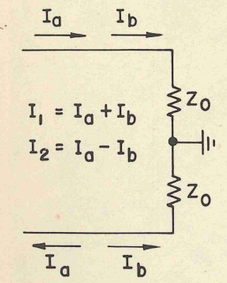

Fig. 2(b) – Resolving the load currents into push-pull and push-push components.

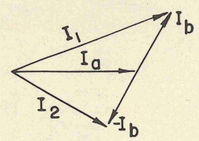

Fig. 2(c) – Vector diagram of the load current components.

If desired, the balun may be used and tested with energy flowing in the opposite direction as shown in Fig. 2a.

Here the balun joins an unbalanced mode generator to a balanced load. Using the reciprocity theorem, the voltages and currents of Fig. 1a are transposed as in Fig. 2a. In the general case, the unequal load currents I_1 and I_2 may be resolved into push-pull components I_a, and push-push components, I_b, as shown in Fig. 2b. Fig. 2c diagrams the vector relationship of the output currents. It is obvious that a simple volt-meter measurement of the output voltages to ground is not sufficient to indicate the balance quality since the relative phase is not taken into account.

Solving for I_b and I_a:

$$I_b = \frac{I_1 - I_2}{2} \tag{5}$$

and

$$I_a = \frac{I_1 + I_2}{2} \tag{6}$$

Therefore

$$\left| \frac{I_b}{I_a} \right| = \left| \frac{I_1 - I_2}{I_1 + I_2} \right| = R \tag{7}$$

Eq. (7) shows that the same ratio R may be obtained as in the previous discussion by measuring the push-push and push-pull components of the output currents. The balanced load impedance in this case must again be equal to the nominal balanced value for which the balun was designed.

The standard procedure thus described for obtaining the balance efficiency is summarized as follows:

If the balun is used to join a balanced generator to an unbalanced load, the internal impedance of the test generator is made equal to the designed balanced impedance of the test balun. The ratio R of the balun output voltages (or currents) is measured for push-push and push-pull driving voltages as in Figs. 1b and 1a, respectively.

If the balun is used to join an unbalanced generator to a balanced load, the ratio R of the unbalanced and balanced components of the output currents is determined. The balanced load in this case must be equal to the impedance for which the balun was designed.

Having determined the ratio R, the balance efficiency is calculated as in Eq. (2).

A typical example of the balance efficiency plotted against frequency is shown in Fig. 3.

An advantage in expressing the quality of balance in this manner is seen in the above

example where the relative absolute magnitudes of the measurements for either type of balun application are apparent at any frequency.

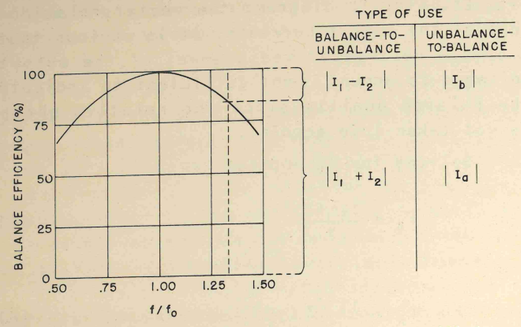

Fig. 3 – A typical example of the balance efficiency plotted vs frequency.

It will be noted again that the balance efficiency measured as outlined is not necessarily the same as that obtained in actual practice since a given antenna system may not conform to the described conditions. Nevertheless, this procedure is valuable in affording a means of accurately comparing different baluns. Future field use may establish some practical lower limit of balance efficiency as measured in this manner.

One means of experimentally determining the data required for calculating the balance efficiency is given by Tomiyasu.[1] Another variation is described below.

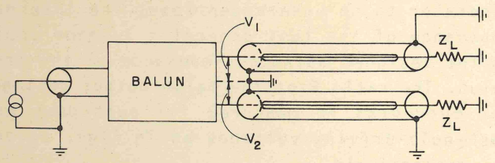

Fig. 4 – Double measuring line method of measuring the balance efficiency.

The balanced output leads of the balun connect to the inner conductors of two slotted coaxial measuring lines as shown in Fig. 4. The characteristic impedance of the two lines is equal to their terminating loads.

As the lines are identical and matched, the relative absolute magnitudes of the output voltages, V_1 and V_2, are found by sampling each line with a probe and receiver.

The phase relationship is measured by the use of two adjustable probes joined by equal length lines to the receiver. The probe depth and position on each of the lines are adjusted for zero receiver indication. Since the phase shift is linear on the two matched lines, the relative phase difference between V_1 and V_2 may be calculated.

Hence, from Eq. (7):

$$R = \left|\frac{I_1 - I_2}{I_1 + I_2}\right| = \left|\frac{V_1 - V_2}{V_1 + V_2}\right| \qquad (8)$$

These methods, however, are cumbersome and require special slotted lines.

The Balance Comparator

The layout of a simpler device to measure the balance efficiency of baluns is drawn in Fig. 5. Two short coaxial lines are positioned at right angles with inner conductors consisting of two small carbon resistors (Z). One end of each resistor is grounded to its respective outer conductor by means of a shorting disc (C). The free ends of the two resistors lead to

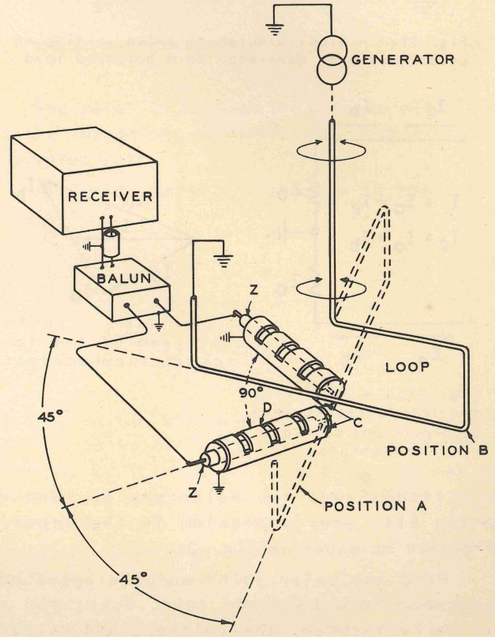

Fig. 5 – Schematic diagram of balance comparator.

the balanced terminals of the balun under test. The outer conductors of the coaxial lines and the balun ground terminal are joined together. The coaxial or unbalanced terminals of the balun connect to a receiver or other indicator.

A generator connects to a single-turn loop that may be rotated on an axis perpendicular to the plane of the two coaxial lines. A number of saw-cuts (D) in each of the coaxial lines provide electrostatic shielding but permit electromagnetic coupling between the loop and resistors. The extension of the resistor axes and the axis of loop rotation intersect in a common point.

With the loop bisecting the right angle formed by the two coaxial lines (position B), equal in-phase voltages are effectively induced in series with the resistors. With the loop rotated 90 degrees to position A, the induced voltages are equal and out-of-phase.

Therefore, the conditions of Figs. 1a and 1b are satisfied if the value of the coaxial resistors, Z, are equal to one-half of the normal operating load of the balun under test.

In operation, the loop is simply rotated to positions B and A, and from the ratio (R) of the corresponding receiver indications, the balance efficiency is calculated by Eq. (2).

As described in the preceding section, identical results will be obtained if the receiver and generator are interchanged.

It is seen that the relative magnitude of the currents I_1 and I_2 of Fig. 2a may also be found by rotating the loop to the 45-degree positions such that it is parallel to each of the resistors, R, of Fig. 5 in turn. Hence the relative phases of the vectors of Fig. 2c may be calculated.

Another application of the device may be in determining the operating characteristics of circuits other than baluns. For example, it might be desired to feed two networks with in-phase or push-push currents only from a common generator. The balance comparator could then be used to determine the extent to which the desired conditions were obtained.

Front and back photographs of the balance comparator are illustrated in Figs. 6 and 7, respectively. Fig. 6 shows the rotating loop housing with the loop coaxial connector. The ungrounded resistor terminals are seen extending from the top of the comparator assembly in the back view of Fig. 7.

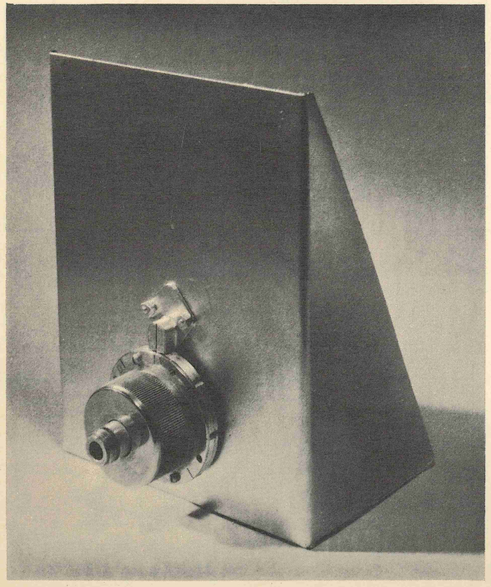

Fig. 6 – Front view of balance comparator.

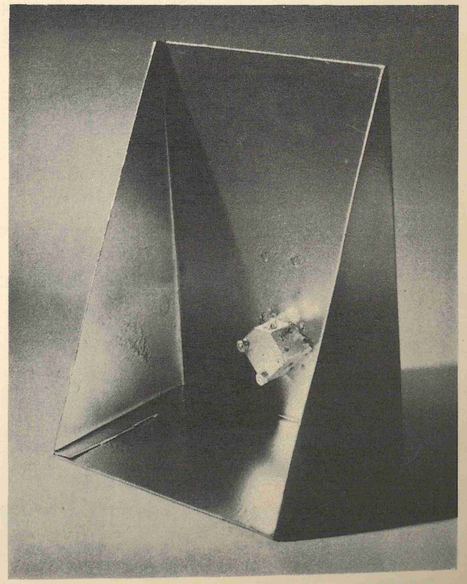

Fig. 7 – Rear view of balance comparator.

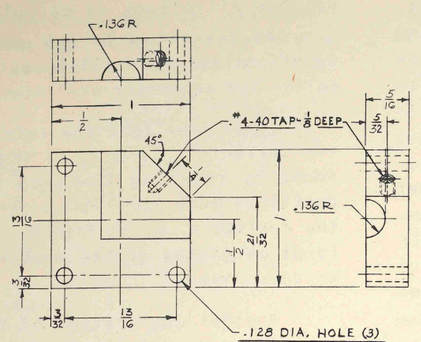

(1) MAT'L. – BRASS

D-229806

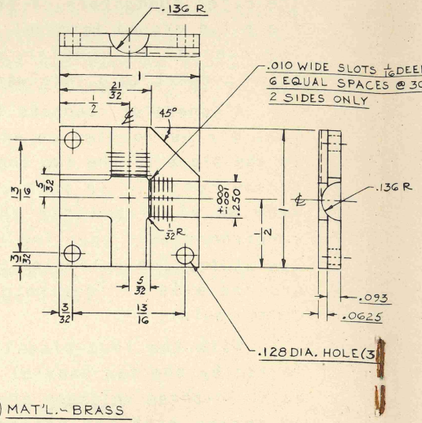

(2) MAT'L. – BRASS

D-229806

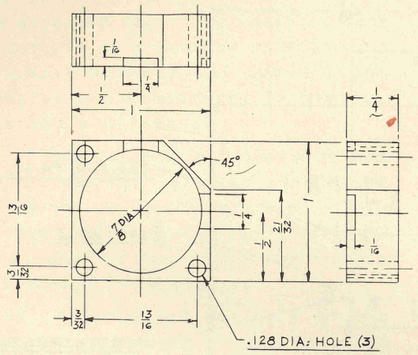

(3) MAT'L. – BRASS

D-229806

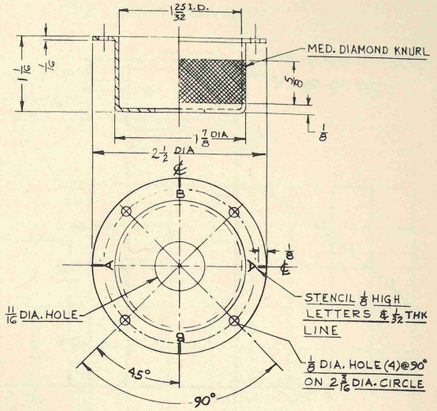

(4) MAT'L. – BRASS

D-229806

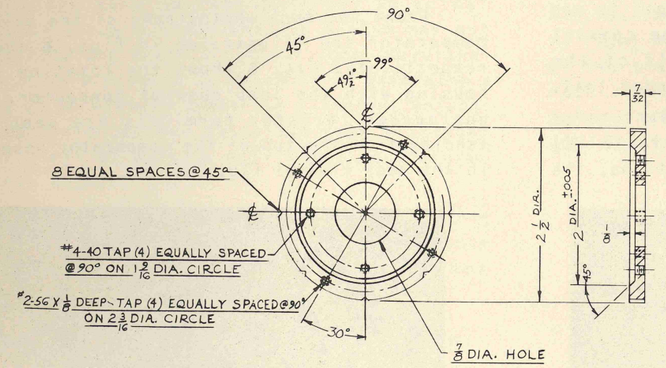
8 EQUAL SPACES @ 45°
#4-40 TAP (4) EQUALLY SPACED @ 90° ON 1 5/16 DIA. CIRCLE
#2-56 X ⅛ DEEP TAP (4) EQUALLY SPACED @ 90° ON 2 3/16 DIA. CIRCLE
⅞ DIA. HOLE

(5) MAT'L. – BRASS

D-229806

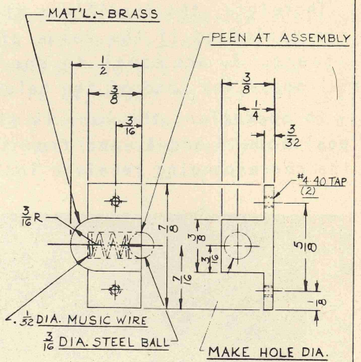

(6) SUB-ASSEM.

D-229806

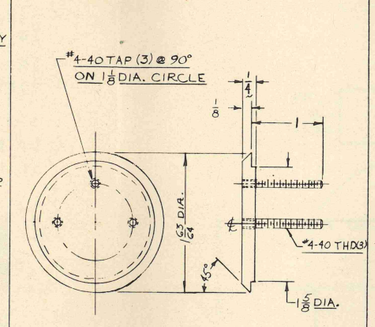

(7) MAT'L. – BRASS

D-229806

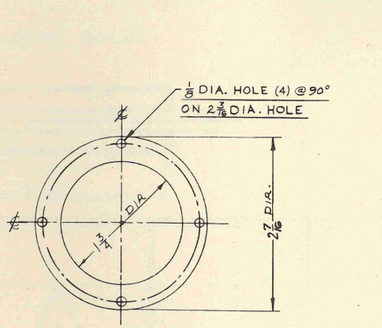

(8) MAT'L. – 1/32 THK. BRASS

D-229806

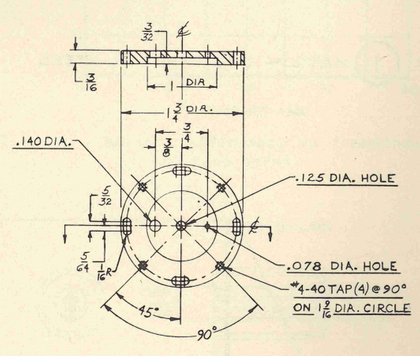

(9) MAT'L. – BRASS

D-229806

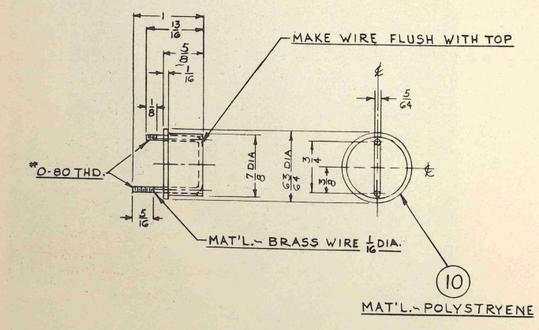

(10) MAT'L. – POLYSTRYENE

D-229806

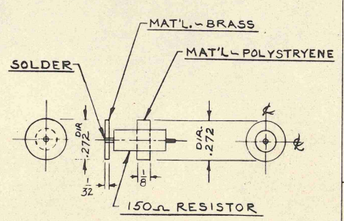

(11) SUB-ASSEMBLY

D-229806

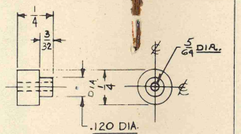

(12) MAT'L. – POLYSTRYENE

D-229806

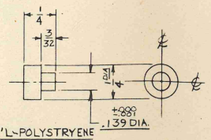

(13) MAT'L. – POLYSTRYENE

D-229806

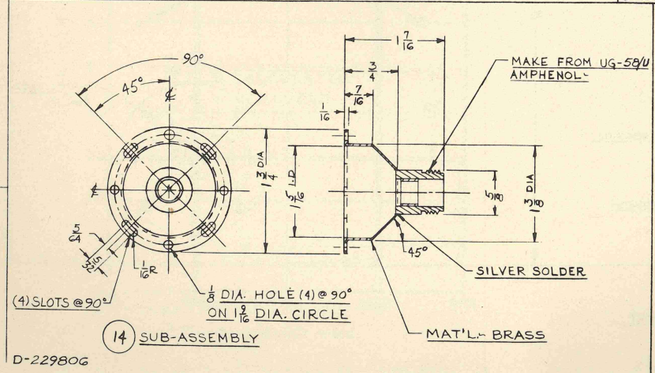

(14) SUB-ASSEMBLY

D-229806

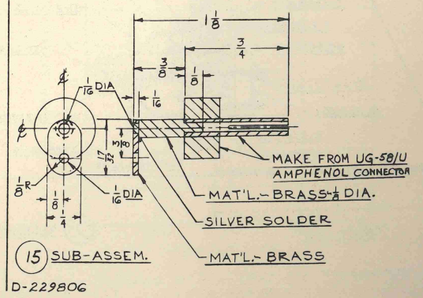

(15) SUB-ASSEM.

D-229806

Fig. 8 – Mechanical details of the balance comparator.

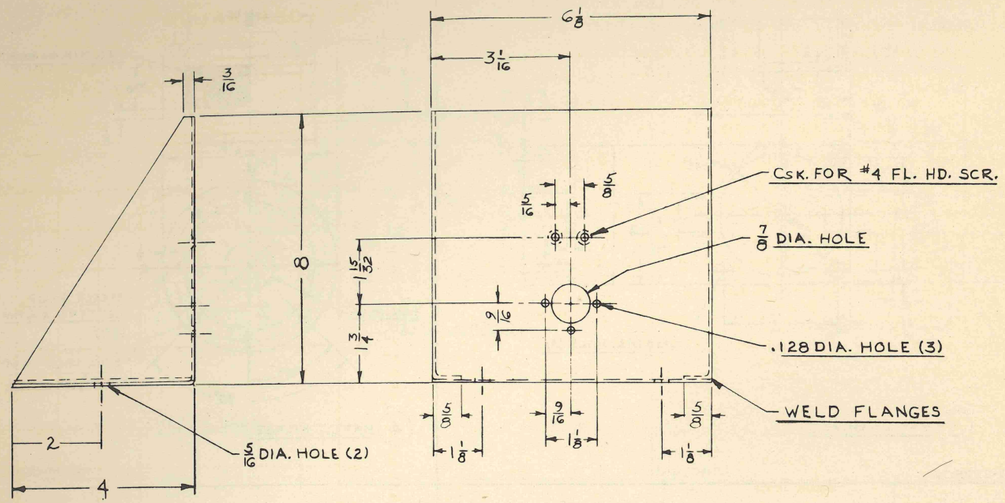

(1) MAT'L.– .046 THK. C.R. STEEL

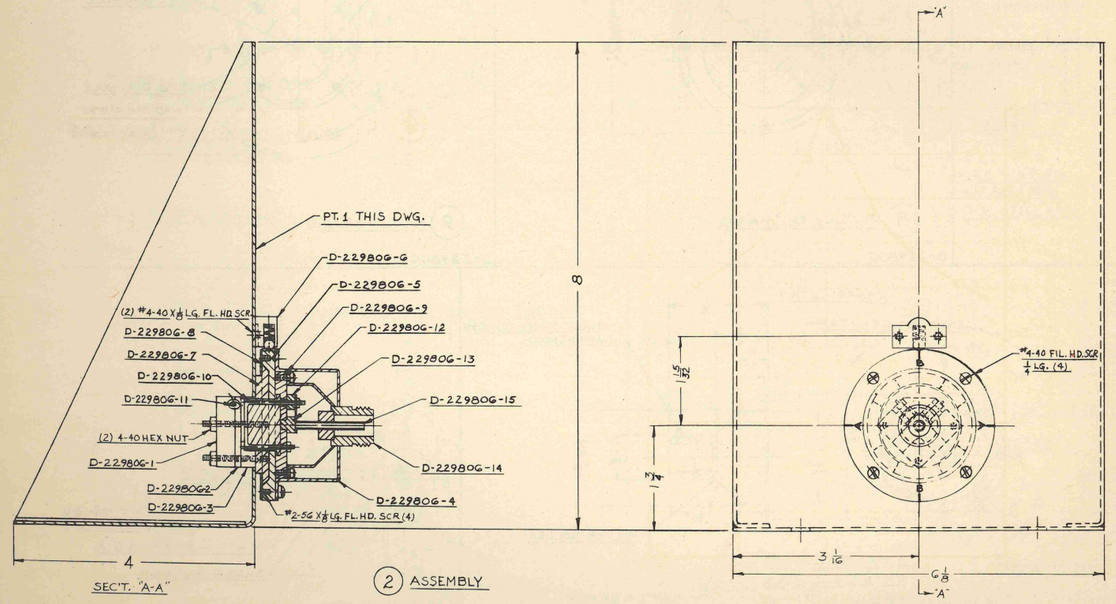

Fig. 9 – Assembly of the balance comparator.

The test balun is mounted on the vertical support plate directly above the resistor terminals. Considerable care must be exercised in maintaining short symmetrical connections between the balun and comparator terminals, especially in the u-h-f band.

As most of the baluns in television use are designed for nominal balanced impedances of 300 ohms, 150-ohm resistors were used in the balance comparator. However, the resistor block assembly is designed so that other values may be easily substituted if necessary.

Mechanical details and assembly of the balance comparator are given in the drawings of Figs. 8 and 9.

Balun Tests

λ/4 SLEEVE BALUN

30.6 OHMS CHARACTERISTIC IMPEDANCE

Fig. 10 – Balance efficiency vs frequency of λ/4 sleeve balun.

λ/2 LOOP BALUN

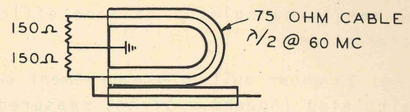

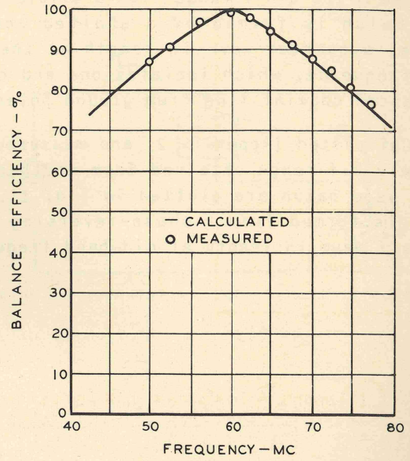

Fig. 11 – Balance efficiency vs frequency of λ/2 loop balun.

SLOTTED BALUN

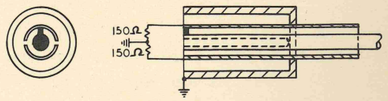

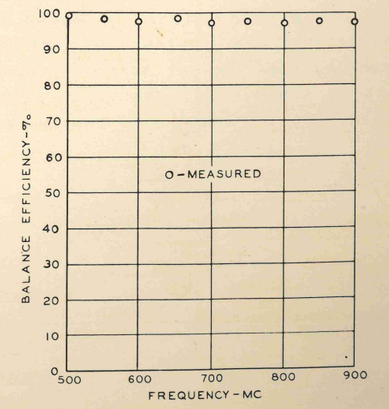

Fig. 12 – Balance efficiency vs frequency of slotted balun.

In order to check the accuracy of the device, measurements were taken on baluns having easily calculated balance efficiency characteristics.

Fig. 10 shows quite close agreement between the calculated (Appendix 1) and measured data obtained in the u-h-f range from a simple balun. This balun is formed by a shorted coaxial sleeve, a quarter-wave in length at the mid-band frequency, which isolates one end of the unbalanced coaxial line from ground potential.

Calculated (Appendix 2) and measured data in the v-h-f range obtained from another commonly used balun are plotted in Fig. 11. This balun is formed from a phase-reversing cable one-half wave in length at mid-band frequency.

The balance characteristics of both types of baluns are seen to be rather sharp in terms of wide-band coverage.

A further check (Fig. 12) was provided by measurements taken on a balun known to be balanced independent of frequency change. This balun consists of two diametrically opposite slots cut in the outer conductor of the unbalanced coaxial line and the inner conductor shorted at the open end to one of the line sections produced by the slot. The slots are one-quarter wave in length at the mid-band frequency for the best impedance characteristic. A quarter-wave sleeve may enclose the slotted assembly as shown in Fig. 12 to provide shielding and a ground terminal near the balanced leads.

O. M. Woodward Jr.

O. M. Woodward, Jr.

Appendix I

Balance Efficiency Calculation of Sleeve Balun

The sleeve balun is formed by a shorted sleeve, one-quarter wave in length at mid-band frequency, around the end of a coaxial line as shown in Fig. 13

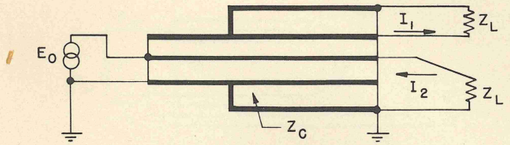

Fig. 13 – Schematic diagram of λ/4 sleeve balun feeding a balanced load.

where Z_c is the characteristic impedance of the line formed by the sleeve and the outer conductor of the coaxial line; θ is its length in electrical degrees; $2Z_L$ is the balanced load impedance.

The reactance presented by the end of the sleeve stub is:

$$Z_s = +jZ_c \tan \theta$$

The equivalent electrical circuit is given in Fig. 14, from which

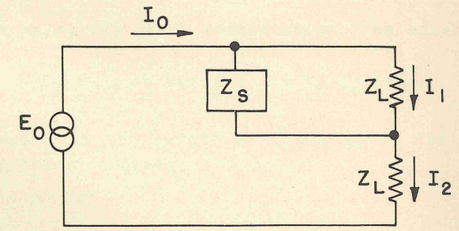

Fig. 14 – Equivalent electrical circuit.

$$I_o = I_2 = \frac{E_o}{Z_L + (Z_L Z_s / Z_L + Z_s)}$$

and

$$I_1 = \frac{E_o (Z_s / Z_L + Z_s)}{Z_L + (Z_L Z_s / Z_L + Z_s)}$$

Hence

$$R = \left| \frac{I_1 - I_2}{I_1 + I_2} \right| = \left| \frac{(Z_s/Z_L + Z_s) - 1}{(Z_s/Z_L + Z_s) + 1} \right| = \left| \frac{-1}{1 + (2Z_s/Z_L)} \right|$$

and the balance efficiency $= \frac{100}{1+R}$

From this it is seen that the balance bandwidth is broadened as the ratio Z_s/Z_L is increased. The greatest unbalance occurs when Z_s, and hence I_1, approaches zero. For I_1 to be zero, the components I_a and I_b must be equal and opposite in that leg of the load. Hence the ratio R is unity and the minimum balance efficiency becomes 50 per cent for this particular balun.

Appendix II

Balance Efficiency Calculation of Half-Wave Balun

This balun is formed from a phase-reversing cable one-half wave in length at mid-band frequency as shown in Fig. 15.

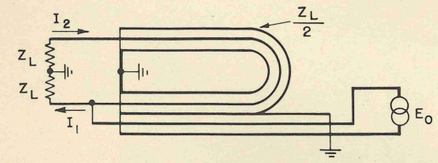

Fig. 15 - Schematic diagram of λ/2 balun feeding a balanced load.

With a balanced load, $2Z_L$, of 300 ohms, the 75-ohm characteristic impedance of the half-wave cable is equal to $Z_L/2$.

Rearranging the circuit as given in Fig. 16,

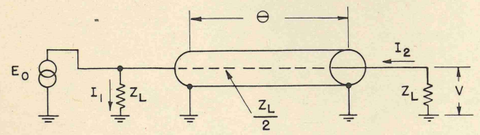

Fig. 16 - Equivalent electrical circuit.

from which

$$I_1 = E_0/Z_L$$

and using the usual transmission line equation;

$$-E_0 = I_2 Z_L \cos\theta + j \tfrac{1}{2} I_2 Z_L \sin\theta$$

where θ is the length of the phasing cable in electrical degrees.

Solving for

$$I_2 = \frac{-E_0}{Z_L (\cos\theta + j \tfrac{1}{2} \sin\theta)}$$

Then

$$R = \left|\frac{I_1 - I_2}{I_1 + I_2}\right| = \left|\frac{(\cos\theta + 1) + j \tfrac{1}{2} (\sin\theta)}{(\cos\theta - 1) + j \tfrac{1}{2} (\sin\theta)}\right|$$

from which the balance efficiency is calculated as before. A minimum balance efficiency of 0 per cent is obtained for phasing cables an integral number of wavelengths long.

The greatest impedance bandwidth is obtained from this type of balun when the phasing cable is matched, or equal to one-half of the balanced load impedance. However, it can be shown that the greatest balance bandwidth is obtained when the ratio of the load impedance to the phasing line impedance is made as large as possible.

RCA

LB-845

COMPOUND DIRECT

RADIATOR LOUDSPEAKER

Property of
Albert E. Linden

RADIO CORPORATION OF AMERICA
RCA LABORATORIES DIVISION
INDUSTRY SERVICE LABORATORY

RADIO CORPORATION OF AMERICA

RCA LABORATORIES DIVISION

INDUSTRY SERVICE LABORATORY

LB-845

Compound Direct Radiator Loudspeaker

This report is the property of the Radio Corporation of America and is loaned for confidential use with the understanding that it will not be published in any manner, in whole or in part. The statements and data included herein are based upon information and measurements which we believe accurate and reliable. No responsibility is assumed for the application or interpretation of such statements or data or for any infringement of patent or other rights of third parties which may result from the use of circuits, systems and processes described or referred to herein or in any previous reports or bulletins or in any written or oral discussions supplementary thereto.

Approved

Stuart W. Seeley

Compound Direct Radiator Loudspeaker

Introduction

The completely closed cabinet as a mounting arrangement for a direct radiator loudspeaker mechanism is generally accepted as superior in performance to that of the open back cabinet. The open back cabinet of conventional dimensions exhibits a serious resonance which accentuates the response at a relatively high frequency in the low frequency range. In addition, the low frequency response is highly attenuated below the resonant frequency. On the other hand, the response at the resonant frequency of a completely closed cabinet of conventional dimensions is not as severely accentuated as in the open back cabinet. In addition, the resonant frequency occurs at a lower frequency than the corresponding open back cabinet. It is for these reasons that the closed cabinet with or without a port has become the standard for high quality sound reproduction in the home, monitoring in broadcasting, television and recording studios, and in other small scale sound reproducing applications.

One of the objections to the closed loudspeaker cabinet with or without a port is the large size required to maintain the response in the low frequency range. There are many applications requiring high fidelity sound reproducing systems in which the cabinet space allocated to the loudspeaker is limited, as for example, combination instruments including television, radio and phonograph in a single integrated unit, built-in custom installations, monitoring loudspeakers in some locations in broadcasting and television applications, etc. As a consequence it is impossible to obtain wide frequency range, high quality sound reproduction for these applications.

In order to obtain adequate low frequency response in a small completely enclosed cabinet some means must be provided for increasing the effective volume of the cabinet. The effective volume of a cabinet may be increased by decreasing the stiffness presented to the radiating loudspeaker mechanism by the cabinet in the low frequency range. It is possible to reduce the effective stiffness of the cabinet by the use of an auxiliary loudspeaker mechanism which drives the radiating loudspeaker mechanism. This system has been termed a compound direct radiator loudspeaker. It is the purpose of this bulletin to describe a compound direct radiator loudspeaker.

Direct Radiator Loudspeaker Mechanism Mounted in a Closed Cabinet

The first consideration will be the relation between the dimensions of the loudspeaker and cabinet and the low-frequency response of a direct radiator loudspeaker mechanism operating in a completely enclosed cabinet. This analysis will show the limitations of the system from the standpoint of the volume of the cabinet and the characteristics of the loudspeaker mechanism.

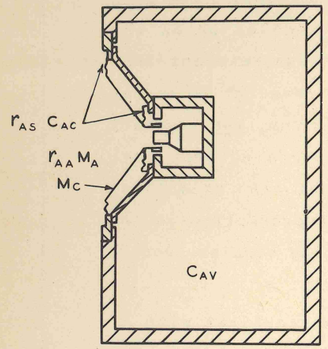

SECTIONAL VIEW

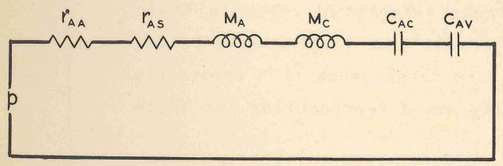

ACOUSTICAL CIRCUIT

Fig. 1 – Sectional view and acoustical circuit of a direct radiator loudspeaker mechanism mounted in a closed cabinet. In the acoustical circuit: p = driving pressure. r_{AA} = acoustical radiation resistance. r_{AS} = acoustical resistance of the suspension system. M_A = inertance of the air load. M_C = inertance of the cone and coil. C_{AC} = acoustical capacitance of the suspension system. C_{AV} = acoustical capacitance of the cabinet.

A sectional view and the acoustical circuit of a direct radiator loudspeaker mechanism mounted in an enclosed cabinet are shown in Fig. 1. The voice coil electrical circuits of the loudspeaker of Fig. 1 are shown in Fig. 2. A photograph of a 12-inch direct radiator loudspeaker mechanism mounted in a closed cabinet having a volume of two cubic feet is shown in Fig. 3. The total acoustical impedance z_{AT}, in acoustical ohms, of the vibrating system of Fig. 1 is given by

$$z_{AT} = r_{AA} + r_{AS} + j\omega M_A + j\omega M_C - j/\omega C_{AC} - j/\omega C_{AV} \qquad (1)$$

where r_{AA} = acoustical resistance due to air load, in acoustical ohms,

r_{AS} = acoustical resistance of the suspension system, in acoustical ohms,

M_A = inertance of the air load upon the cone, in grams per (centimeter)^4,

M_C = m_c/A^2 = inertance of the cone and coil, in grams per (centimeter)^4,

A = Area of the cone, in square centimeters,

m_c = mass of the cone and coil, in grams,

C_{AC} = acoustical capacitance of the suspension system, in (centimeter)^5 per dyne,

C_{AV} = $V/\rho c^2$ = acoustical capacitance of the volume of the cabinet, in (centimeter)^5 per dyne,

ρ = density of air, in grams per cubic centimeter,

c = velocity of sound, in centimeters per second,

V = volume of the cabinet, in cubic centimeters,

The volume current $\dot{X}$, in cubic centimeters per second, in the system is given by

$$\dot{X} = \frac{p}{z_{AT}} = \frac{p}{r_{AA} + r_{AS} + j\omega M_A + j\omega M_C - j/\omega C_{AC} - j/\omega C_{AV}} \qquad (2)$$

where $p = f_M/A$ = pressure developed by the voice coil, in dynes per square centimeter,

f_M = Bli = force developed in the voice coil, in dynes,

B = flux density in the air gap, in gausses,

l = length of the voice coil conductor, in centimeters,

i = current in the voice coil, in abamperes,

A = area of the cone, in square centimeters

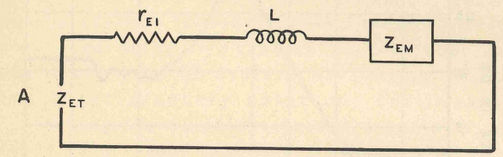

ELECTRICIAL CIRCUIT

Fig. 2 (A) – Electrical circuit of the voice coil of the mechanism of Fig. 1. z_{ET} = total electrical impedance of the voice coil. r_{E_1} = electrical resistance of the voice coil. L_1 = inductance of the voice coil. z_{EM_1} = motional electrical impedance of the voice coil.

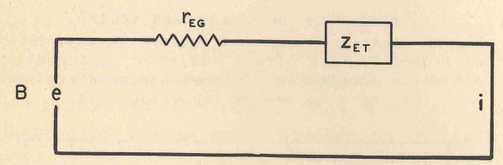

ELECTRICIAL CIRCUIT

Fig. 2 (B) – Electrical circuit of the generator and voice coil. e = open circuit voltage of the generator. r_{EG} = electrical resistance of the generator. i = current in the circuit.

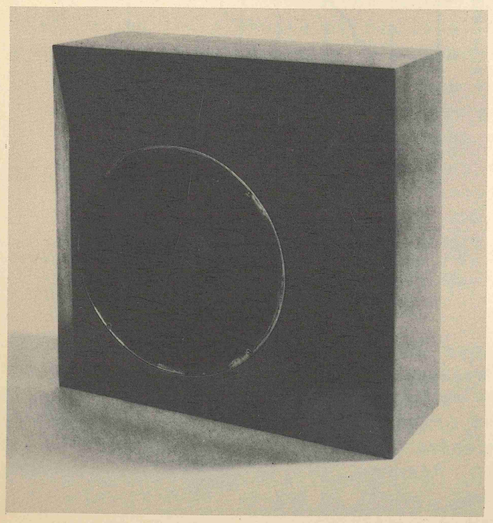

Fig. 3 – Photograph of a twelve inch direct radiator loudspeaker mechanism mounted in a closed cabinet having a volume of two cubic feet.

The motional electrical impedance z_{EM_1}, in abohms, of the voice coil is given by

$$z_{EM_1} = \frac{(Bl)^2}{z_{AT}A^2} \qquad (3)$$

The electrical circuit of the voice coil is shown in Fig. 2A. The total electrical impedance z_{ET}, in abohms, of the voice coil is given by

$$z_{ET} = r_{E_1} + j\omega L_1 + z_{EM_1} \qquad (4)$$

where r_{E_1} = electrical resistance of the voice coil, abohms, and

L_1 = inductance of the voice coil in abhenries.

The electrical circuit of the voice coil and generator is shown in Fig. 2B. The electrical current i, in abamperes, is given by

$$i = \frac{e}{r_{EG} + z_{ET}} \qquad (5)$$

where e = open circuit voltage of the generator, in abvolts and

r_{EG} = electrical resistance of the generator, in abohms.

The acoustical power output P, in watts, is given by

$$P = r_{AA}\dot{X}^2 \cdot 10^{-7} \qquad (6)$$

The performance of a dynamic direct radiator loudspeaker mounted in a completely enclosed cabinet can be predicted from Eqs. 1 to 6 inclusive. To show the effect of the volume of the cabinet upon the response of a direct radiator dynamic loudspeaker mechanism the theoretical and experimental performance of a typical 12-inch loudspeaker mechanism mounted in an enclosed cabinet will be described. The specifications of the loudspeaker mechanism used in these tests are as follows: Effective diameter of the cone = 10.5 inches. Mass of the cone, voice coil and air load = 25.5 grams. Length of the voice coil conductor = 522 centimeters. Electrical resistance of the voice coil = 2.8×10^9 abohms. Inductance of the voice coil = 8.9×10^4 abhenries. Flux density in the air gap = 10,000 gausses. Resonant

frequency of the mechanism = 70 cycles. The acoustical resistance of the suspension system = 0.003 acoustical ohms. The generator electrical resistance = 1.4×10^9 abohms. The acoustical radiation resistance of the air load upon the cone can be obtained from the conventional formulas[1] for these quantities. The performance may be predicted from the above data and the cabinet volume.

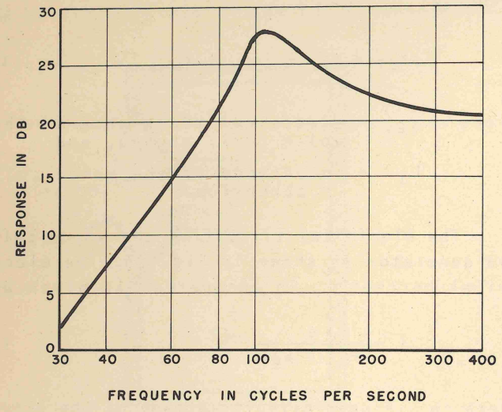

Fig. 4 – Theoretical response frequency characteristic of a twelve inch direct radiator loudspeaker mechanism mounted in a closed cabinet having a volume of two cubic feet.

The theoretically determined acoustical power output characteristic of the above mechanism operating in cabinet of two cubic feet is shown in Fig. 4. The corresponding experimentally determined acoustical output characteristic is shown in Fig. 5. The experimentally determined response of the same system but with damping material in the cabinet is shown in Fig. 6. Referring to Figs. 5 and 6 it will be seen that the combined resonant frequency of the cabinet and mechanism is 113 cycles. The response falls off quite rapidly below 90 cycles. Therefore, the low-frequency performance of the 12-inch direct radiator loudspeaker mechanism in a cabinet of two cubic feet is not satisfactory for a high quality reproducing system.

There are many expedients that may be employed to increase the low-frequency range of the combination of a direct radiator loudspeaker mechanism mounted in a completely enclosed cabinet. These systems will be described below.

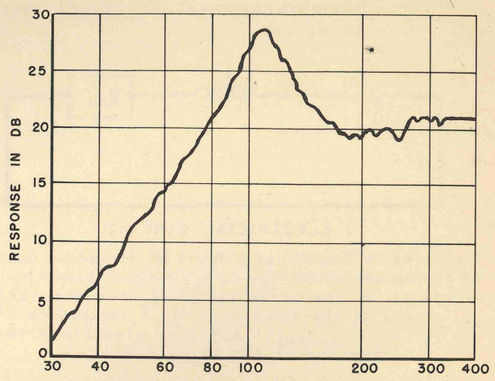

Fig. 5 – Measured response frequency characteristic of a twelve inch direct radiator loudspeaker mechanism mounted in a closed undamped cabinet having a volume of two cubic feet.

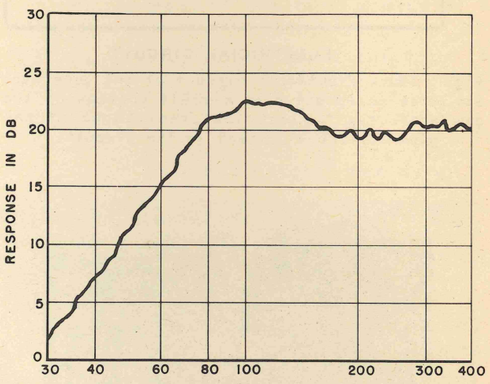

Fig. 6 – Measured response frequency characteristic of a twelve inch direct radiator loudspeaker mechanism mounted in a closed damped cabinet having a volume of two cubic feet.

Referring to Eq. (1) it will be seen that the resonant frequency of the combination of the mechanism and the cabinet can be lowered and hence the low-frequency response range extended by increasing the volume of the cabinet. However, as previously pointed out, a large cabinet is not suitable or possible for some applications.

The resonant frequency of the system consisting of the mechanism and cabinet can be

[1] Olson, ELEMENTS OF ACOUSTICAL ENGINEERING, D. Van Nostrand Company, New York, N. Y., 1947.

lowered by increasing the compliance of the suspension of the vibrating system of the mechanism. However, even if the stiffness of the suspension system were made zero, that is, an infinite compliance, the resonant frequency of the 12-inch loudspeaker mechanism described above operating in a cabinet of two cubic feet would still be 88 cycles. Obviously, this is not a satisfactory solution. Furthermore, decreasing the stiffness beyond a certain value leads to a ragged response frequency characteristic in the mid-frequency range due to "break up" of the limp suspension system.

The resonant frequency of the combination of loudspeaker mechanism and cabinet can be lowered by increasing the inertance of the cone. The inertance of the cone of the mechanism described above can be increased by increasing the mass of the cone and voice coil. In order to obtain a resonant frequency of 72 cycles in a cabinet of two cubic feet with the same suspension system would require an increase in mass of $2\frac{1}{2}$ times. Since the air load mass is unchanged this would require an increase in mass of the cone and voice coil of approximately 4 times. This system is impractical from the standpoint of efficiency and response.

The inertance of the cone can be increased by decreasing the diameter of the cone. Decreasing the diameter of the cone in the mechanism described above by a factor of one half but retaining the same voice coil will increase the inertance by 3.6 times. A mechanism employing this cone will give satisfactory response in the low-frequency range. However, for the same output the amplitude of the smaller cone will be four times that of the larger cone. If large outputs are not required this is a satisfactory solution.

An examination of the above loudspeaker systems for improving the low-frequency response indicates that there is a deviation from the conventional systems. It appears that a practical solution for this problem would be the addition of some means to a conventional loudspeaker mechanism so that the performance would be equivalent to that of a large cabinet. It is the purpose of the next section to describe an adjunct which accomplishes this result.

Compound Direct Radiator Loudspeaker

One solution of the problem of maintaining adequate response in the low-frequency region in a small closed cabinet is to employ some means for reducing the stiffness presented to the cone of the loudspeaker mechanism by the cabinet. This can be accomplished by employing a second loudspeaker mechanism with a small cone coupled to the first loudspeaker mechanism with the large radiating cone. This system has been termed a compound direct radiator loudspeaker.

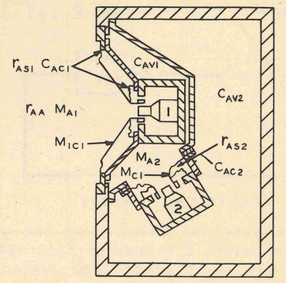

SECTIONAL VIEW

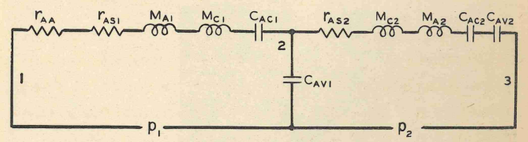

ACOUSTICAL NETWORK

Fig. 7 – Sectional view and acoustical circuit of a compound direct radiator loudspeaker mounted in a closed cabinet. In the acoustical circuit: p_1 and p_2 = driving pressure of mechanism 1 and 2. r_{AA} = acoustical radiation resistance. r_{AC_1} and r_{AC_2} = acoustical resistance of the suspensions of mechanisms 1 and 2. M_{A_1} and M_{A_2} = inertances of cones and voice coils of mechanisms 1 and 2. C_{AS_1} and C_{AS_2} = acoustical capacitances of the suspensions of mechanisms 1 and 2. C_{AV_1} = acoustical capacitance of the volume between the loudspeaker mechanisms 1 and 2. C_{AV_2} = acoustical capacitance of the volume behind loudspeaker mechanism 2.

A sectional view and the acoustical network of the compound direct radiator loudspeaker system are shown in Fig. 7. The electrical circuits of the loudspeaker system of Fig. 7 are shown in Fig. 8. A photograph of the components of a compound direct radiator loudspeaker is shown in Fig. 9.

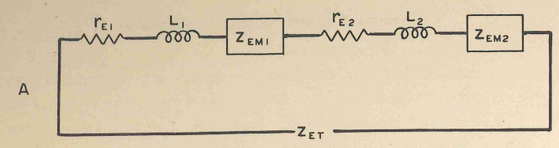

ELECTRICAL CIRCUIT

Fig. 8 (A) – Electrical circuit of the voice coils of mechanisms 1 and 2 of Fig. 7 connected in series. z_{ET} = total electrical impedance. r_{E_1} = electrical resistance of the voice coil of mechanism 1. L_1 = inductance of the voice of mechanism 1. z_{EM_1} = motional electrical impedance of the voice coil of mechanism 1. r_{E_2} = electrical resistance of the voice coil of mechanism 2. L_2 = inductance of the voice coil of mechanism 2. z_{EM_2} = motional electrical impedance of voice coil 2.

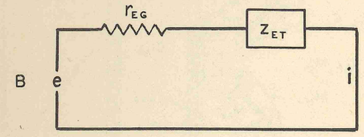

ELECTRICAL CIRCUIT

Fig. 8 (B) – Electrical circuit of the generator and voice coils. e = open circuit voltage of the generator. r_{EG} = electrical resistance of the generator. i = current in the circuit.

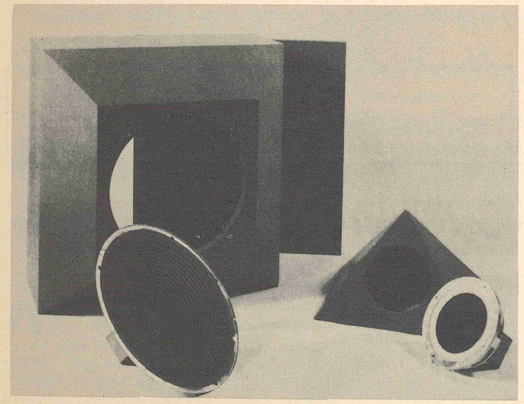

Fig. 9 – Photograph of the components of a compound direct radiator loudspeaker showing the 12-inch and the 5-inch loudspeaker mechanisms, the coupler and a closed cabinet having a volume of two cubic feet.

The volume current $\dot{X}_1$, in cubic centimeters per second, in branch 1 of Fig. 7, is given by

$$\dot{X}_1 = \frac{p_1(z_{A2} + z_{A3})}{D} + \frac{p_2(z_{A2})}{D} \qquad (7)$$

where p_1 = pressure delivered by loudspeaker 1, in dynes per square centimeter,

p_2 = pressure delivered by loudspeaker 2, in dynes per square centimeter,

$D = z_{A_1}z_{A_2} + z_{A_1}z_{A_3} + z_{A_2}z_{A_3}$

$z_{A_1} = r_{AA} + r_{AS_1} + j\omega M_{A_1} + j\omega M_{C_1} - j/\omega C_{AC_1}$

$z_{A_2} = - j/\omega C_{AV_1}$

$z_{A_3} = r_{AS_2} + j\omega M_2 - j/\omega C_{AC_2} - j/\omega C_{AV_2}$

r_{AA} = acoustical resistance due to the air load, upon the cone of loudspeaker 1, in acoustical ohms,

r_{AS_1} = acoustical resistance of the suspension of loudspeaker 1, in acoustical ohms,

M_{A_1} = inertance of the air load upon the cone of loudspeaker 1 in grams per (centimeter)^4,

M_{C_1} = inertance of the cone and coil of loudspeaker 1, in grams per (centimeter)^4,

C_{AC_1} = acoustical capacitance of the suspension system of loudspeaker 1, in (centimeter)^5 per dyne,

C_{AV_2} = acoustical capacitance of the volume behind loudspeaker 2, in (centimeters)^5 per dyne.

r_{AS_2} = acoustical resistance of the suspension system of loudspeaker 2, in acoustical ohms.

M_{C_2} = inertance of the cone of loudspeaker 2, in grams per (centimeter)^4,

M_{A_2} = inertance of the air load upon the cone of loudspeaker 1, in grams per (centimeter)^4,

C_{AC_2} = acoustical capacitance of the suspension of loudspeaker 2, in (centimeters)^5 per dyne,

$p_1 = f_{M_1}/A_1$ = driving pressure, in dynes per square centimeter,

$f_{M_1} = B_1 l_1 i$ = driving force, in dynes,

B_1 = flux density in the air gap of loudspeaker 1, in gausses,

l_1 = length of the voice coil conductor of loudspeaker 1, in centimeters,

A_1 = area of the cone of loudspeaker 1, in square centimeters,

i = current in the voice coil, in abamperes,

$p_2 = f_{M_2}/A_2$ = driving pressure, in dynes per square centimeter,

$f_{M_2} = B_2 l_2 i$ = driving force, in dynes

B_2 = flux density in the air gap of loudspeaker 2, in gausses,

l_2 = length of the voice coil conductor of loudspeaker 2, in centimeters,

A_2 = area of the cone of loudspeaker 2, in square centimeter.

The volume current $\dot{X}_2$, in cubic centimeters per second, in branch 3 of Fig. 5 is given by

$$\dot{X}_2 = \frac{p_2(z_{A_2} + z_{A_1}) + p_1 z_{A_2}}{D} \qquad (8)$$

Since the electrical current is the same in the voice coils of loudspeaker mechanisms 1 and 2, there follows the relation

$$p_1/p_2 = B_1 l_1 A_2 / B_2 l_2 A_1 = K \qquad (9)$$

where K = constant given by Eq. 9.

From Eqs. 7 and 9, the acoustical impedance, in acoustical ohms, at p_1 of Fig. 7 is

$$z'_{A_1} = \frac{p_1}{\dot{X}_1} = \frac{D}{z_{A_2} + \frac{z_{A_2}}{K} + z_{A_3}} \qquad (10)$$

From Eqs. 8 and 9, the acoustical impedance, in acoustical ohms, at p_2 of Fig. 7 is

$$z'_{A_2} = \frac{p_2}{\dot{X}_2} = \frac{D}{z_{A_1} + z_{A_2} + Kz_{A_2}} \qquad (11)$$

The motional electrical impedance z_{EM_1}, in abohms, of the voice coil of loudspeaker mechanism 1 is given by

$$z'_{EM_1} = (B_1 l_1)^2 / z_{A_1} A_1^2 \qquad (12)$$

The motional electrical impedance z_{EM_2}, in abohms, of the voice coil of loudspeaker mechanism 2 is given by

$$z'_{EM_2} = (B_2 l_2)^2 / z_{A_2} A_2^2 \qquad (13)$$

The electrical circuit consisting of the voice coils of loudspeaker mechanisms 1 and 2 is shown in Fig. 8A. The total electrical impedance z_{ET}, in abohms, of the voice coils of loudspeaker mechanisms 1 and 2 in series is given by

$$z_{ET} = r_{E_1} + j\omega L_1 + z_{EM_1} + r_{E_2} + j\omega L_2 + z_{EM_2} \qquad (14)$$

where r_{E_1} = electrical resistance of the voice coil of loudspeaker 1, in abohms,

L_1 = inductance of the voice coil of loudspeaker 1, in abhenries,

r_{E_2} = electrical resistance of the voice coil of loudspeaker 2, in abohms,

L_2 = inductance of the voice coil of loudspeaker 2, in abhenries

The electrical circuit of the voice coils and generator is shown in Fig. 8B. The electrical current i, in abamperes, is given by

$$i = \frac{e}{r_{EG} + z_{ET}} \qquad (15)$$

where e = voltage of the generator, in abvolts and

r_{EG} = electrical resistance of the generator, in abohms.

The acoustical output is produced by loudspeaker mechanism 1. The acoustical power output P, in watts, is given by

$$P = r_{AA}\dot{X}_1^2 \cdot 10^{-7} \qquad (16)$$

The performance of the compound direct radiator loudspeaker can be determined from Eqs. 7 to 16 inclusive. To demonstrate the effectiveness of the compound loudspeaker in extending the low frequency range, the loudspeaker mechanism described in the preceding section was used as the radiating loudspeaker and designated as 1 in the compound loudspeaker system of Fig. 7. The total cabinet volume was two cubic feet. The volume behind the loudspeaker mechanism was 1.8 cubic feet. The specifications of the loudspeaker mechanism 2 are as follows: Effective diameter of the cone = 5 inches. Length of the voice coil conductor = 321 centimeters. Electrical re-

sistance of the voice coil = 7×10^8 abohms. Inductance of the voice coil = 2.2×10^4 abhenries. Flux density in the air gap = 11,250 gausses. The acoustical capacitance of the suspension = 0.049 (centimeters)^5 per dyne. Mass of the cone, air load and voice coil = 4 grams. The acoustical resistance of the suspension system = 0.0015 to 0.003 acoustical ohm. The generator electrical resistance = 1.7×10^9 abohms. From the above data the performance of the compound direct radiator loudspeaker may be predicted.

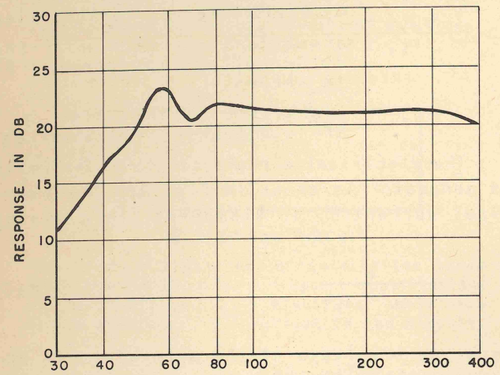

Fig. 10 – Theoretical response frequency characteristic of a compound direct radiator loudspeaker mechanism mounted in a closed cabinet of two cubic feet. The radiator is a twelve-inch mechanism.

The theoretically determined acoustical output characteristic of the compound direct radiator loudspeaker is shown in Fig. 10. The experimentally determined characteristic is shown in Fig. 11. Comparing Figs. 10 and 11 with Figs. 4, 5 and 6 it will be seen that for the same cabinet volume the low frequency range is extended by the use of the compound direct radiator loudspeaker system. As a matter of fact, the output characteristic of the compound direct radiator loudspeaker system operating in a cabinet of two cubic feet is the same as that of the single loudspeaker system operating in a very large cabinet of several cubic feet. The efficiency of the compound system in the high-frequency range is practically the same as that of loudspeaker mechanism 1 alone because the electrical impedance of loudspeaker mechanism 2 is small compared to that of loudspeaker 1 in the region above 300 cycles. Below 300 cycles the combined characteristics of the two mechanisms conspire to extend the low-frequency range and smooth out the response.

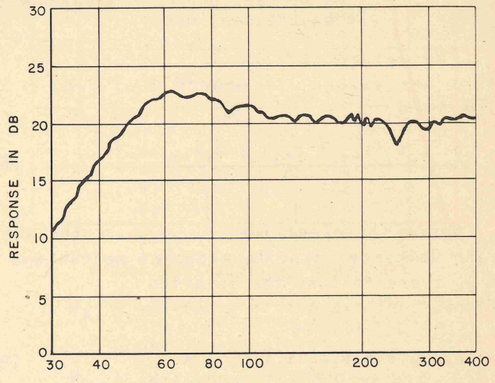

Fig. 11 – Measured response frequency characteristic of a compound direct radiator loudspeaker mechanism mounted in a closed cabinet of two cubic feet. The radiator is a twelve-inch mechanism.

The loudspeaker mechanism 2 must be capable of executing excursions four times that of loudspeaker 1 in order that the power handling capacity of the compound system will not be limited by the loudspeaker mechanism 2. Above 400 cycles mechanism 2 does not influence the response of the system. Therefore, the performance of the loudspeaker mechanism 2 in the region above 400 cycles is of no consequence. Under these conditions the entire attention as to performance of loudspeaker mechanism 2 can be confined to the low frequency region. For example, the breakup of the limp suspension system in the loudspeaker mechanism 2 in the mid and high frequency ranges is not important as would be the case if it were the radiating loudspeaker. A consideration of Fig. 7 and Eqs. 7 to 16 inclusive shows that a small amount of distortion in loudspeaker mechanism 2 will be reduced to a negligible amount by the radiating loudspeaker. These factors conspire to make the design of loudspeaker mechanism a rather simple task.

The compound direct radiator loudspeaker may be used with a closed cabinet equipped with a port and thereby increase the amplitude of the response over a portion of the low-frequency region at the expense of a higher low-frequency

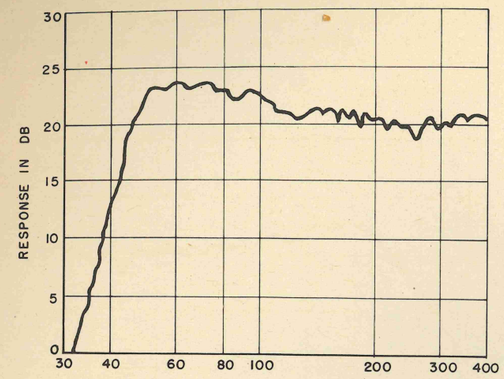

Fig. 12 – Measured response frequency characteristic of a compound direct radiator loudspeaker mechanism mounted in a closed cabinet of two cubic feet equipped with a port. The radiator is a twelve inch mechanism.

cutoff. The experimentally determined response frequency characteristic of the compound direct radiator loudspeaker operating in a closed cabinet equipped with a port is shown in Fig. 12. It will be seen that the output is increased over a closed cabinet in the region from 45 to 150 cycles. However, the low-frequency cutoff is sharper than that of a closed cabinet.

In a second application of the compound direct radiator loudspeaker, a 10-inch loudspeaker was used as the radiating loudspeaker. The total cabinet volume was one cubic foot. The response frequency characteristic of the ten inch loudspeaker mechanism mounted in a closed cabinet of one cubic foot is given by the curve A of Fig. 13. The response frequency characteristic of a compound loudspeaker system consisting of the same ten-inch loudspeaker mechanism as the radiating loudspeaker, a small

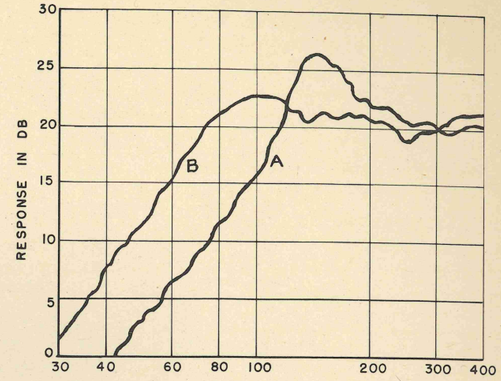

Fig. 13 (A) – Measured response frequency characteristic of a ten inch direct radiator loudspeaker mechanism mounted in a closed cabinet having a volume of one cubic foot.

Fig. 13 (B) – Measured response frequency characteristic of a compound direct radiator loudspeaker mounted in a closed cabinet having a volume of one cubic foot. The radiating mechanism is a ten inch mechanism.

second mechanism and a cabinet with a volume of one cubic foot is given by the curve B of Fig. 13.

The compound direct radiator loudspeaker as described above, provides a system for obtaining adequate low-frequency response in a cabinet of small volume. In other words, if the cabinet is restricted to a relatively small volume, the addition of a second smaller direct radiator loudspeaker mechanism supplies an adjunct, which in combination with a conventional direct radiator loudspeaker mechanism, makes it possible to obtain the same low-frequency response in a small cabinet as would be obtained with the conventional mechanism operating alone in a relatively large cabinet.

Everett G. May

Everett G. May

John Preston

John Preston

Harry F. Olson

Harry F. Olson

LB-848

ELIMINATION OF MOIRÉ EFFECTS IN TRI-COLOR KINESCOPES

Property of
Albert E. Linden

RADIO CORPORATION OF AMERICA
RCA LABORATORIES DIVISION
INDUSTRY SERVICE LABORATORY

RADIO CORPORATION OF AMERICA
RCA LABORATORIES DIVISION
INDUSTRY SERVICE LABORATORY

LB-848

Elimination of Moiré Effects in Tri-Color Kinescopes

This report is the property of the Radio Corporation of America and is loaned for confidential use with the understanding that it will not be published in any manner, in whole or in part. The statements and data included herein are based upon information and measurements which we believe accurate and reliable. No responsibility is assumed for the application or interpretation of such statements or data or for any infringement of patent or other rights of third parties which may result from the use of circuits, systems and processes described or referred to herein or in any previous reports or bulletins or in any written or oral discussions supplementary thereto.

Approved

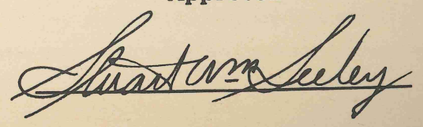

Elimination of Moiré Effects in Tri-Color Kinescopes

Introduction

Moiré effects which may arise in aperture mask tri-color kinescopes are spurious intensity variations in the picture in the nature of beat patterns between the scanning lines and the aperture array in the shadow mask. The visibility of these effects depends on the relative magnitudes of the scanning line width, mask aperture size, aperture spacing, and line separation, on the orientation of the scanning pattern relative to the mask, and, finally, on the picture content.

For the narrow aperture spacing normally employed (e.g., 215,000 apertures in a rectangular picture area of 104 square inches or 195,000 apertures in the somewhat smaller area defined by the framing mask) and for the preferred orientation of the scanning pattern, however, the moire effects are negligible. They may become noticeable, in the form of dot or bar patterns, if the aperture spacing is increased or the orientation of the scanning pattern relative to the mask is changed.

The variation in the line transmission of the mask indicates directly the degree to which the mask may distort transmitted intensity values. It increases with a reduction in the ratios of line width and aperture diameter to aperture spacing and with a departure from the preferred orientation of the scanning pattern relative to the mask. Again, for the preferred orientation and within the range of spot sizes required for optimum resolution, the variation in line transmission is negligible--one per cent or less. Furthermore, since the increase in the variation in transmission with departure from the preferred orientation is quadratic, the picture quality is insensitive to small deviations from the optimum orientation.

The Nature of the Moiré Introduced by the Mask

The introduction of the mask, with its regular hexagonal array of apertures, into the aperture mask tri-color kinescope[1] causes intensity variations in the image which are not present in a kinescope for monochrome reproduction. As long as these variations are limited to areas of the order of a picture element--as they would be, e.g., if the mask were simply bombarded by a uniform spray of electrons--they do not affect the picture; at the normal viewing distance the eye recognizes only the average brightness of a picture element and this, by assumption, is unaffected (in relative measure) by the mask.

[1] See H. B. Law, "A Three-Gun Shadow Mask Color Kinescope," *Proc. I.R.E.*, October 1951.

It will be shown that this condition applies also for actual television pictures which are formed by a set of equally spaced scanning lines, even though for uniform picture signal the intensity distribution on a kinescope screen, without mask, is not uniform. The brightness fluctuation, which is repeated identically for every line spacing, is greatest if the line width is small compared to the line spacing. Since, however, the latter lies close to the limit of visual resolution, this brightness fluctuation is scarcely perceived under normal circumstances.

The introduction of the mask, with its rows of apertures with a periodicity which differs, in general, from that of the scanning lines, will give rise to brightness fluctuations on the screen with a period which may be much greater than the spacing of either the mask aperture lines or the scanning lines. It will be assumed, to begin with, that scanning lines and mask aperture lines are aligned as shown in Fig. 1. Minimizing, in this manner, the vertical spacing of the mask-aperture lines serves to minimize the effect of the mask on vertical resolution and the prominence of spurious intensity fluctuations. The transmission of electrons through a row of apertures will be a maximum when a scanning line is centered on it; it will be least when its center line falls midway between two scanning lines. Thus, if, e.g., the spacing of the rows of apertures, $a/2$, is but slightly less than the line separation h the brightness of the field for uniform signal will be amaximum for the first condition and a minimum for the second, which will be reached $n-\frac{1}{2}$ scanning lines down the picture:

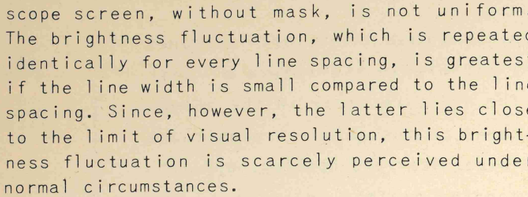

Fig. 1 – Preferred Orientation of Scanning Lines Relative to Mask.

$$(n - \tfrac{1}{2})\ h = \tfrac{1}{2}\ na; \qquad n = \frac{1}{2 - \frac{a}{h}} \qquad (1)$$

Hence there may be gross intensity fluctuations, or moiré, in the vertical direction with a period of $2n - 1$ scanning lines.

It is seen from Eq. 1 that the periodicity of the moiré is determined exclusively by the ratio of the dot separation a on the mask to the separation h of the scanning lines. The relative amplitude of the fluctuation, on the other hand, is determined only by the ratios of the line width d_s (for a given form of intensity distribution in the line) and the aperture diameter B to the line separation h.

If the scanning pattern is rotated relative to the mask by an angle θ, both the periodicity and direction of the moiré changes. Essentially, the intensity distribution in the field is given by the superposition of sinusoidal intensity variations of constant amplitude and differing frequency and direction. The amplitude is determined, as before, by the ratios of the line width and aperture diameter to the line separation. If the period of one of the sinusoidal components is much larger than that of any other, a line moiré, consisting of a sequence of broad bars, is obtained for uniform signal. If there are two components of nearly equal period, a dot moiré (with periods greater than the line separation) will be present.

The intensity distribution on the screen obtained for uniform signal does not, however, tell the full story of the effect of the mask on the picture. The picture signal contains, in effect, information regarding the variation in brightness of the sequence of equally spaced lines forming the scanning pattern. Hence, a proper measure of the error introduced by the mask is the variation in the transmission of the mask for these scanning lines, depending on the relative position of the scanning line and the aperture array in the mask. Fig. 2 compares schematically the intensity of a dot in a uniform-signal field and the line transmission. The dot intensity is the transmission

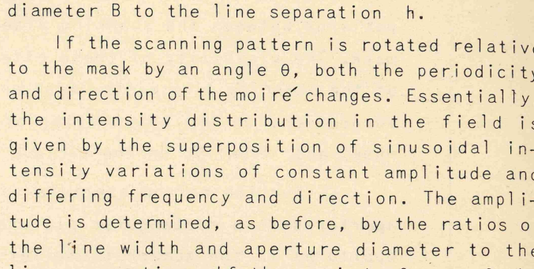

Fig. 2 – Schematic Representation of Dot Intensity and Line Transmission.

of a single mask aperture for the whole scanning pattern, whereas the line transmission is the transmission of the entire aperture mask for a single scanning line. The fluctuation in the dot intensity will be larger than that of the transmission as long as the spacing of aperture lines is less than the spacing of scanning lines; this condition is always satisfied in practice for the optimum orientation of the scanning pattern relative to the mask (Fig. 1).

This smaller fluctuation of the transmission is to be expected, since here electron current is, in effect, integrated over a coarser unit (the scanning line rather than the aperture line). In return for the greater coarseness of the information supplied, the transmission yields information not only regarding fluctuations in a uniform-signal field, but also for a field in which the line brightness may vary in some prescribed fashion (e.g., a succession of dark and light horizontal bars). If the scanning pattern is disoriented with respect to the mask, the transmission fluctuation rapidly increases, reaching a maximum for a displacement of 30 degrees relative to the optimum position; here the fluctuation in transmission greatly exceeds that in (dot) intensity for uniform signal, since the spacing of aperture rows (e.g., a = 0.023 or 0.030 inch) is materially greater than the scanning line spacing h (placed at 0.018 inch).

Basic Assumptions

The following calculations are made for a tube with a 9 x 12 inch scanning raster of 500 lines[2] and a line separation of 0.018 inch. A sequence of values, from 0.009 to 0.018 inch and from 0.0075 to 0.013 inch, are assumed for the line width d_s and the aperture diameter B. The separation of nearest neighbors in the aperture array, a, is made equal, in general, to 0.023 and 0.030 inch, although most of the results can readily be extended to any other values. The following exponential distribution is assumed for the scanning line:

$$f(y) = \frac{1}{b\sqrt{\pi}}\, e^{-y^2/b^2} = \frac{1.662}{d_s\sqrt{\pi}}\, e^{-(1.662y/d_s)^2} \qquad (2)$$

Here the "line width" d_s is defined as the transverse distance between two points at which the brightness of the line has dropped to $\frac{1}{2}$ of its maximum value. A "flat field" would correspond approximately to $d_s/h = 1$. The results reported here do not, of course, depend on the absolute dimensions of mask and scanning pattern, but only on the ratios d_s/h, B/h (or B/a), and a/h.

Intensity Distribution for Uniform Signal

The intensity transmitted by any one mask aperture may be written as a cosine series in terms of c/h, c being the distance between the center of the aperture and the center of the nearest scanning line:

$$I(c/h) = \frac{\pi B^2}{2\sqrt{3}a^2}\left(1 + \sum_{n=1}^{\infty} k_n \cos\frac{2\pi nc}{h}\right) \qquad (3)$$

Here, for convenience of comparison, the external coefficient has been set equal to the average transmission of the mask; in other words, the intensity falling on the total mask area per aperture has been set equal to unity. The values of k_n depend on the ratios of the line width and aperture diameter to the line separation, d_s/h and B/h. Tabulated below, they were calculated by the formulas derived in the Appendix.

Table I. Values of k_1

B in.		0.013	0.0115	0.009	0.0075	0
B/h		0.7222	0.6389	0.5	0.4167	0
d_s in.	d_s/h					
0.018	1	0.0277	0.0331	0.0416	0.0461	0.0576
0.0127	0.707	0.1631	0.1950	0.2450	0.2717	0.3394
0.009	0.5	0.3962	0.4732	0.5948	0.6596	0.8240

Table II. Values of k_2

B in.		0.013	0.0115	0.009	0.0075	0
B/h		0.7222	0.6389	0.5	0.4167	0
d_s in.	d_s/h					
0.018	1	$-1.5\cdot10^{-7}$	$-5\cdot10^{-6}$	$2.5\cdot10^{-7}$	$4.9\cdot10^{-7}$	$1.38\cdot10^{-6}$
0.0127	0.707	$-1.76\cdot10^{-4}$	$-5.9\cdot10^{-6}$	$3.02\cdot10^{-4}$	$5.9\cdot10^{-4}$	$1.66\cdot10^{-3}$
0.009	0.5	−0.00612	−0.00204	0.01045	0.02050	0.0576

[2] Or, e.g., a 8.45 x 11.27 inch raster of 470 lines. This refers to the raster on the mask. The picture area is some 5 per cent larger.

It is seen that even the second Fourier coefficient is quite insignificant, being 0.02 in the least favorable case considered. (The last column represents the Fourier coefficients of the intensity distribution without mask). Thus the intensity variation, as function of c/h, is practically sinusoidal and the relative amplitude of its fluctuations is given directly by the values of k_1.

Whereas the amplitude of the fluctuations is given by k_1, their periodicity in a vertical direction, for the alignment between aperture rows and scanning lines shown in Fig. 1, is given by Eq. 1. In particular for the values a = 0.030 in (a/h = 1,6667) and a = 0.023 in (a/h = 1.2778) the period of the fluctuation becomes 5 and 1.78 scanning lines. Since, in the second case, the period is of the same order as the dot separations, the effect would be here quite unnoticeable. With the larger spacing employed in some earlier experimental tubes a modulation of the vertical intensity should be readily visible even at viewing distance large enough that the line structure and the dot patterns are no longer resolved. It may be noted that, for the narrower spacing, a fluctuation with a somewhat larger period (1.99 h) is observed in a direction forming an angle of about 26 degrees with the vertical (see below).

The moiré for uniform signal when an angle θ is formed between the scanning lines and the x-axis (Fig. 1), which is imagined as fixed on the mask, is determined as follows: The intensity function I (Eq. 3) for the individual dot, with c replaced by y cos θ − x sine θ, is multiplied by a Fourier expansion which represents the array of the dot centers:

$$J(x, y; \theta) = \frac{B^2}{2\sqrt{3}a^2}\left[1 + \sum_{\substack{k,l=-\infty \\ k+l=2n \\ (k,l)\neq(0,0)}}^{\infty} k_1 \cos\frac{2\pi}{N_{kl}h}(x\cos\alpha_{kl} + y\sin\alpha_{kl})\right] \tag{5}$$

with

$$N_{kl} = \left[\left(\frac{kh}{a} + \cos\theta\right)^2 + \left(\frac{lh}{a\sqrt{3}} - \sin\theta\right)^2\right]^{-\frac{1}{2}} \tag{6}$$

and

$$\tan\alpha_{kl} = \frac{\frac{kh}{a} + \cos\theta}{\frac{lh}{a\sqrt{3}} - \sin\theta} \tag{7}$$

This represents the full solution for the intensity pattern obtained with uniform picture signal. The fluctuation components are all of the same amplitude k_1 but vary in the ratio N_{kl} of their period to the scanning line separation as well as in the direction of intensity variation α_{kl}; referred to the horizontal scanning lines this direction is $\alpha_{kl} - \theta$.

Only the terms of lowest order in h and k are significant since for higher order N_{kl} rapidly becomes small. Fig. 3 shows the variation of N_{kl} and $\alpha_{kl} - \theta$ as function of θ for the components which yield, for small values of θ, the largest values of N_{kl}. Here, again, it is assumed that a = 0.030 (a/h = 1.667) and 0.023 (a/h = 1.2778) inches.

$$J(x, y; \theta) = \frac{B^2}{2\sqrt{3}a^2}\left[1 + \sum_{n=1}^{\infty} k_n \cos\frac{2\pi n}{h}(y\cos\theta - x\sin\theta)\right]$$
$$\left[1 + 2\sum_{k=1}^{\infty}\cos\frac{4\pi k y}{a} + 2\sum_{l=1}^{\infty}\cos\frac{4\pi l x}{a\sqrt{3}} + 2\sum_{k,l=1}^{\infty}(1 + (-1)^{k+l})\cos\frac{2\pi k y}{a}\cos\frac{2\pi l x}{a\sqrt{3}}\right] \tag{4}$$

This formula assumes in effect that the intensity transmitted by each aperture is concentrated at the center of the corresponding dot. Since the dot size lies beyond the range of visual resolution this leads to no erroneous conclusions regarding any visible, macroscopic, intensity fluctuations. If the dot-structure

Transmission of Mask for a Scanning Line

The calculation of the transmission of the mask for a scanning line is indicated in detail in the Appendix. It is, of course, independent

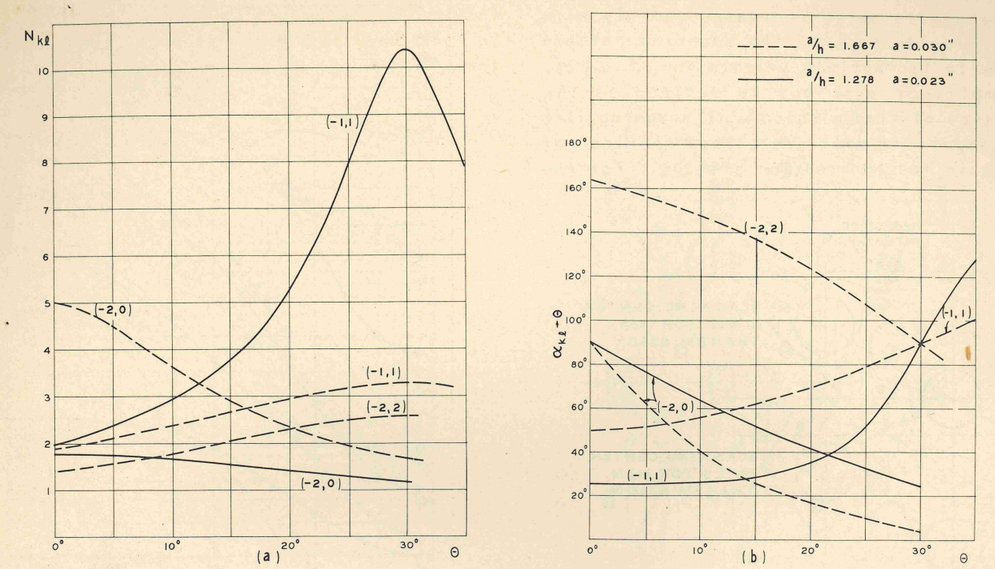

Fig. 3 – Variation (a) of Moiré Periods N_{kl} Measured in Multiples of the Scanning Line Separation and (b) of Directions of Corresponding Intensity Variations Relative to the Horizontal Scanning Lines as Function of Angle θ between Actual and Preferred Orientation of Scanning Lines Relative to Mask.

of h and, instead, a function of the two ratios B/d_s and B/a, namely of the ratios of the aperture diameter to the line width and the aperture separation. An amplitude factor k_T, corresponding to k_1 in Table I, may be introduced to describe the variation in transmission as the scanning line is displaced relative to the center line of a row of apertures by a distance varying from 0 to a/4. This factor is given, for comparison with Table I, in Table 3. It is also plotted, more extensively, in Fig. 7.

Table III. Values of k_T

a in.	B in. / d_s in.	0.013	0.0115	0.009	0.0075	0
0.030	0.018	0.004	0.005	0.008	0.007	0.012
0.030	0.01273	0.050	0.066	0.095	0.108	0.155
0.030	0.009	0.179	0.242	0.344	0.408	0.551
0.023	0.018					0.0003
0.023	0.01273		0.005	0.011	0.01	0.026
0.023	0.009		0.042	0.100	0.127	0.228

As already mentioned these fluctuation amplitudes are materially smaller than the values of k_1 listed in Table I. Identical values of k_T and k_1 are reached for a = 0.036 (a/2 = h), for which moiré effects are also most prominent, the period of the vertical intensity variation approaching infinity.

A plot of the actual transmissions as function of the aperture diameter B is given in Fig. 4.

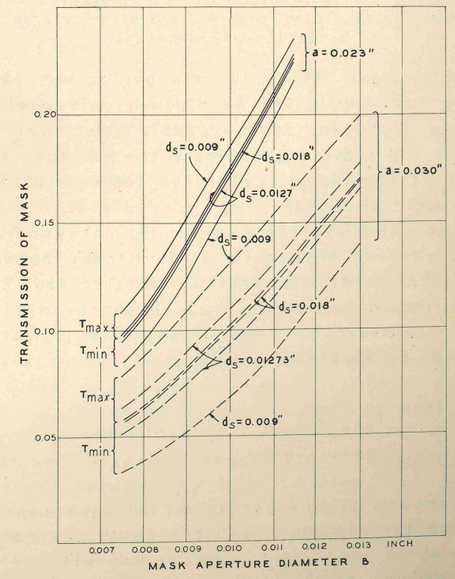

Fig. 4 – Maximum and Minimum Mask Transmissions as Function of the Mask Aperture Diameter.

The amplitude k_T increases rapidly with angular displacement of the scanning pattern relative to its optimum orientation (Fig. 1). This amplitude must now be defined as the fluctuation of transmission with scanning line displacement for some prescribed "period" of the mask in the x-direction (Fig. 5). For the

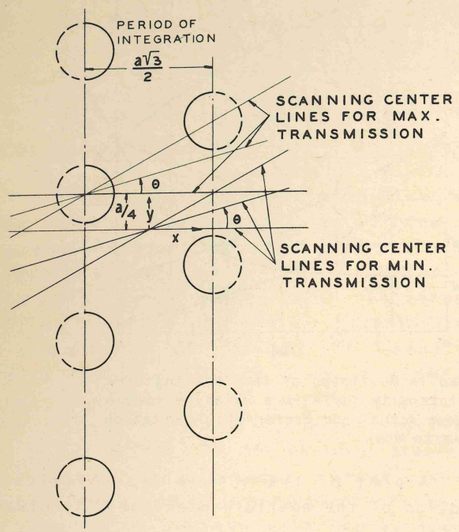

Fig. 5 – Determination of Mask Transmission When Scanning Line Forms Angle θ with Preferred Direction of Scanning.

results shown in Fig. 6, the period was taken to be $\frac{a\sqrt{3}}{2}$, which is the minimum period which may be employed. It is readily seen that for both θ = 0 and θ = 30 degrees the maximum value of the transmission is obtained for rays passing through the center of an aperture within the period, whereas the minimum is obtained for rays passing through a point midway between both horizontal and vertical aperture rows. The same should apply, to a close approximation, for intermediate values of angle. k_T, plotted in Fig. 6, is then given by

$$k_T = \frac{T_{max} - T_{min}}{T_{max} + T_{min}} \qquad (8)$$

The choice of the period of integration--in effect the distance in a horizontal direction over which intensities are summed--will affect the values of k_T only for angles between

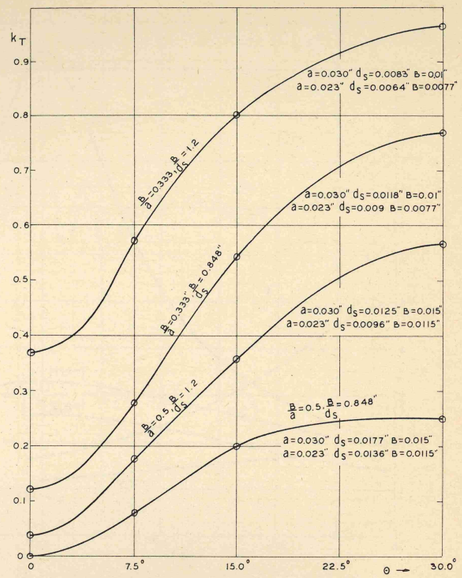

Fig. 6 – Fluctuation in Transmission as Function of Angle θ between Actual and Preferred Scanning Direction.

0 degrees and 30 degrees, not at the endpoints; the greater the period of integration, the less the fluctuation amplitude at intermediate points. The fluctuation amplitudes of the transmission for the endpoints, i.e., the most and the least favorable orientations of the scanning pattern (θ = 0° and θ = 30°), are plotted as function of the number of apertures in the picture area in Fig. 7.

Discussion of Results

The results for the moiré which is present with uniform signal are given by the data in Table I and Fig. 3. Table I shows that the amplitude of the moiré increases very rapidly as the scanning line is narrowed and more slowly, as the mask apertures are narrowed. For a scanning line width of 0.0127 inch and an aperture diameter of 0.009 inch, e.g., the modulation factor of the intensity is 0.25. With the larger aperture spacing (0.030 in.) this modulation has a period of 5 scanning line separations for the preferred orientation of the scanning pattern relative to the mask

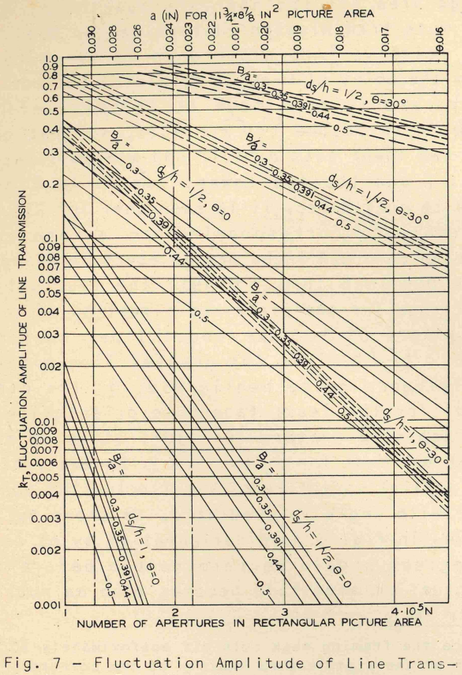

Fig. 7 – Fluctuation Amplitude of Line Transmission as Function of Number of Apertures in Mask.

(Fig. 1) line separations. The intensity variation is in the form of horizontal bars. In more detail, the intensity distribution given by the three terms with the largest periods in the range θ = 0 to θ = 30 degrees may be represented by an intensity contour pattern, such as that shown in Fig. 8. Not much weight can be attached to the finer structure of the pattern since the higher-frequency components of the intensity distribution have been omitted. The predominant importance of the term $N_{-2,0}$, with a vertical periodicity of 5 scanning line separations is, however, clearly evident.

As the scanning pattern is disoriented with respect to the mask, the system of horizontal bars also changes its orientation and contracts, eventually merging into a dot moiré with a periodicity of two to three line separations.

For the smaller aperture spacing (0.023 in.) the behavior is quite different. For the preferred orientation of the scanning pattern with respect to the mask, an unobjectionable dot moiré close to the limit of resolution (i.e.,

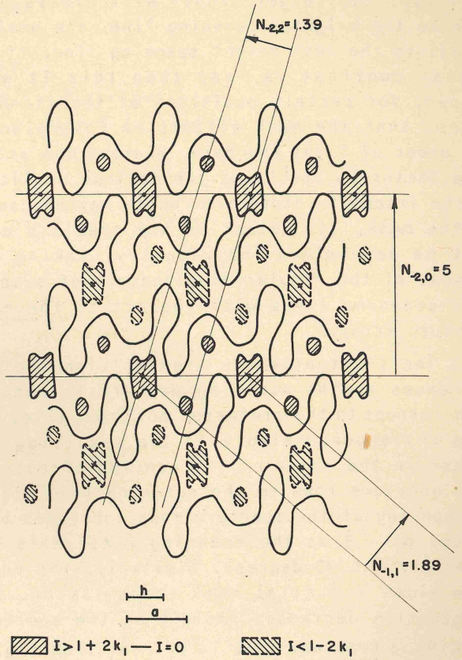

Fig. 8 – Approximate Intensity Contours for Uniform Signal, Computed for a/h = 1.667, θ = 0 from the Fourier Terms (-2,0), (-1,1), and (-2,2).

with periodicities of 2.0 and 1.8 scanning line separations) exists. With disorientation this gives way to a bar mosaic which reaches a maximum period of over 10 scanning line separations when the disorientation attains 30 degrees. Whereas, for uniform signal, the moiré pattern becomes less objectionable with disorientation for the tube with wide dot spacing, it is scarcely evident in the tube with narrow dot spacing unless there is a considerable departure from the preferred orientation.

The fluctuation in the transmission of the mask for a scanning line with vertical displacement of the line, as given by Table 3 and Figs. 4, 6, and 7, may serve as an index for the degree to which the mask permits the reproduction of fine (vertical) picture detail. In effect, it establishes a lower limit for the contrast between the picture signals for two scanning lines which will assure qualitatively correct reproduction. Thus if the ratio of the two picture signals (or, more precisely, the resulting beam currents) exceeds $(1 + k_T)/$

$(1 - k_T)$, the larger signal will always give rise to the brighter scanning line, the smaller signal to the less bright scanning line. If the signal contrast is less than this it will happen, for certain positions of the scanning lines, that the mask effects an inversion of the order of light and dark. Whereas the amplitude factor k_T specifies the maximum amplitude in the intensity distortion which may be caused by the mask, its extent in any specific case must be determined individually, taking due account of the regular displacement of successive scanning lines with respect to the mask aperture array.

The fluctuation in transmission rapidly increases as the scanning pattern is rotated with respect to the preferred position (Fig. 6). This corresponds simply to the resulting increase in the ratio of the spacing of successive aperture rows to the scanning line width; the spacing of the aperture rows increases by a factor of $\sqrt{3}$ as the scanning pattern is rotated through 30 degrees. Similarly, for equal line width and total mask transmission, the fluctuation decreases rapidly as the aperture spacing is reduced. This is evident from Fig. 7, where the fluctuation amplitude is plotted as function of the number N of apertures in the image area (or the aperture spacing a) with the mask transmission (determined by B/a) and the relative line width d_s/h as parameters. From the point of view of obtaining the maximum sharpness in the image it is pointless to lower d_s/h beyond $1/\sqrt{2} = 0.71$, so that only the two lower sets of full and broken lines in Fig. 7 and the two lowest curves in Fig. 6 need be considered. It is seen that for 215,000 apertures[3], corresponding to an aperture spacing of 0.023 inch, and an aperture diameter of 0.009 inch (B/a = 0.391) the fluctuation amplitude for the preferred direction of scanning ($\theta = 0$) is just about 1 per cent for $d_s/h = 1/\sqrt{2}$, less for greater line widths. It is hence quite negligible. On the other hand, for the least favorable orientation of the scanning pattern ($\theta = 30^\circ$) it is as much as 35 per cent for $d_s/h = 1/\sqrt{2}$. However, since the initial variation of the fluctuation amplitude with angle is quadratic, as shown by the curves in Fig. 6, a disorientation by at least 2 degrees should be permissible before the fluctuation amplitude becomes even as much as 2 per cent.

[3] Since the framing mask cuts off approximately 10 per cent of the picture area (mainly at the corners), the corresponding number of apertures contributing to the framed picture is 195,000.

E. G. Ramberg

Mathematical Appendix

Calculation of the Dot Intensity

If $I_o(c/h)$ is the intensity distribution of the scanning pattern for unit current falling on unit area,

$$I\left(\frac{c}{h}\right) = \frac{4}{a^2\sqrt{3}} \int_{-B/2}^{B/2} \sqrt{(B/2)^2 - y^2}\; I_o\left(\frac{y-c}{h}\right) dy \qquad (8)$$

with

$$I_o\left(\frac{y}{h}\right) = \frac{h}{b\sqrt{\pi}} \sum_{m=-\infty}^{m=\infty} e^{-\frac{(y + mh)^2}{b^2}}$$

$$= 1 + \sum_{n=1}^{\infty} a_{on} \cos \frac{2\pi n y}{h} \qquad (9)$$

$$= 1 + 2 \sum_{n=1}^{\infty} e^{-(\pi^2 n^2 b^2)/h^2} \cos \frac{2\pi n y}{h}$$

Substitution of Eq. 9 in Eq. 8 leads to

$$I\left(\frac{c}{h}\right) = \frac{\pi B^2}{2a^2\sqrt{3}} \left(1 + \frac{4}{\pi} \sum_{n=1}^{\infty} e^{-(\pi^2 n^2 b^2)/h^2} \int_{-1}^{1} \sqrt{1-s^2} \cos \frac{\pi n B s}{h}\, ds \cos \frac{2\pi m c}{h}\right)$$

$$= \frac{\pi B^2}{2a^2\sqrt{3}} \left(1 + \sum_{n=1}^{\infty} k_n \cos \frac{2\pi n c}{h}\right). \qquad (10)$$

The Fourier coefficient in this equation becomes:

$$k_n = 2e^{-(\pi^2 n^2 b^2)/h^2} \sum_{m=0}^{\infty} \frac{(-1)^m}{(m+1)\,(m!)^2} \left(\frac{\pi B n}{2h}\right)^{2m} \qquad (11)$$

Calculation of the Transmission

If the scanning pattern is in the preferred orientation (Fig. 1) relative to the mask, the transmission of the mask for the scanning line is given by

$$T\left(\frac{c}{a}\right) = \frac{2}{ab\sqrt{3\pi}} \sum_{n=-\infty}^{\infty} \int_{\frac{na-B}{2}}^{\frac{na+B}{2}} \sqrt{\left(\frac{B}{2}\right)^2 - \left(y - \frac{na}{2}\right)^2}\; e^{-\left(\frac{y-c}{b}\right)^2} dy$$

$$= \frac{2}{ab\sqrt{3\pi}} \sum_{n=-\infty}^{\infty} \int_{-B/2}^{B/2} \sqrt{\left(\frac{B}{2}\right)^2 - y^2}\; e^{-(1/b^2)\,(y-c+\frac{na}{2})^2} dy. \qquad (12)$$

A comparison of Eq. 12 with Eq. 8 shows that the transmission T is obtained from the dot intensity I if, in the latter, h is re-

placed by a/2. It follows, as already mentioned, that line transmission and dot intensity become identical for a = 2h.

For purposes of integration it is convenient to introduce the two variables

$$\beta = 2c/a \quad \text{and} \quad \alpha = [B/(2b)]^2 = (0.834B/d_s)^2.$$

Then Eq. 12 becomes

$$T\left(\frac{\beta}{2}\right) = \frac{B}{a}\sqrt{\frac{\alpha}{3\pi}} \int_{-1}^{1} \sqrt{1-s^2} \sum_{n=-\infty}^{\infty} e^{-\alpha\left(s-\beta+\frac{na}{B}\right)^2} ds \qquad (13)$$

If the scanning line is inclined by an angle θ to the preferred direction the transmission, calculated for the period shown in Fig. 5, becomes

$$T\left(\frac{\beta}{2}\right) = \frac{B}{a}\sqrt{\frac{\alpha}{3\pi}} \cos\theta \sum_{n=-\infty}^{\infty} \left[\int_{\frac{2na}{B}-1}^{\frac{2na}{B}+1} ds \int_{-\frac{\sqrt{3}a}{B}}^{-\frac{\sqrt{3}a}{B}+\sqrt{1-s^2}} d\xi + \int_{\frac{2na}{B}-1}^{\frac{2na}{B}+1} ds \int_{\frac{\sqrt{3}a}{B}-\sqrt{1-s^2}}^{\frac{\sqrt{3}a}{B}} d\xi \right]$$

$$\cdot e^{-\alpha[(s-\beta)\cos\theta - \xi\sin\theta]^2} \qquad (14)$$

with $s = \frac{2y}{B}, \qquad \xi = \frac{2x}{B}.$

This integral can be brought into a form convenient for quadrature by introducing polar coordinates with origin at the centers of the several apertures over which the integration is carried out. The result is:

$$T\left(\frac{\beta}{2}\right) = \frac{B}{2a}\sqrt{\frac{\alpha}{3\pi}} \cos\theta \left[\int_0^{\frac{\pi}{2}} \frac{d\varphi}{\sin^2\varphi} [F_1(\varphi) + F_1(-\varphi) + F_2(\varphi) + F_2(-\varphi)] \right.$$

$$\left. + \int_{\pi/2-\theta}^{\pi/2} \frac{d\phi}{\sin^2\varphi} [F_1(\varphi) - F_1(-\varphi) - F_2(\varphi) + F_2(-\varphi)] \right] \qquad (15)$$

with $F_j(\varphi) = \sum_{n=-\infty}^{\infty} \left[\frac{1}{\alpha} [e^{-\alpha q_{nj}^2} - e^{-\alpha(q_{nj}+\sin\varphi)^2}] \right.$

$$\left. + \sqrt{\frac{\pi}{\alpha}}\, q_{nj} [P(\sqrt{\alpha} q_{nj}) - P(\sqrt{\alpha}\,(q_{nj}+\sin\varphi))] \right]$$

$$q_{n1} = [\beta - \frac{2a}{B}(n+\tfrac{1}{4})] \cos\theta - \frac{\sqrt{3}}{2}\frac{a}{B}\sin\theta,$$

$$q_{n2} = [\beta - \frac{2a}{B}(n+\tfrac{3}{4})] \cos\theta + \frac{\sqrt{3}}{2}\frac{a}{B}\sin\theta,$$

$$P(y) = \frac{2}{\sqrt{\pi}} \int_0^y e^{-x^2} dx.$$

LB-866

NOISE FACTOR CONSIDERATIONS AND MEASUREMENT TECHNIQUES AT UHF

Property of
Albert E. Linden

RADIO CORPORATION OF AMERICA
RCA LABORATORIES DIVISION
INDUSTRY SERVICE LABORATORY

RADIO CORPORATION OF AMERICA

RCA LABORATORIES DIVISION

INDUSTRY SERVICE LABORATORY

LB-866

Noise Factor Considerations and Measurement Techniques at UHF

This report is the property of the Radio Corporation of America and is loaned for confidential use with the understanding that it will not be published in any manner, in whole or in part. The statements and data included herein are based upon information and measurements which we believe accurate and reliable. No responsibility is assumed for the application or interpretation of such statements or data or for any infringement of patent or other rights of third parties which may result from the use of circuits, systems and processes described or referred to herein or in any previous reports or bulletins or in any written or oral discussions supplementary thereto.

Approved

Stuart W. Seeley

Noise Factor Considerations and Measurement Techniques at UHF

Introduction

In the course of making noise-factor measurements on uhf television receivers, several precautions were found necessary in order to avoid error. As a result, an investigation of several phases of the problem was conducted, including a study of the operating levels required at the receiver video detector, an evaluation of the c-w and noise-diode methods of measurement, and a consideration of the less commonly used two-point noise-diode method.

Several charts which were prepared in the course of this investigation to simplify the required calculations, are included in this bulletin. The design data for the construction of two types of coaxial 50-to-75-ohm transformers are also included.

General Discussion

The two systems of noise-factor measurement commonly used are the c-w signal-generator method and the one-point noise-diode method,[1] the video detector of the receiver being used in both instances as the output device. The method of linearizing the detector differs for each method. When using a noise diode, linearization is obtained by the introduction of a c-w signal, so that the noise appears as modulation of this c.w. The a-c output then becomes a linear function of noise voltages at the detector input. In the signal-generator method, however, the detector must respond to a combination of c-w and noise, so that its exact behavior is dependent on the i-f and detector bandwidths.[2] This method requires an accurate knowledge of receiver bandwidth, and measurement of the d-c output of the detector, with the attendant error due to the presence of detector contact potential.

[1] LB-775, "Noise Factor and Its Measurement".
LB-776, "A Television and FM Noise Generator".

[2] W. R. Bennett, "Response of a Linear Rectifier to Signal and Noise", *Bell System Technical Journal*, Vol. 23, p. 97, Jan. 1944.

Signal-Generator Method

Detector linearization is obtained for the signal generator method by increasing the receiver gain until sufficient noise voltage appears at the detector. Experience has shown that, for the conventional video detector to operate linearly, the d-c level due to noise alone must be approximately one volt (Fig. 1). Measurements made on vhf television receivers indicate that in some instances, because of low receiver noise factor and moderate i-f gain, this minimum d-c level necessary for linearization cannot be obtained. This is indicated by the low values of measured noise factor at the lower values of detector d-c output. In such instances the measured noise figure may be low by as much as 5 db from the correct value.

The dotted curve in Fig. 1 also indicates the possibility of error in the opposite direction. Thus the measured noise figure may increase at low detector levels if excessive bias is applied to the r-f tube. In this instance, the degradation of noise figure due to the increased mixer noise contribution overrides the apparent improvement in the noise figure due to detector non-linearity. Fig. 1 also

shows the rise in measured noise figure at high detector noise levels because of receiver overload.

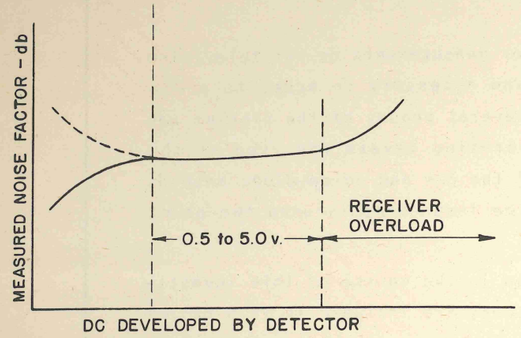

Fig. 1 – Noise factor vs d-c detector output level for the c-w method.

If the forward resistance of the detector is independent of level and frequency, the presence of a c-w input power equal to that of the receiver noise will increase the d-c output of the detector to a value 45 per cent greater than that due to receiver noise alone.[2] Then, for an equivalent c-w generator open-circuit voltage of e_o, a receiver input impedance of R_a and a noise bandwidth of Δf, the noise factor is given by the familiar relation:

$$F \text{ (in db)} = 10 \log 62 \frac{e_o^2}{R_a \Delta f}$$

where e_o is in μvolts

R_a is in ohms

and Δf, the noise bandwidth, is in megacycles.

For convenience, this relation has been plotted in Fig. 2 for several bandwidths and input impedances.

Noise-Diode Method

The noise-diode method has proven generally more satisfactory than the signal-generator method. The advantages of this method are that the receiver bandwidth need not be known, that the detector is required to handle noise signals only, and that an a-c voltmeter is employed thus removing the problem of contact potential. The detector is linearized by the injection of a c-w carrier of such amplitude that the noise voltages appear effectively as modulation of that c.w. For this condition, when the noise-diode power (as read from the instrument) is made equal to the noise power originating in the receiver, the a-c output of the detector is increased by 3 db. If there are spurious responses of appreciable magnitude, the measured noise factor will appear lower than the actual noise factor. Normally, this is a second-order effect. Thus for an image response down as little as 10 db, the measured noise figure will be degraded by 0.5 db.

Fig. 3 indicates that some caution must be used in choosing an operating point. The indicated a-c output range of 10 to 50 millivolts is representative, although this will vary with receiver design. Below this range, the measured noise figure may increase if excessive bias is applied to the r-f tube.

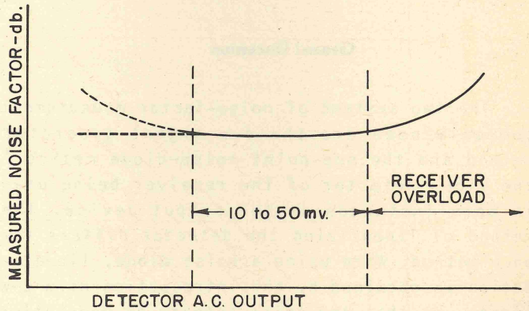

Fig. 3 – Noise factor vs detector a-c output level for the noise-diode method.

Two-Point Noise-Diode Method

When uncertainty exists as to linearity of the detector, the two-point noise-diode method may be used (LB-775, page 13). This method consists basically of calibrating the detector at two a-c output levels using a noise diode, and then using these same detector levels for making the actual measurement (see Fig. 4). Because the calibration is dependent upon the receiver noise factor, an appreciable

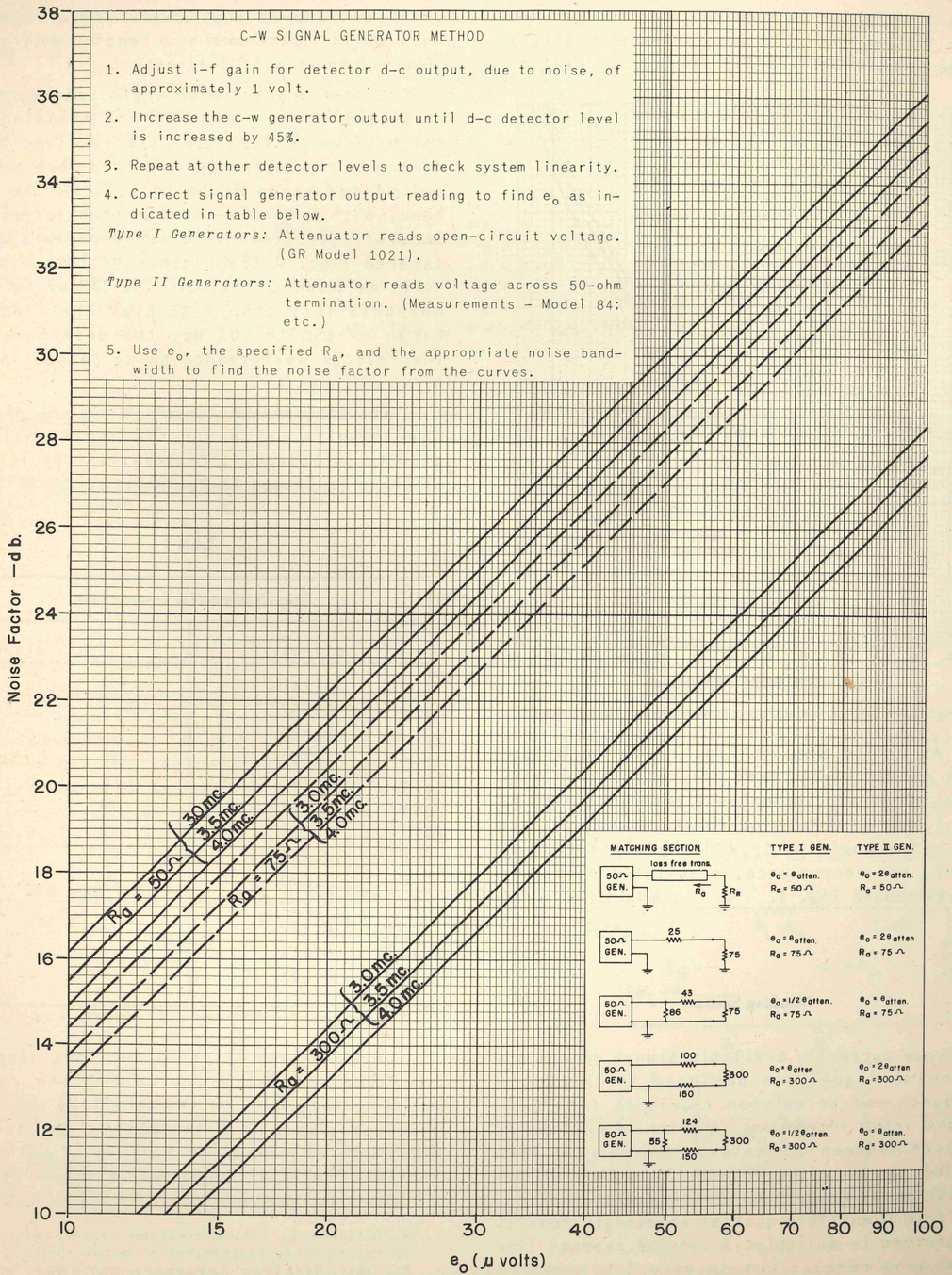
C-W SIGNAL GENERATOR METHOD
1. Adjust i-f gain for detector d-c output, due to noise, of approximately 1 volt.
2. Increase the c-w generator output until d-c detector level is increased by 45%.
3. Repeat at other detector levels to check system linearity.
4. Correct signal generator output reading to find e_o as indicated in table below.
Type I Generators: Attenuator reads open-circuit voltage. (GR Model 1021).
Type II Generators: Attenuator reads voltage across 50-ohm termination. (Measurements – Model 84; etc.)
5. Use e_o, the specified R_a, and the appropriate noise bandwidth to find the noise factor from the curves.
Noise Factor – d b.
e_o (μ volts)
Ra = 50 Ω
Ra = 75 Ω
Ra = 300 Ω
3.0 mc.
3.5 mc.
4.0 mc.
MATCHING SECTION
TYPE I GEN.
TYPE II GEN.
loss free trans.
50Ω GEN.
e_o = eatten. Ra = 50 Ω
e_o = 2eatten. Ra = 50 Ω
25
75
e_o = eatten. Ra = 75 Ω
e_o = 2eatten Ra = 75 Ω
43
86
75
e_o = 1/2 eatten. Ra = 75 Ω
e_o = eatten. Ra = 75 Ω
100
150
300
e_o = eatten Ra = 300 Ω
e_o = 2eatten Ra = 300 Ω
124
55
e_o = 1/2 eatten. Ra = 300 Ω
e_o = eatten. Ra = 300 Ω

Fig. 2 – Chart for conversion from e_o to noise factor for common receiver impedances and bandwidth.

correction factor is required when the receiver noise figure is of the same order of magnitude as the noise-diode levels used for calibrating.

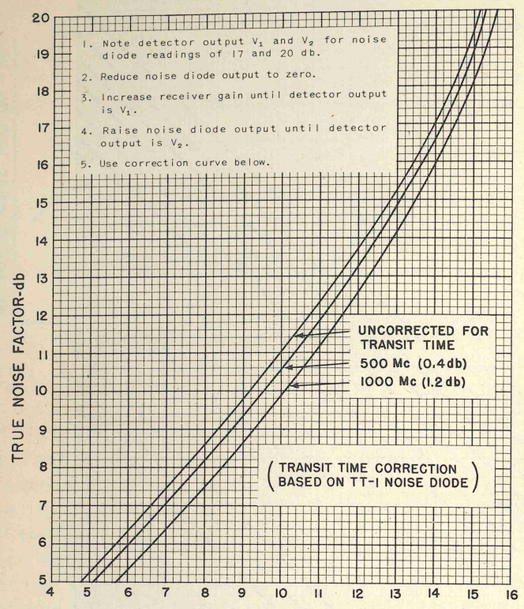

Fig. 4 - Two-point noise-diode correction curve.

As can be seen in Fig. 4, if the noise-diode output levels used for calibration were 20 and 17 db and the noise figure indicated by use of these calibration points was 15 db, the true value would be 19.4 db, a difference of 4.4 db. For convenience, a suitable procedure is outlined in Fig. 4.

Matching Sections

Since currently available signal generators and noise diodes are designed for a 50-ohm impedance and television receivers for 75 or 300-ohm input impedances, a matching section is required between generator and receiver. This section can be either of the loss-free or resistive type. For a 50 to 75-ohm transformation, some form of multiple-quarter wavelength coaxial transformer is suitable. A coaxial tapered line gives good results but is more difficult to construct and is physically larger since it must be at least one wavelength long at the lowest frequency of interest.

Single quarter-wavelength transformation sections provide a theoretical standing-wave ratio of up to 1.25 over the required 2-to-1 frequency range. For two cascaded sections this calculated value drops to 1.1. On the other hand, with a triple-section transformer[3] the theoretical performance is comparable with a tapered line. A transformer of this type was built as shown in Fig. 5b. The SWR of this unit measured less than 1.15 over the frequency range of 450 to 900 Mc, the departure from theoretical performance being caused largely by its connectors.

The tapered line shown in Fig. 5a gave the same results, although the additional complexity is apparent. Diameter values for each step are indicated in Table I.

Table 1

Step Diameters for Tapered Line			
S	diameter	S	diameter
1	0.261	14	0.212
2	0.257	15	0.208
3	0.253	16	0.205
4	0.249	17	0.202
5	0.245	18	0.199
6	0.241	19	0.195
7	0.237	20	0.192
8	0.233	21	0.188
9	0.229	22	0.186
10	0.226	23	0.183
11	0.222	24	0.179
12	0.219	25	0.177
13	0.215		

Dissipative matching sections generally have the configuration of Fig. 6a where a match is made both to the generator and to the receiver. Thus, at either AA' or BB' the same impedance is seen when looking in either direction. The result obtained is the elimination of standing waves on both the generator and

[3] W. Dallenbach, "Transformation Section with Transformation Ratio Independent of Wavelength", abstract No. 1511, *Wireless Engineer*, May 1944, p. 231.

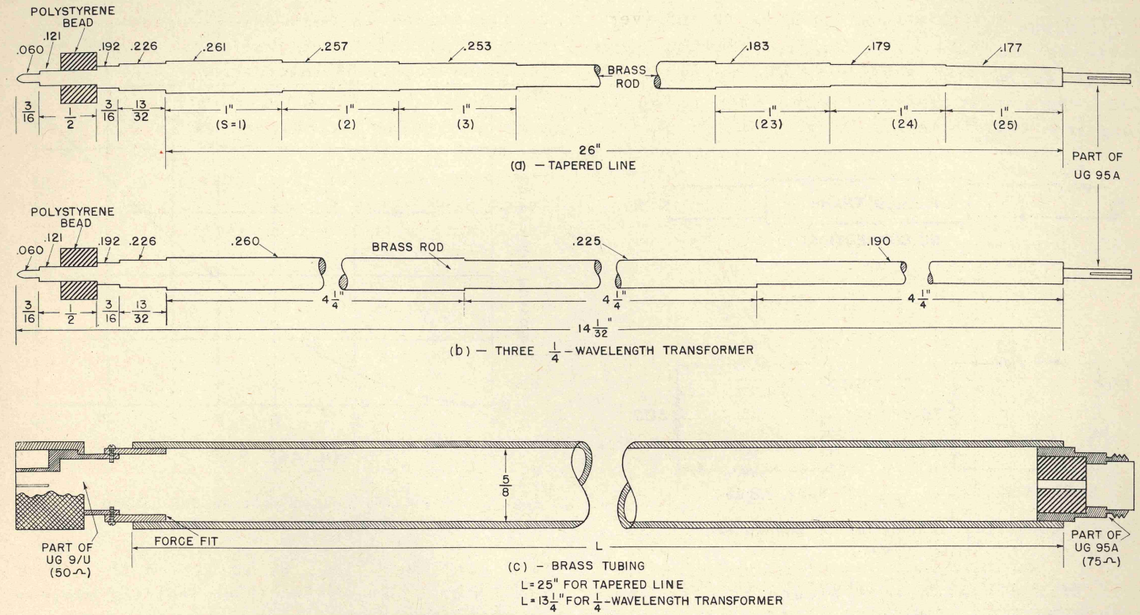

Fig. 5 - Two types of 50-75 ohm coaxial transformer.

receiver transmission lines when the receiver is matched to its transmission line.

Since the generator line is usually of the unbalanced coaxial type, reflections in this line can be tolerated. Should a single resistive element be used as indicated in Fig. 6b, the receiver line will be matched and no trouble from reflections will arise, provided the receiver matches its line and the generator matches the generator line. The main advantages of this arrangement are its lower attenuation, a factor of importance when using a noise diode, and the smaller number of resistors required, a significant consideration at uhf where the reactive components of resistors become important. The resistance values required for typical configurations and the corresponding corrections when using the signal-generator method are given on Fig. 2. Since the

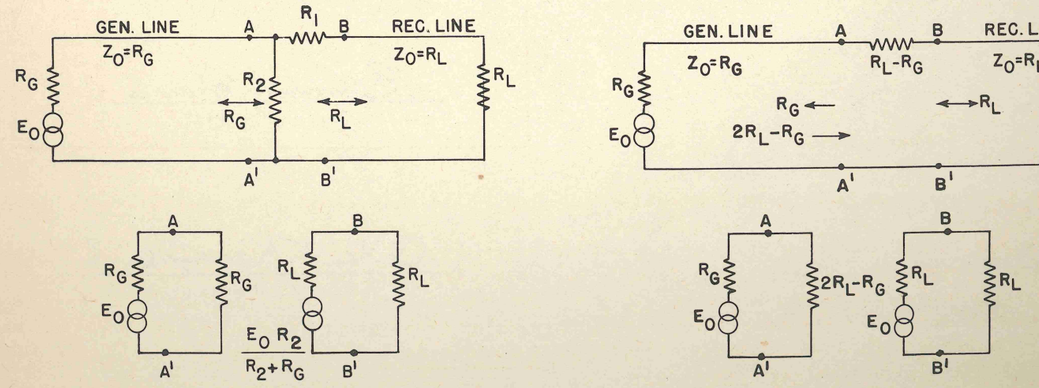

(a) Pad matches both transmission lines.

(b) Pad matches load transmission line only.

Fig. 6 - Two types of resistive matching section and equivalent circuits.

noise diode is calibrated for a 50-ohm load, a different correction is required. These are indicated in Fig. 7 for the non-terminated pads. No correction is needed when using a loss-free transformer.

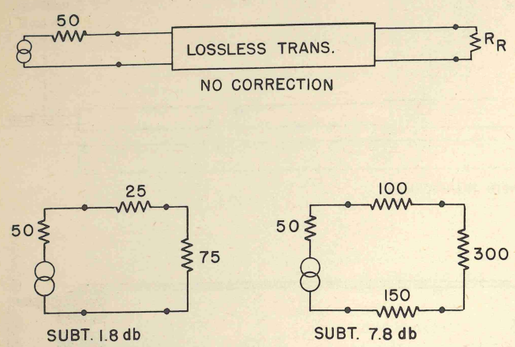

Fig. 7 – Matching section losses when using a noise diode.

If a mismatch loss occurs because the actual receiver impedance differs from its nominal value, the noise figure measured is indicative of receiver operation under typical conditions. This noise figure is independent of line length between generator and receiver, assuming that the generator matches its line. Some indication of the order of magnitude of the receiver mismatch can be obtained by inserting an adjustable shorting-stub into the receiver input line. By adjusting this stub both in position and length so that the minimum input signal for a given detector output is determined, the ratio of the squares of the generator voltages required with and without the stub will give the mismatch loss. A large input signal should be used during the measurement so that the noise originating in the receiver is only a small part of the total output voltage. Fig. 8 enables conversion from the mismatch loss (in db) to SWR.

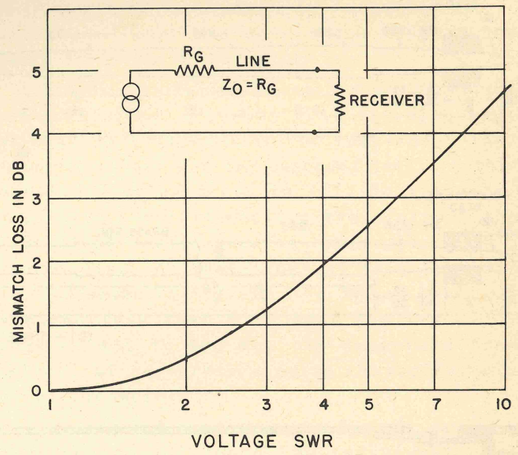

Fig. 8 – Mismatch loss vs voltage SWR caused by receiver mismatched to line.

Bernard Harris
Bernard Harris

Alan T. Brennan
Alan T. Brennan

LB-854

PERFORMANCE OF THE VIDICON, A SMALL DEVELOPMENTAL TELEVISION CAMERA TUBE

Property of
Albert E. Linden

RADIO CORPORATION OF AMERICA
RCA LABORATORIES DIVISION
INDUSTRY SERVICE LABORATORY

RADIO CORPORATION OF AMERICA
RCA LABORATORIES DIVISION
INDUSTRY SERVICE LABORATORY

LB-854

Performance of the Vidicon, a Small Developmental Television Camera Tube

This report is the property of the Radio Corporation of America and is loaned for confidential use with the understanding that it will not be published in any manner, in whole or in part. The statements and data included herein are based upon information and measurements which we believe accurate and reliable. No responsibility is assumed for the application or interpretation of such statements or data or for any infringement of patent or other rights of third parties which may result from the use of circuits, systems and processes described or referred to herein or in any previous reports or bulletins or in any written or oral discussions supplementary thereto.

Approved

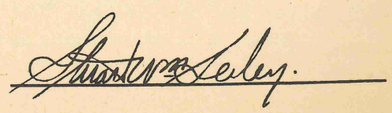

ABSTRACT

The performance of developmental Vidicons utilizing three different developmental types of photoconductive layers is described in this bulletin. Data are given on gamma, sensitivity, illumination considerations, spectral response, persistence, and life. Vidicon construction and operation as well as signal-to-noise limitations are discussed.

Performance of the Vidicon, a Small Developmental Television Camera Tube

Introduction

The Vidicon is a developmental television camera tube employing a thin layer of photoconductive material as its light-sensitive element. This bulletin describes the performance of developmental Vidicons employing several different types of photoconductive layers. Although the operation of the Vidicon has been presented in detail in other papers[1], the principles of operation and a description of its construction will be given so that the significance of the performance data will be evident.

Principles of Operation

Fig. 1 illustrates the basic principles of Vidicon operation. In this tube the electron beam is of low velocity as in the scanning section of the image orthicon. As shown in the illustration, the photoconductive layer, or photolayer, which is scanned by the electron beam, is backed by a signal plate which is maintained positive with respect to the cathode by an externally applied voltage. The electron beam current is maintained sufficiently high so that each element of surface on the gun side of the photolayer remains near cathode potential. In the interval between scans, wherever the photolayer is conductive due to the presence of light, the migration of charge through the layer causes its surface potential to rise toward that of the signal plate. On the next scan a sufficient number of electrons is deposited to return the surface to cathode potential. The result of this deposition is a current in the circuit which produces across the load resistor a voltage drop proportional to the charge built up between scans. The fluctuations in the voltage across the load resistor become the video signal applied to the first amplifier stage.

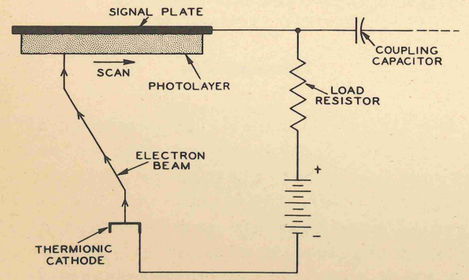

Fig. 1 – Basic principles of Vidicon operation.

[1] P. K. Weimer, S. V. Forgue, and R. R. Goodrich, "The Vidicon Photoconductive Camera Tube", *Electronics*, Vol. 23, pp. 70–73, May, 1950. Also, *RCA Review*, Vol. XII, No. 3, pp. 306–313, Sept. 1951.

Electrical Requirements of the Photoconductive Material

The photosensitivity of the photoconductive material may be as high as attainable, but in order that the signal produced be approximately proportional to the conductivity, the illumination in the picture highlights should be limited to a value such that the surface-potential change is small compared to the signal-plate potential. With the 1/30 second television frame time and the dielectric constant of the order of 10 for photoconductors, the resistivity in the highlights should not be lower than about 10^{10} ohm cm. The dark resistivity should be large compared to this value.

Vidicon Construction and Operation

In the developmental Vidicon, the signal plate is a coating of transparent conductive material deposited on the inside of the glass faceplate so that the optical image may be projected through it to the photolayer. Fig. 2 shows the arrangement of parts in the tube together with the positioning of the associated components. Grid No. 2 accelerates the beam of electrons emitted by the thermionic cathode.

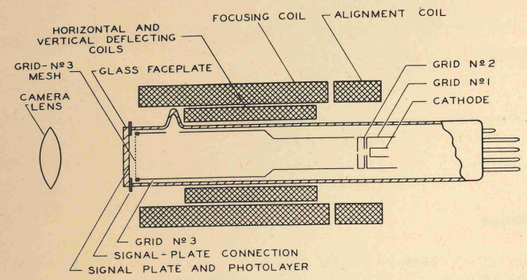

Fig. 2 – Arrangement of parts in Vidicon and positioning of associated components.

Grid No. 1, the control grid, operates at 0 to −100 volts with respect to the cathode. A small fraction of the electron-beam current passes through the small aperture (0.002 inch in diameter) at the faceplate end of grid No. 2. The beam passing through the aperture is imaged on the photolayer by the magnetic field produced by the external focusing coil. Deflection is obtained by external coils placed within the focusing field. The long electrode, grid No. 3, controls the potential of most of the space through which the electrons move. Focus adjustment is obtained by varying either the current through the focusing coil or the grid-No. 3 voltage, which is slightly less than 300 volts. A 500-mesh screen at the faceplate end of grid No. 3 provides a uniform decelerating field for the electrons. For the particular focusing coil and focusing-coil-current value used when the data described in this bulletin were taken, the electrons make one loop between the grid-No. 2 aperture and the photolayer. The potential of the signal plate is approximately 30 volts positive with respect to the cathode. The thickness of the photoconductive layer, approximately 0.0002 inch, is small compared to the diameter of the electron-beam spot and, hence, any lateral conductivity is negligible.

A photograph of the developmental Vidicon is given in Fig. 3. The tube is one inch in diameter, has an over-all length about 6¼ inches, and has a useful sensitive area about 5/8 inch in diameter. For a 3 to 4 aspect ratio the image is 3/8 inch high and ½ inch wide.

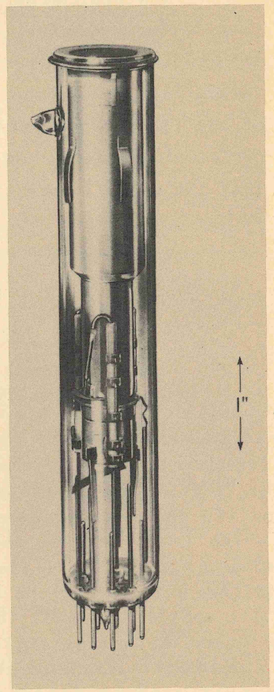

Fig. 3 – Photograph of developmental Vidicon.

Performance Data

The Vidicon is capable of resolving at the center of the picture at least 350 television lines per vertical picture height; with a suitable amplifier, 500 to 600 lines can usually be seen. A more complete specification of the ability of the tube to show detail is given in Fig. 4 which shows the amplitude-response-factor curve for a typical tube. This curve indicates that a pattern of 300 lines provides a response about 20 per cent of that of large-area blacks and whites. The curve was obtained with an average signal output of 0.2 microampere. When the signal output is larger, some loss of resolution is observed because the larger beam current required does not provide as sharp a spot.

The noise contributed by the Vidicon is small compared to that contributed by the associated circuit. With the usual peaked amplifier response, the noise is equivalent to about 0.002 microampere in the load resistor. A 0.2-microampere output signal, therefore, should have a signal-to-noise ratio of about 100 to 1.

Although the sensitivity of the Vidicon increases with increasing signal-plate voltage, a limit is set by the dark current which increases with a higher exponential power of signal-plate voltage than the signal. The useful limit is determined by the amount of nonuniformity in the dark-current signal background which can be tolerated under the conditions of use. The data given in this bulletin were taken within the limitation of a maximum tolerable dark current of 0.04 microampere.

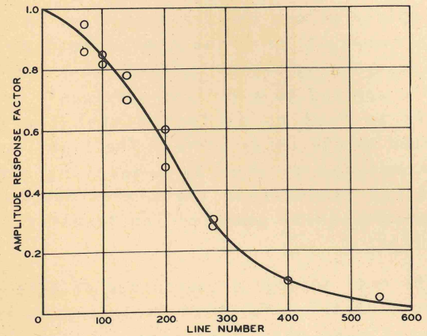

Fig. 4 – Amplitude response factor of typical developmental Vidicon.

Photoconductive Layer

Three developmental types of photolayers are discussed in this bulletin. These types are referred to as 1, 2, and 3. The material of which type 1 is made is amorphous selenium[2], type 2 is of antimony trisulfide[3], and type 3 is a developmental modification of type 2.

[2] P. K. Weimer and A. D. Cope, "Photoconductivity in Amorphous Selenium". *RCA Review*, Vol. XII, No. 3, pp. 314–334, Sept. 1951.

[3] S. V. Forgue, R. R. Goodrich, and A. D. Cope, "Properties of Some Photoconductors, Principally Antimony Trisulfide", *RCA Review*, Vol. XII, No. 3, pp. 335–349, Sept. 1951.

Gamma, Sensitivity, and Illumination Considerations

Fig. 5 is a typical log-log plot of signal output versus light flux for each of the three photosensitive layers. In all cause the slopes of the lines are less than unity; the output, therefore, is not proportional to the applied illumination. In the usual operating range between 0.02 and 0.2 microampere, the approximate slopes, or gammas, are 0.9 for type 1, 0.75 for type 2, and 0 7 for type 3. A low-gamma camera tube provides compression of the electrical signal range which is desirable for amplification and transmission and which also helps to compensate for the high gamma of the kinescope. Because the response of the Vidicon is nonlinear, it is necessary to specify the light or signal level and to require uniform illumination over the scanned area when sensitivity is being determined. Sensitivity is specified here at a low signal level, 0.02 microampere, because the lowlights are most critical for amplification of the signal. With this definition, the sensitivity of developmental Vidicons having photoconductive layers 1, 2, and 3 is, respectively, 100, 300, and 50 microamperes per lumen. As an example of illumination requirements, one millilumen on the useful photosensitive area 3/8 inch by ½ inch, which yields a signal output in the useful range between 0.02 and 0.2 mic oampere for any of the three types, represents a tube illumination of about ¾ of a foot candle. With an f:2 lens

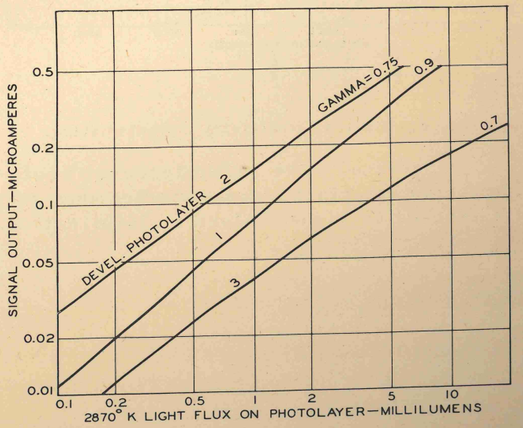

Fig. 5 – Transfer characteristics.

and a scene reflectance of 50 per cent, the scene illumination would be about 30 foot-candles of incandescent light.

Spectral Response, Persistence, and Life

There are several possible ways of defining the spectral sensitivity of a nonlinear device. For the data given in this bulletin the spectral sensitivity is taken as the reciprocal of the amount of energy at each wavelength required to obtain the same signal. This signal is chosen to be 0.02 microampere. As shown in Fig. 6, the response of photolayer 1 is limited to the blue end of the spectrum, photolayer 2 peaks in the red or yellow, and photolayer 3 peaks in the blue or green but has an appreciable response throughout the visible region. The spectral response curve for 3 is close to that of the RCA image orthicon type 5820.

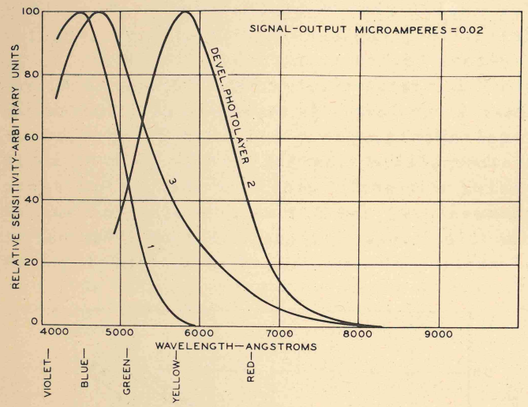

Fig. 6 – Spectral sensitivity characteristics.

In general, the persistence of photoconductive materials becomes shorter when they are exposed to higher values of illumination.

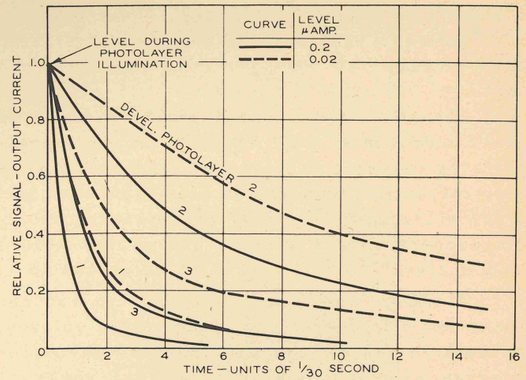

Fig. 7 – Decay characteristics.

Fig. 7 shows measurements of electrical signal decay made with each of the three photo-sensitive layers after the illumination had been suddenly cut off. Photosensitive layers 1 and 3 have persistence short enough for use in motion-picture work where the subject does not normally move rapidly across the field of view. As shown by the curve, type 2 has the slowest decay. The corresponding signal build-up when light is suddenly applied to a Vidicon previously in the dark is as fast as or faster than the rate indicated by the decay curves. The light output of a kinescope excited by a decaying signal will decay faster than the signal due to the greater-than-unity gamma of its transfer characteristic.

The most serious disadvantage of type 1 is its short useful life which is in the order of 300 hours even when operation is at the low face-plate temperature of around 35 degrees C. Development has not progressed far enough to lengthen this life materially. Types 2 and 3 have better life which should be more nearly commercially acceptable, and, in addition, in these types, the face plate temperature may safely be 60 degrees C in operation.

F. S. Veith

R. B. Janes

B. H. Vine

Tube Dept.
RCA Victor Division

LB-853

INTERLACED SAMPLING-SIGNAL GENERATOR

RADIO CORPORATION OF AMERICA

RCA LABORATORIES DIVISION

INDUSTRY SERVICE LABORATORY

RADIO CORPORATION OF AMERICA
RCA LABORATORIES DIVISION
INDUSTRY SERVICE LABORATORY

LB-853

Interlaced Sampling-Signal Generator

This report is the property of the Radio Corporation of America and is loaned for confidential use with the understanding that it will not be published in any manner, in whole or in part. The statements and data included herein are based upon information and measurements which we believe accurate and reliable. No responsibility is assumed for the application or interpretation of such statements or data or for any infringement of patent or other rights of third parties which may result from the use of circuits, systems and processes described or referred to herein or in any previous reports or bulletins or in any written or oral discussions supplementary thereto.

Approved

Stuart W. Seeley

Interlaced Sampling-Signal Generator

Introduction

The operation of dot- or frequency-interlaced color television systems requires a source of sinusoidal color-sampling or color sub-carrier signal having a frequency which is an odd multiple of one-half line frequency. In order that the proper relationship between the sampling frequency and one-half line frequency be maintained, a signal at 31.5 kc which is suitable for driving a standard monochrome synchronizing signal generator (such as the RCA TG-1A) must be derived, by appropriate frequency division operations, from the sampling-frequency oscillator signal. Part I of this bulletin describes a unit for this purpose employing regenerative frequency dividers, which was developed for experimental work in color television. It derives a 31.5-kc driving signal from a crystal-controlled 3.89 Mc (nominal) signal. The 31.5-kc signal is the double-line frequency and 3.89 Mc the color-sampling frequency tentatively standardized by the National Television System Committee.

Part II of this bulletin describes a companion unit for the Interlaced Sampling-Signal Generator which provides distribution amplifiers for the sampling-signal and a source of marker pulses of 0.01 H repetition period.

Part I

General Discussion

Either the regenerative divider or the trigger-circuit-type counter can be employed to perform frequency division. Considerations which recommend the use of the former include its relative insensitivity to supply-voltage variations and its relative economy of tubes. At the frequencies encountered in this application the elements of the required tuned circuits of a regenerative-type divider are of convenient size and adequate stability.

A single divider stage consists of a mixer section and a multiplier section as shown in Fig. 1. For division from 5 Mc to 1 Mc, for example, the mixer plate circuit is tuned to 1 Mc and the multiplier plate circuit is tuned to 4 Mc. In the steady state, the mixer combines the input signal at 5 Mc and the signal from the multiplier plate at 4 Mc and selects the difference frequency of 1 Mc in its tuned circuit. This provides the input to the multiplier section, which multiplies by four and which completes the regenerative loop. In the transient state in which the signal levels are building up, the input signal must excite the mixer tuned circuit, and there must be sufficient loop gain that regeneration will occur and the desirable steady state condition will be achieved. It is also desirable, though not

absolutely essential, to limit loop gain so that in the absence of an input signal the circuits are quiescent, preventing a spurious signal output.

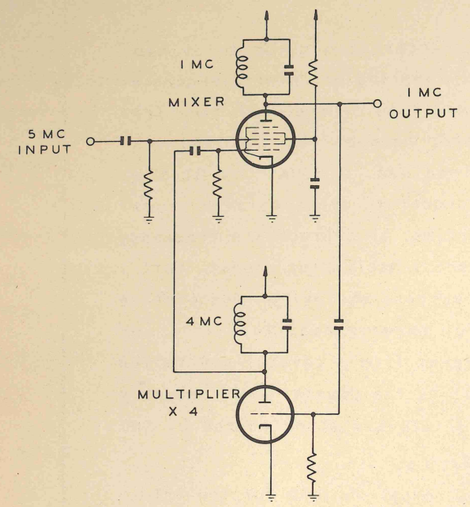

Fig. 1 – Typical single stage of regenerative division.

Description of Circuits

The unit, the schematic of which is shown in Fig. 2, may be considered in five sections: oscillator and buffer section, three sections of division, and 31.5-kc output. The buffer provides the color sampling-frequency output. The divisions are by five-fourths, nine and eleven.

Section (1) consists of a conventional crystal oscillator, V101, and a buffer-amplifier, V102. The buffer provides an output of approximately 20 volts p-p amplitude at a nominal impedance level of 75 ohms.

Section (2), the first stage of division, is a conventional regenerative divider made up of a mixer V103, and a multiplier, V104A. The mixer is driven by the buffer-amplifier of section (1). This stage performs a division of five-to-four; the desired divided output is present at the plate of the multiplier, V104A.

Section (3), which isdriven by the section (2) multiplier, performs a nine-to-one frequency division. This stage is a conventional regenerative divider, V105 being a mixer, and V104-B being a multiplier. The desired output is developed at the plate of the divider, V105.

Section (4), which is driven by the section (3) divider, again is a conventional regenerative divider circuit, V107 being a mixer, and V106A being a multiplier. This stage performs an eleven-to-one frequency division. The divided output is present at the plate of V107.

Section (5) is a resistance-coupled amplifier, V106B, providing the 31.5-kc output. This stage is driven by V107 through the RC filter formed by the 82K resistor and 51-μμf capacitor at the grid of V106B. This filter serves to attenuate the eleventh harmonic component present in the V107 plate current; the output of V106B approximates a 31.5-kc sine wave.

The 31.5-kc output is adjustable from 0-100 volts by means of potentiometer P1, and is intended to drive into a high impedance. The 31.5 kc signal at the top of P1 is also brought out to J12 to provide drive for the companion unit described in Part II of this bulletin.

The unit is assembled on a standard 5¼ inch dishpan-type chassis. Figs. 3 and 4 show front and rear views, respectively. Seven miniature tubes, and a crystal oven operating

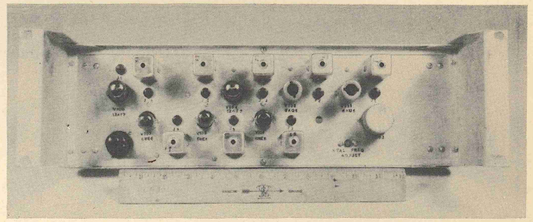

Fig. 3 – Front view of Interlaced Sampling-Signa Generator.

from the heater supply are employed. Power supply requirements are 100 ma at 300 volts and 3.1 amps at 6.3 volts. An RCA VC-1-C crystal ground for 3,898.125 kc at 75 degrees C, is mounted in a James Knights Co. JK02 crystal oven, operating at 75 degrees C, with a maximum

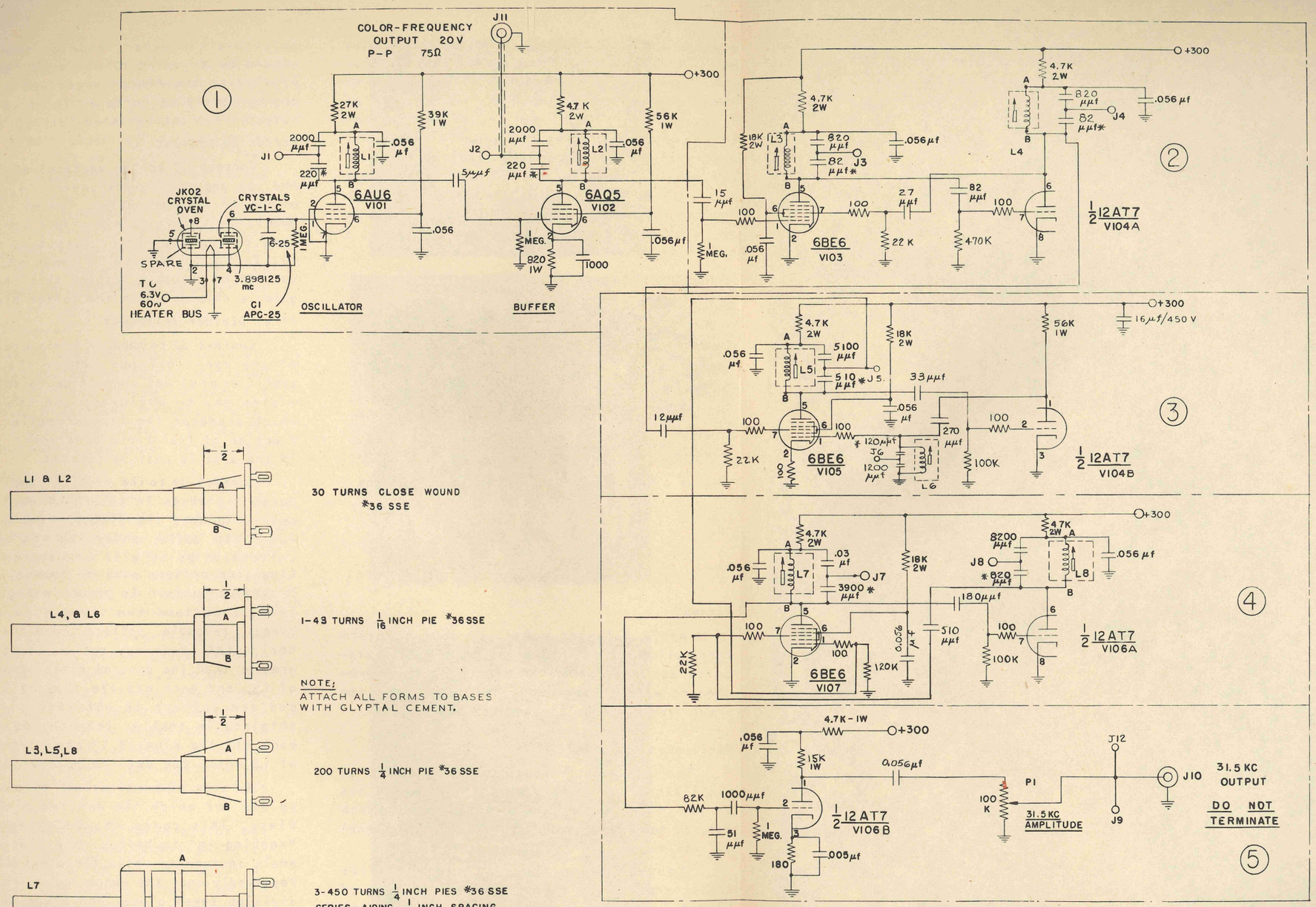

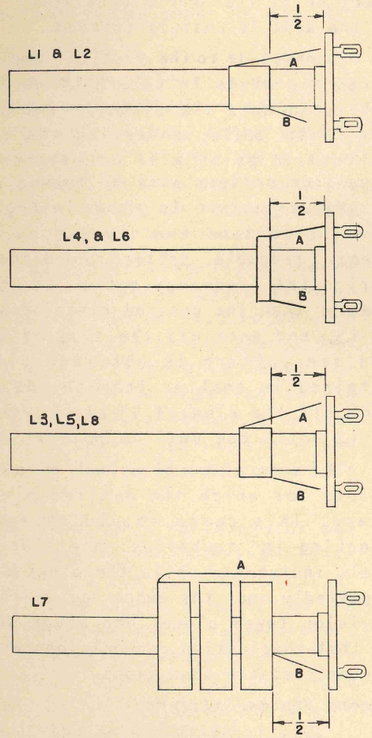
L1 & L2
1/2
A
B
30 TURNS CLOSE WOUND *36 SSE
L4, & L6
1-43 TURNS 1/16 INCH PIE *36 SSE
L3, L5, L8
200 TURNS 1/4 INCH PIE *36 SSE
L7
3-450 TURNS 1/4 INCH PIES *36 SSE SERIES AIDING, 1/16 INCH SPACING BETWEEN COILS.

NOTE:
ATTACH ALL FORMS TO BASES WITH GLYPTAL CEMENT.

COIL FORM ASSEMBLY RCA PART NO. 917848-504
1/4" FORM 7/8" SQUARE CAN

NOTE:
FOR USE WITH RCA TG-1A SYNCH. GENERATOR CONNECT 31.5KC OUTPUT TO EXT. SYNCH. INPUT TERMINAL; ADJUST 31.5KC AMPLITUDE FOR 15V P-P AT J9.

* SILVERED MICA 5% CAPACITORS —— RESISTOR TOLERANCES 5% —— GROUND ONE SIDE OF FILAMENT

Fig. 2 – Schematic Diagram of Interlaced Sampling-Signal Generator.

temperature cycling range of ±2 degrees C. The maximum range of frequency variation for this configuration is ±12 cps; a typical range of frequency variation is ±6 cps. The range of frequency adjustment afforded by the crystal trimmer-capacitor is approximately 800 cps, permitting adequate compensation for aging or crystal replacement. The outputs of the unit are 3.89 Mc at 20 volts p-p amplitude at a nominal impedance level of 75 ohms, and 31.5 kc adjustable to 0-100 volts p-p amplitude at a high impedance level.

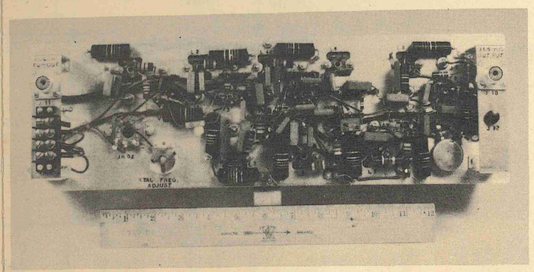

Fig. 4 - Rear view of Interlaced Sampling-Signa Generator.

Adjustment

General

Apply filament power, connect a 75-ohm termination to J11, and allow ten minutes warm-up to assure crystal stability, before proceeding with further adjustment. Apply plate power from a 300-volt regulated supply.

Oscillator Adjustment

For this and the remaining adjustments, an oscilloscope which focuses sharply, which has at least one wide-band channel, and which affords some gain at 400 kc in the other channel is required.

Connect J1 to the vertical amplifier input, and use any sweep. Advance the slug of L1 until oscillation is initiated. Note the signal amplitude. Continue to advance the slug of L1, noting the maximum signal amplitude. This immediately precedes an abrupt cessation of oscillation. Back off the slug of L1 until the amplitude is approximately 70 per cent of the maximum amplitude previously noted. The grid-to-plate capacitance of the oscillator should be adjusted by means of lead dress to provide an oscillator rectified grid bias of approximately 15 volts at 70 per cent maximum output. This assures stability of oscillation.

Buffer Adjustment

Connect J2 to the vertical amplifier input and use any convenient sweep. Adjust the slug of L2 for maximum output. Tuning of the buffer should have a negligible effect upon the amplitude of the oscillator output as measured at J1. This will be true if leads and components are placed in such a fashion that the oscillator grid is shielded from the buffer plate circuit.

First Divider Alignment

Connect J2 to produce horizontal deflection of the oscilloscope. Either the horizontal amplifier or direct connection to the deflection plates may be employed; use the connection which produces the largest deflection. A deflection of less than a centimeter is adequate if the spot is sharply focused.

Connect J4 to the vertical amplifier input. Screw the slugs in L3 and L4 well out of the coils. Advance the slugs by equal increments into both coils, observing the oscilloscope pattern. A point will be reached at which a Lissajous pattern will be formed. The correct Lissajous pattern is shown in Fig. 5a. Slight readjustment of the slugs should produce a steady, readable, pattern. Read the vertical to horizontal frequency ratio. If this ratio is greater than the desired ratio advance the slug of L3, and back off the slug of L2 until the desired pattern is obtained. If the ratio obtained is smaller than the desired ratio, back off the slug of L3 and advance the slug of L2 until the desired pattern is obtained.

A range of combinations of slug positions exists for which the desired division takes place. This range should be explored by a "rocking-in" technique: one slug is moved in small increments while the other slug is moved repeatedly over the range for which the desired division takes place. The slugs should be set in that combination of positions which produces the most stable conditions.

Second Divider Alignment

Leave J4 connected to the vertical amplifier input. Connect J5 to the horizontal amplifier input. Advance the slug of L5 to the

middle of its range. Gradually advance the slug of L6 until a Lissajous pattern is formed on the oscilloscope. The correct Lissajous pattern is shown in Fig. 5b. It may be necessary to readjust the slug of L5 in order to achieve a stable pattern. Read the vertical to horizontal frequency ratio. If this ratio is greater than the desired ratio, back off the slug of L5 and gradually advance the slug of L6 until the desired pattern is obtained. If the ratio obtained is smaller than the desired ratio, advance the slug of L5 and gradually back off the slug of L6 until the desired pattern is obtained. The slugs should then be adjusted for the most stable condition.

Third Divider Alignment

Connect J9 to the vertical amplifier input. Leave J5 connected to the horizontal amplifier input. Proceed as with the *second divider*, but read the horizontal to vertical frequency ratio. L7 corresponds to L5; L8 corresponds to L6. The desired Lissajous pattern is shown in Fig. 5c.

31.5-kc Output Adjustment

The amplitude of the 31.5-kc signal provided by the 31.5-kc output stage is adjustable to a maximum of 100 volts p-p by potentiometer P1, and may be measured at J9. The output impedance level is high; it should be recognized that the capacitance of the connecting cable will contribute to the load impedance.

In general, synchronizing-signal generators derive their output signals from an internal source of voltage at 31.5 kc of high amplitude and high impedance level. The 31.5-kc signal provided by the Interlaced Sampling-Signal Generator should be supplied to the synchronizing-signal-generator in such a fashion as to duplicate as nearly as possible the signal amplitude and source impedance of this internal source.

The RCA TG1A Synchronizing Generator may be driven by the Interlaced Sampling-Signal Generator by connecting the 31.5-kc output of the latter to the "Ext. Sync." terminal on the bottom chassis of the synchronizing generator, and placing the "Frequency Control" switch in the "Ext." position. The 31.5-kc amplitude should be set at 15 volts p-p at J9 of the Interlaced Sampling-Signal Generator.

When the Interlaced Sampling-Signal Generator 31.5-kc signal has been supplied to the

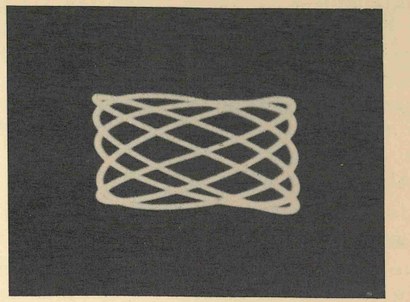

(a)

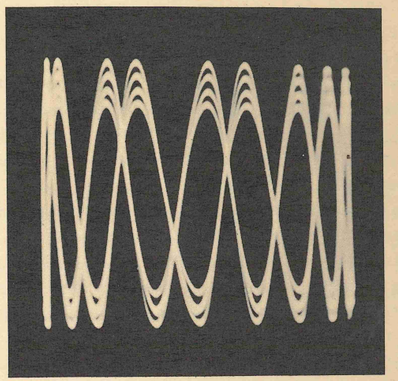

(b)

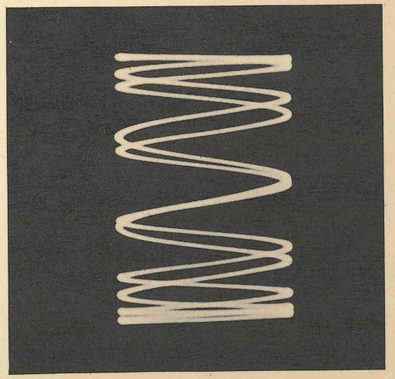

(c)

Fig. 5 - Lissajous figures employed in alignment of Interlaced Sampling-Signal Generator.

sync-generator, observe the composite sync-and-blanking waveform on the oscilloscope, using a

60-cycle sine-wave sweep. When the sync-generator is properly controlled, the waveform will rotate slowly at the difference frequency between the power-line frequency and the field frequency. An erratic pattern, or a pattern which rotates at more than a few tenths of a cycle per second, indicates that the sync-generator is not properly controlled.

Oscillator Frequency Adjustment

When a precise adjustment of oscillator frequency is desired, the following method may be employed. The auxiliary equipment required consists of a communications receiver, a calibrated 2.5-Mc crystal source (such as the RCA WR-39-B Television Calibrator), an audio oscillator, and an oscilloscope. The 2.5-Mc crystal may be calibrated with respect to the Standard Frequency Transmissions of station WWV, Washington, D. C. These transmissions are at 2.5, 5, 10, 15, 20, 25, 30, and 35 Mc. By adjustment of the 2.5-Mc crystal frequency, a zero beat may be obtained between one of these transmissions and a harmonic of the crystal frequency. The audio oscillator may be calibrated with respect to the 31.5-kc output of the Interlaced Sampling-Signal Generator; a calibration at 10,500 cps is close to the frequency required in adjustment of oscillator frequency, and may be obtained by forming a three-to-one Lissajous figure on the oscilloscope. (This 31.5-kc reference is inaccurate only to an extent proportional to the inaccuracy of oscillator frequency. At the extremes of the range of the crystal trimmer-capacitor, the oscillator frequency is in error less than 0.03 per cent.)

For measurement of the 3.89 Mc frequency (3,898,125 cps design frequency) connect the Color Frequency Output (J11) to the input connector (J18) of the sampling signal distribution amplifier (or equivalent amplifier) which is a part of the Companion Unit described in Part II of this bulletin. There should be a 75-ohm termination at J15. Adjust the slug of L12 for maximum output at J19.

Connect J19 (terminated in 75 ohms) to the 2.5-Mc crystal calibrator input with a short wire, and connect a 1N34 germanium crystal diode from the input terminal to ground. The crystal may be connected with either polarity grounded.

A signal at the difference frequency between the 59th harmonic of the 3.89-Mc frequency (229,989,375 cps) and the 92nd harmonic of the 2.5-Mc crystal (230,000,000 cps) will appear at the output of the crystal calibrator detector. This difference frequency is dependent on the particular frequency of the 3.89 Mc crystal oscillator, and may be varied from a frequency well above the audible range, through zero beat, and to another frequency above audibility on the other side of zero beat, by varying oscillator trimmer capacitor C1.

In order to obtain optimum amplitude of the difference frequency some slight readjustment of the plate tuning of V102 and V301 will be required. The following procedure has been used.

Set the trimmer capacitor C1 so that the difference frequency is readily audible. A frequency of 3,000 to 5,000 cps has been found satisfactory. As mentioned previously, beat notes may be obtained on both sides of zero beat; these correspond to two positions of trimmer capacitor C1. The higher capacitance position is the proper one. Next, adjust the slug of L2 for maximum amplitude of the difference frequency. This adjustment may "pull" the oscillator frequency slightly; once this adjustment has been made, do not change the position of the slug in L2.

After the slug in L2 has been adjusted for maximum amplitude of the difference frequency, the plate tuning of V301 should also be adjusted for maximum amplitude of the difference frequency. This tuning adjustment should not pull the frequency of the oscillator.

The difference frequency may now be compared to a signal from the audio oscillator by means of the oscilloscope, and should be coupled to the oscilloscope through a 200-μμf capacitor to minimize the effect of hum present in the output of the television calibrator. Because of oven-temperature cycling, the detected difference frequency will vary over a range of about one thousand cycles at approximately one minute intervals. If the audio oscillator is set at a frequency within this range, it will be possible to observe the zero-beat condition when the detected difference frequency swings past the audio oscillator frequency. Now vary the audio oscillator frequency so as to maintain the zero-beat condition, and follow the detected difference

signal over its range. Note the audio oscillator frequencies at the two extremes of this range, and compute from them the mid-range frequency. This mid-range frequency should be adjusted, by means of trimmer capacitor C1, to 10,625 cps. An error of 59 cycles per second at the frequency of the detected signal arising from errors such as those incurred in audio oscillator calibration represents an error of one cycle per second at the color sampling frequency.

Part II

Companion Unit to Interlaced Sampling-Signal Generator

General Discussion

The horizontal synchronizing signal utilized for experimental transmissions of the National Television System Committee color-television system includes, in addition to the horizontal blanking pulse and horizontal sync pulse, a burst of the color-sampling frequency riding on a burst pedestal. The timing and duration of the components of this signal are usually given in decimal parts of H, the line repetition period. Adjustment of the waveform to the required values is facilitated by a source of marker pulses which repeat at a known decimal part of H.

One section of the Companion Unit to the Interlaced Sampling-Signal Generator provides such a source of marker pulses, adjustable in phase, occurring at a repetition period of 0.01 H.

The other section of the Companion Unit consists of three distribution amplifiers for the color sampling signal, providing three independent outputs. Independence of outputs is particularly advantageous for experimental work.

Description of Circuits

The marker-pulse section of the Companion Unit, the schematic of which is shown in Fig. 6, is composed of four stages: a multiplier stage, a limiter stage, an amplifier-rectifier stage, and an output stage.

The multiplier stage utilizes one section of a 6J6, V201A. It is driven from the 31.5-kc signal originating at the plate of the 31.5-kc output stage, V106B, of the Interlaced Sampling-Signal Generator. This signal is available at J12 in that unit. J12 should be connected to J15 of the Companion Unit; J15 is connected to the variable phase-shift network, which is in turn connected to the multiplier grid. The phase-shift is controlled by the *Marker-Pulse Position* potentiometer, P2.

The output of the multiplier, at 787.5 kc (25 x 31.5 kc), is amplified and limited by V201B, the second section of the 6J6. The signal at the grid of the limiter is shown in Fig. 7a.

The limiter drives the amplifier, V202A, one section of a 12AU7. The limiter output, measured at the grid of V202A, is shown in Fig. 7b. The double-ended plate load is shunt-fed; the balanced signal is full-wave rectified by two 1N34 crystal diodes. The repetition frequency of this signal is thus 2 x 787.5 kc, or 1575 kc which is 100 times the 15,750 cps horizontal sync frequency.

The full-wave rectified signal drives the cathode-follower output stage, V202B. The cathode load is the *Marker-Pulse Amplitude* potentiometer, P3. The *Marker-Pulse Output* is made available at the coax-receptacle, J16, and at the pin-jack, J17. The output signal consists of positive pulses of 0-8 volts amplitude, adjustable, occurring at a repetition period of 0.01 H. The marker-pulse output is shown in Fig. 7c. The pulse-position is adjustable over the full range of the repetition period.

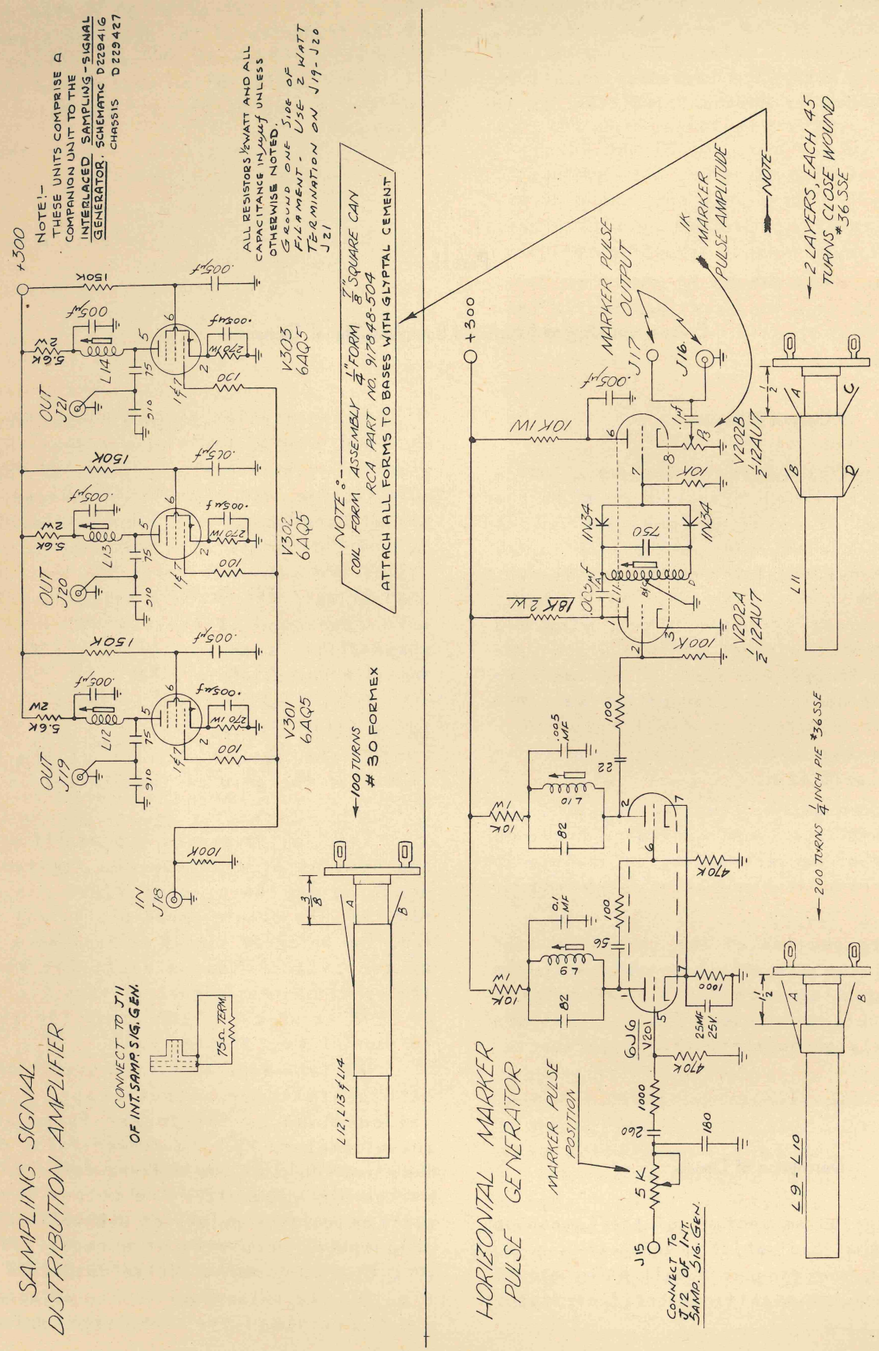
NOTE:- THESE UNITS COMPRISE A COMPANION UNIT TO THE INTERLACED SAMPLING-SIGNAL GENERATOR. SCHEMATIC D229416 CHASSIS D229427
ALL RESISTORS ½WATT AND ALL CAPACITANCE IN μμF UNLESS OTHERWISE NOTED. USE OF FILAMENT - USE 2 WATT TERMINATION ON J19-J20 J21
NOTE:- 2 LAYERS EACH 45 TURNS CLOSE WOUND #36 SSE
NOTE:- COIL FORM - ASSEMBLY ½" FORM & ½" SQUARE CAN RCA PART NO. 91-348-504 ATTACH ALL FORMS TO BASES WITH GLYPTAL CEMENT
100 TURNS #30 FORMEX
200 TURNS ¼ INCH PIE #36 SSE
+300
MARKER PULSE OUTPUT J17
1K MARKER PULSE AMPLITUDE
OUT J21
OUT J20
OUT J19
IN J18
V303 6AQ5
V302 6AQ5
V301 6AQ5
V201 6U6
V202A ½12AU7
V202B ½12AU7
SAMPLING SIGNAL DISTRIBUTION AMPLIFIER
CONNECT TO J11 OF INT. SAMP. SIG. GEN.
HORIZONTAL MARKER PULSE GENERATOR
MARKER PULSE POSITION
CONNECT TO J12 OF INT. SAMP. SIG. GEN.
J15
J16
L7, L8, L9, L10
L11
D17-67

Fig. 6 - Schematic diagram of Companion Unit to Interlaced Sampling-Signal Generator.

The distribution amplifier section of the Companion Unit is composed of three 6AQ5 amplifiers, V301, V302, and V303. The outputs are available at the coaxial receptacles, J19, J20, and J21. The amplifiers are designed to be driven from the *Color-Frequency Output*, terminated, of the Interlaced Sampling-Signal Generator. This termination may be a terminated line, permitting further utilization of the *Color-Frequency Output*.

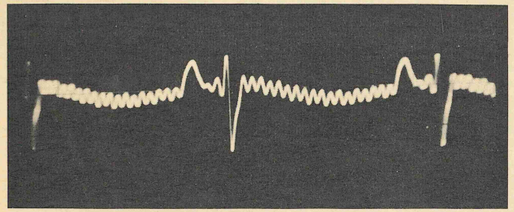

(a) Waveform at grid of limiter, V201B; 8v p-p.

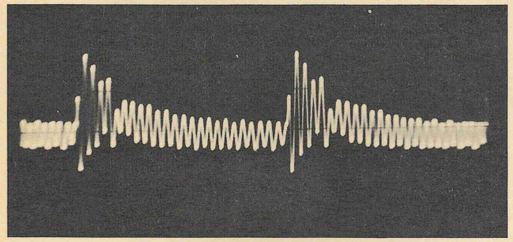

(b) Signal at grid of V202A; 8v p-p.

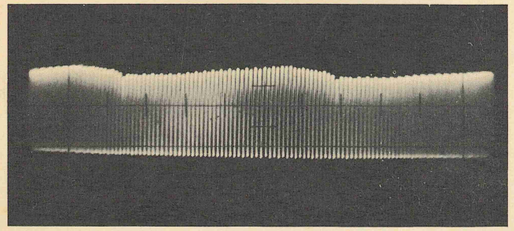

(c) Output of marker-pulse generator; 8v p-p.

Fig. 7 - Waveforms of marker pulse generator.

Both sections are mounted on a standard 3½-inch dishpan chassis. Power requirements are 150 ma at 300 volts and 2 amps at 6.3 volts. Front and rear views are shown in Figs. 8 and 9.

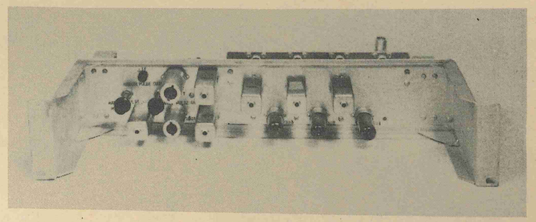

Fig. 8 - Front view of Companion Unit.

Adjustment

The Companion Unit should be mounted either immediately above or below the Interlaced Sampling-Signal Generator. A short wire, terminated in pin-plugs is used to connect J12 of the latter unit to J15 of the former.

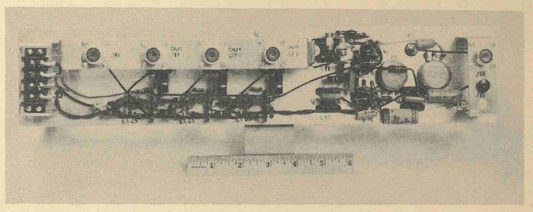

Fig. 9 - Rear view of Companion Unit.

The plate loads of V201A, V201B, and V202A in the Companion Unit must now be tuned to 787.5 kc. This is most readily accomplished by observation of the *Marker-Pulse Output* on an oscilloscope, the sweep of which is synchronized by horizontal drive, or the 31.5-kc output available at J9. The waveform observed will consist of a full-wave rectified sinusoid of high frequency, with irregularities in amplitude which repeat symmetrically at 31.5-kc repetition rate. L9, L10, and L11 should be tuned to maximize this signal; this will greatly reduce the irregularities in amplitude. For proper tuning, there are 50 pulses in a repetition interval. The pulses in a repetition interval should be counted and the coils should be tuned to achieve the proper number of pulses. Tuning L9, in the multiplier plate load, is most effective.

The marker pulse section of the Companion Unit has now been adjusted. The *Marker-Pulse*

Output may be employed conventionally to blank the trace of the oscilloscope presentation of any waveform whose repetition rate is controlled by the Interlaced Sampling-Signal Generator. It may also be convenient to add marker pulses to the signal to be observed. To accomplish this, the *Marker-Pulse Output* may be coupled by a small capacitor (e.g., 18 μμf) to the terminated line carrying the signal in question. The differentiated marker pulses thus added to the signal are approximately sawtooth in form; they effectively interrupt the signal at 0.01 H intervals. The combined signal may be adjusted to the desired appearance by the *Marker-Pulse Amplitude* control.

The color-frequency distribution amplifier section of the Companion Unit is driven from the Color-Frequency Output of the Interlaced Sampling-Signal Generator. A short length of cable should be connected from J11 of the latter unit to a coaxial Tee mounted on J18 of the Companion Unit. The free arm of the Tee should be terminated. The outputs at J19, J20, and J21 may be adjusted by tuning L12, L13, and L14, respectively; 30 volts p-p into 75 ohms is available at these outputs, and 2-watt terminations should be used.

T. O. Stanley

N. D. Larky

D. D. Holmes